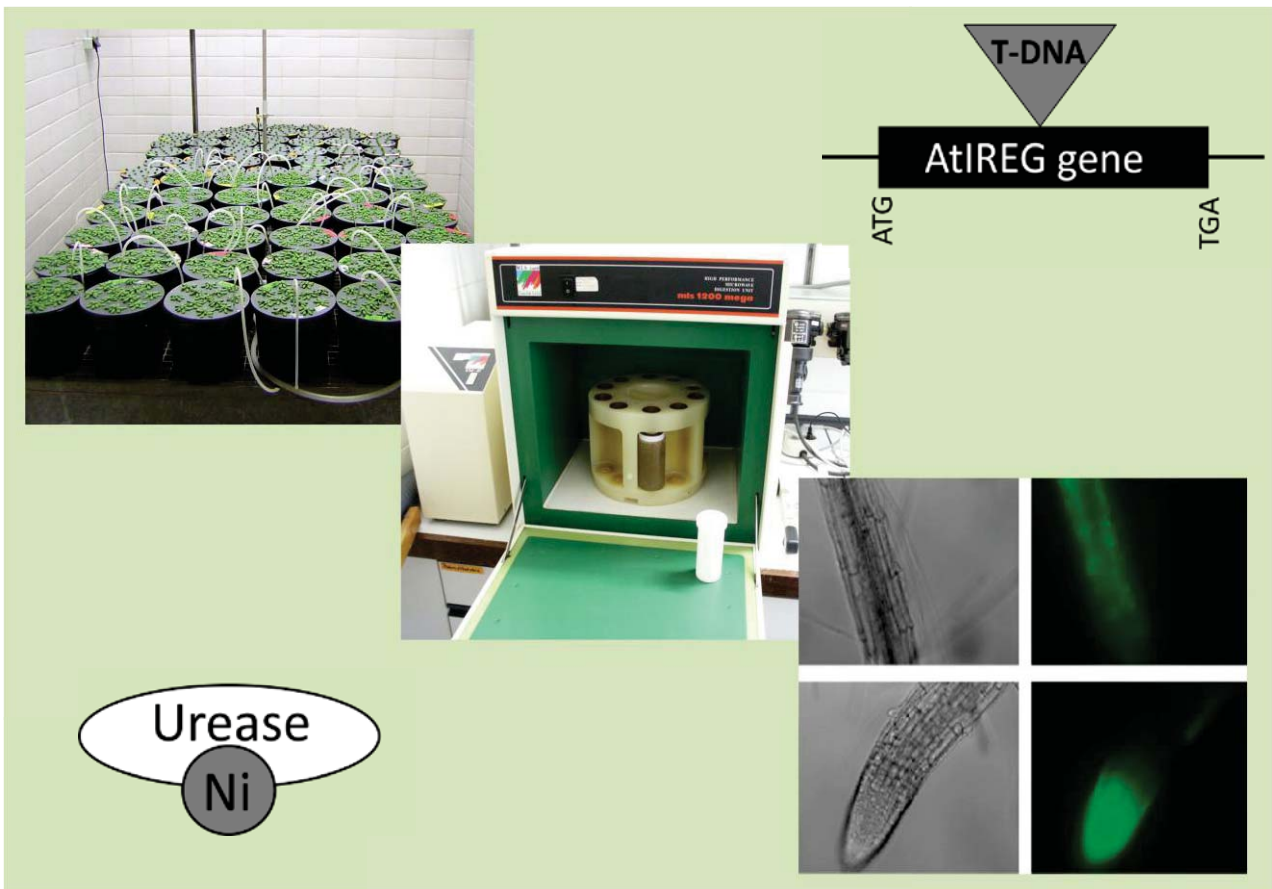


Silvia Kirchner

## The AtIREGs – Characterization of a new family of metal transporters in *Arabidopsis thaliana*



Institute of Plant Nutrition

University of Hohenheim

Prof. Dr. N. von Wirén

**The AtIREGs - Characterization of a new family of  
metal transporters in *Arabidopsis thaliana***

Dissertation

Submitted in fulfilment of the requirements for the degree

„Doktor der Agrarwissenschaften“

(Dr. Sc. Agr. / Ph. D. in Agricultural Sciences)

to the Faculty Agricultural Sciences

of the University of Hohenheim

presented by

**Silvia Kirchner**

from Neu-Ulm

2009

This thesis was accepted as a doctoral dissertation in fulfilment of the requirements for the degree “Doktor der Agrarwissenschaften” by the Faculty of Agricultural Sciences at the University of Hohenheim.

Date of oral examination: 3<sup>rd</sup> March 2009

**Examination Committee**

Supervisor and reviewer	Prof. Dr. Nicolaus von Wirén
Co-reviewer	Prof. Dr. Gerd Weber
Additional examiner	Prof. Dr. Wolfgang Hanke
Vice dean and head of the committee	Prof. Dr. Werner Bessei

## Table of contents

<b>1 Summary – Zusammenfassung .....</b>	<b>1</b>
1.1 Summary .....	1
1.2 Zusammenfassung .....	3
<b>2 Introduction .....</b>	<b>5</b>
2.1 Heavy metals: definition and terminology .....	5
2.2 Metal homeostasis in higher plants: dealing with deficiency and toxicity .....	5
2.2.1 The physiological role of heavy metals in plants .....	6
2.2.2 Heavy metal toxicity .....	9
2.2.3 Heavy metal homeostasis and detoxification .....	11
2.3 Iron uptake in higher plants .....	17
2.4 Crosstalk between the Fe nutritional status and metal homeostasis of higher plants .....	20
2.5 The IREG gene family .....	21
2.6 Aims of the thesis .....	25
<b>3 Materials and Methods .....</b>	<b>28</b>
3.1 Yeast growth experiments .....	28
3.2 Transformation of Arabidopsis plants .....	28
3.3 Generation of plasmids and transgenic Arabidopsis lines .....	29
3.4 Isolation and complementation of Arabidopsis T-DNA insertion lines .....	30
3.5 Localization experiments .....	32
3.6 Plant culture and growth conditions .....	32
3.6.1 Arabidopsis plate experiments .....	32
3.6.2 Hydroponic culture .....	33
3.7 RNA gel blot analysis .....	34
3.8 Reverse transcription (RT)-PCR .....	34
3.9 Vacuole isolation from Arabidopsis leaves .....	35
3.10 Visualization of ROS (reactive oxygen species) formation in Arabidopsis .....	36

<b>4 Results</b> .....	<b>37</b>
<b>4.1 <i>In silico</i> analysis of the IREG gene family in Arabidopsis</b> .....	<b>37</b>
<b>4.2 AtIREG1</b> .....	<b>42</b>
4.2.1 Expression of <i>AtIREG1</i> .....	42
4.2.2 Characterization of the growth phenotype of <i>AtIREG1</i> overexpressing Arabidopsis lines ...	46
4.2.3 Characterization of the growth phenotype of <i>AtIREG1</i> T-DNA insertion lines .....	50
4.2.4 Localization of AtIREG1 proteins and <i>AtIREG1</i> expression in Arabidopsis .....	57
4.2.5 Influence of <i>AtIREG1</i> expression level on nickel and cobalt transport and distribution .....	60
<b>4.3 AtIREG2</b> .....	<b>69</b>
4.3.1 Yeast experiments .....	69
4.3.2 Expression of <i>AtIREG2</i> .....	70
4.3.3 Characterization of the growth phenotype of <i>AtIREG2</i> overexpressing Arabidopsis lines ...	71
4.3.4 Characterization of the growth phenotype of <i>AtIREG2</i> T-DNA insertion lines .....	73
4.3.5 Intracellular localization of AtIREG2 <i>in planta</i> .....	81
4.3.6 Influence of <i>AtIREG2</i> expression level on nickel transport and distribution <i>in planta</i> .....	83
<b>4.4 Assessment of a functional relationship between AtIREG1 and AtIREG2</b> .....	<b>87</b>
4.4.1 Comparative analysis of the phenotype of transgenic lines with altered expression of <i>AtIREG1</i> and <i>AtIREG2</i> .....	87
4.4.2 Characterization of the double T-DNA insertion line <i>ireg1ireg2</i> .....	89
4.4.3 Ni-induced ROS (reactive oxygen species) production in dependency of the <i>AtIREG1</i> and <i>AtIREG2</i> expression level .....	90
<b>4.5 AtIREG3</b> .....	<b>93</b>
<b>5 Discussion</b> .....	<b>95</b>
<b>5.1 <i>AtIREG2</i> encodes a tonoplast transport protein involved in nickel detoxification in <i>Arabidopsis thaliana</i> roots</b> .....	<b>95</b>
<b>5.2 <i>AtIREG1</i> encodes a plasma membrane protein involved in nickel and cobalt detoxification in <i>Arabidopsis thaliana</i></b> .....	<b>99</b>
<b>5.3 AtIREG1 and AtIREG2 share similar functions but different localization, substrate specificity and regulation</b> .....	<b>103</b>
<b>5.4 Preliminary characterization of AtIREG3</b> .....	<b>106</b>

5.5 The AtIREGs constitute a previously uncharacterized metal transporter gene family in Arabidopsis .....	107
6 References .....	113
7 Appendix .....	125
8 Acknowledgements .....	129
9 Curriculum vitae .....	131

# 1 Summary / Zusammenfassung

## 1.1 Summary

Essential transition metals are required in all plant cells for the activities of numerous metal-dependent enzymes and proteins, but can become toxic when present in excess. For the detoxification of heavy metals and to adjust to changes in micronutrient concentrations in the environment, plants possess a tightly controlled metal homeostasis network. In this regard, transition metal transporters are of central importance. Many metal transporters have already been identified, but a large number of candidates for heavy metal transport proteins still have to be analyzed at the biochemical level and within the plant metal homeostasis network. Based on the description of the animal IREG1 metal transporter as an iron exporter in vertebrates, a phylogenetic analysis of eukaryote and prokaryote sequences with similarity to IREG1 showed three homologous genes in Arabidopsis, which were named *AtIREG1*, *AtIREG2* and *AtIREG3*. As these *AtIREG* family members were candidates for yet uncharacterized metal transporters, the main objective of this thesis was to investigate the physiological function of this newly identified transporter family in plants.

In spite of the homology of *AtIREG1* and *AtIREG2* to vertebrate Fe exporters, heterologous expression in yeast and characterization of transgenic Arabidopsis lines did not indicate a Fe transport function of either transporter. Instead, *AtIREG2* could be described as a Ni transporter at the vacuolar membrane. A role in vacuolar Ni transport was supported by the localization of *AtIREG2*-GFP fusion proteins to the tonoplast in Arabidopsis suspension cells and root cells of intact plants. Transgenic plants overexpressing *AtIREG2* showed an increased Ni tolerance, whereas *AtIREG2* T-DNA insertion lines were more sensitive to toxic concentrations of Ni, particularly under Fe deficiency, and accumulated less Ni in roots. Furthermore, gene expression analysis allowed relating the function of *AtIREG2* to *AtIRT1*. As part of the Fe uptake system in root cells, *AtIRT1* can cause the accumulation of other transition metals especially in

Fe-deficient plants, due to its low metal specificity. As *AtIREG2* is co-regulated with *AtIRT1* by the transcription factor FIT, *AtIREG2* can counterbalance the low substrate specificity of *AtIRT1* by vacuolar loading of excess cytoplasmic Ni. Thus, *AtIREG2* may represent a novel component in the Fe-deficiency stress response.

Parallel analyses of *AtIREG1* also revealed a function in Ni detoxification, which is supported by an increased Ni tolerance of *AtIREG1* overexpressing lines, and a higher Ni sensitivity of T-DNA insertion lines lacking the expression of *AtIREG1*. Furthermore, an additive action of *AtIREG1* and *AtIREG2* in Ni detoxification is presented by the characterization of a double T-DNA insertion line that lacks the expression of both corresponding genes. This line was more sensitive to Ni and showed higher Ni-induced production of reactive oxygen species than either of the single T-DNA insertion lines. Despite of this functional similarity of *AtIREG1* and *AtIREG2*, *AtIREG1*-GFP fusion proteins localised to the plasma membrane in *Arabidopsis* protoplasts and thus revealed a different subcellular localization of both transporters. Ni-dependent urease activity was employed as a biochemical marker to assess a Ni export function of *AtIREG1* over the plasma membrane, showing that overexpression of *AtIREG1* decreased urease activity in root tissue, while a defective expression led to higher urease activity. In contrast to *AtIREG2*, *AtIREG1* also transported Co except Ni. *AtIREG1* was not under transcriptional control of FIT and was not upregulated in plants under Fe deficiency. A phenotypic analysis of *AtIREG1* T-DNA insertion lines revealed no Fe deficiency-dependent enhancement of the Ni-sensitive phenotype. Thus, *AtIREG1* is described as a transporter that functions in the detoxification of Ni and Co, irrespective of the Fe nutritional status of the plant.

A preliminary characterization of T-DNA insertion lines lacking the expression of *AtIREG3* did not provide hints for a metal transport function of *AtIREG3*.

## 1.2 Zusammenfassung

Essentielle Übergangsmetalle werden für die Aktivität zahlreicher metallabhängiger Enzyme und Proteine in allen pflanzlichen Zellen benötigt. Wenn sie im Überschuss vorhanden sind können diese Metalle jedoch toxisch wirken. Um Schwermetalle zu entgiften und um Veränderungen in Mikronährstoff-Konzentrationen in der Umwelt auszugleichen, besitzen Pflanzen ein streng kontrolliertes Homöostase-Netzwerk. In diesem Zusammenhang spielen besonders Metalltransporter eine wichtige Rolle. Viele Metalltransporter wurden bereits identifiziert, es gibt jedoch eine Reihe von Kandidaten für putative Metalltransport-Proteine, die noch auf biochemischer Ebene und innerhalb des pflanzlichen Metallhomöostase-Netzwerks analysiert werden müssen. Basierend auf der Entdeckung des tierischen IREG1 Metalltransporters, der in Vertebraten eine Funktion im Eisenexport besitzt, wurde eine phylogenetische Analyse eukaryotischer und prokaryotischer Sequenzen mit Ähnlichkeiten zu IREG1 durchgeführt. Dadurch konnten drei homologe Gene in *Arabidopsis* identifiziert werden, die daraufhin *AtIREG1*, *AtIREG2* und *AtIREG3* genannt wurden. Da diese Mitglieder der *AtIREG* Genfamilie Kandidaten für bisher uncharakterisierte Metalltransporter sind, war es das Hauptziel der vorliegenden Arbeit, die physiologische Funktion dieser neu identifizierten Transporterfamilie in Pflanzen zu untersuchen.

Trotz der Ähnlichkeit von *AtIREG1* und *AtIREG2* zu Eisenexportern von Wirbeltieren konnte durch heterologe Expression in Hefe und durch die Untersuchung transgener *Arabidopsis*-Linien keine Eisentransport-Funktion für *AtIREG1* oder *AtIREG2* nachgewiesen werden. Stattdessen konnte *AtIREG2* in der vorliegenden Arbeit als ein an der Vakuolenmembran lokalisierter Ni-Transporter beschrieben werden. Hinweise auf eine Rolle im vakuolären Substrattransport lieferte die Lokalisierung von *AtIREG2*-GFP Fusionsproteinen am Tonoplasten, sowohl in Protoplasten aus einer *Arabidopsis* Suspensions-Zellkultur als auch in Wurzelzellen intakter Pflanzen. Transgene Pflanzen in denen *AtIREG2* überexprimiert ist zeigten eine erhöhte Ni-Toleranz, während *AtIREG2* T-DNA-Insertionslinien, speziell unter Fe-Mangel-Bedingungen, empfindlicher gegenüber Ni waren und weniger Ni im Wurzelgewebe akkumulierten. Zusätzlich zeigte eine Genexpressions-Analyse einen Zusammenhang zwischen der Funktion von *AtIREG2* und *AtIRT1*. Als Teil des Eisenaufnahmesystems in Wurzelzellen von *Arabidopsis* kann *AtIRT1* die Akkumulation anderer

Übergangsmetalle verursachen, vor allem unter Eisenmangel-Bedingungen. Der Grund dafür ist die niedrige Substratspezifität von AtIRT1. *AtIREG2* wird, genauso wie *AtIRT1*, durch den Transkriptionsfaktor FIT reguliert und gleicht die niedrige Substratspezifität von AtIRT1 durch den Transport von überschüssigem cytoplasmatischem Ni in die Vakuole aus. AtIREG2 könnte daher eine neue Komponente in der Antwort von Pflanzen auf Eisenmangel-Stress darstellen.

Parallele Untersuchungen zeigten für AtIREG1 ebenfalls eine Funktion in der Entgiftung von Ni. Unterstützt wurde dieses Ergebnis durch die erhöhte Ni-Toleranz von *AtIREG1*-überexprimierenden Pflanzen, und einer höheren Sensitivität von T-DNA-Insertionslinien mit fehlender *AtIREG1* Genexpression gegenüber erhöhten externen Ni-Konzentrationen. Zusätzlich wird mit Hilfe der doppelten T-DNA Insertionslinie *ireglireg2*, in der weder AtIREG1 noch AtIREG2 exprimiert werden, gezeigt, dass die beiden Transporter eine additive Funktion in der Ni-Entgiftung haben. *Ireglireg2* Pflanzen waren sensitiver gegen Ni und zeigten eine höhere durch Ni induzierte Produktion von reaktiven Sauerstoffspezies als jede der beiden einzelnen T-DNA Insertionslinien. Trotz dieser funktionalen Ähnlichkeit zwischen AtIREG1 und AtIREG2 zeigte der Nachweis von AtIREG1-GFP Fusionsproteinen an der Plasmamembran eine unterschiedliche subzelluläre Lokalisation der beiden Transporter. Um für AtIREG1 eine Ni-Exportfunktion über die Plasmamembran nachzuweisen, wurde die Ni-abhängige Urease-Aktivität als ein biochemischer Marker verwendet. Diese Experimente zeigten, dass eine Überexpression von *AtIREG1* die Urease-Aktivität in Wurzeln verminderte, während eine verringerte Expression zu einer Erhöhung der Urease-Aktivität führte. Im Gegensatz zu AtIREG2 transportierte AtIREG1 außer Ni auch Co. Außerdem wurde *AtIREG1* auf transkriptioneller Ebene nicht durch FIT kontrolliert und zeigte keine erhöhte Expression in Eisenmangel-Pflanzen. Eine phänotypische Analyse von *AtIREG1* T-DNA-Insertionslinien ergab keine Hinweise auf eine eisenmangelabhängige Verstärkung des Ni-empfindlichen Phänotyps. Daher wird AtIREG1 als ein Transporter beschrieben, der eine Funktion in der Entgiftung von Ni und Co erfüllt, die unabhängig vom Fe-Ernährungszustand der Pflanze ist.

Eine vorläufige Untersuchung von T-DNA-Insertionslinien mit fehlender Expression von AtIREG3 ergab keinen Hinweis auf eine Metalltransport-Funktion von AtIREG3.

## 2 Introduction

### 2.1 Heavy metals: definition and terminology

The term “heavy metal” is only loosely defined, leading to many different definitions based on density, atomic number, atomic weight or sometimes even on chemical properties or toxicity. In an IUPAC technical report on the different definitions given for heavy metals, the author found at least 38 different definitions and therefore calls the term *heavy metal* “meaningless and misleading”, due to the lack of a “coherent scientific basis” (Duffus, 2007). In this thesis I will refer to heavy metals as elements with a density higher than 5 g/cm<sup>3</sup>, following the definition given in numerous scientific books (e. g. Wiberg, 1985). Following this definition, the group of heavy metals includes - amongst others - zinc (Zn, with a density of 7.14 g/cm<sup>3</sup>), manganese (Mn, 7.47 g/cm<sup>3</sup>), iron (Fe, 7.87 g/cm<sup>3</sup>), cadmium (Cd, 8.65 g/cm<sup>3</sup>), cobalt (Co, 8.90 g/cm<sup>3</sup>), nickel (Ni, 8.91 g/cm<sup>3</sup>), copper (Cu, 8.92 g/cm<sup>3</sup>), molybdenum (Mo, 10.28 g/cm<sup>3</sup>), lead (Pb, 11.34 g/cm<sup>3</sup>) and mercury (Hg, 13.55 g/cm<sup>3</sup>).

### 2.2 Metal homeostasis in higher plants: dealing with deficiency and toxicity

Some non-essential heavy metals like Cd, Pb or Hg are toxic to plants and disturb the plant metabolism already in very low concentrations, leading to reduced plant growth, lower yield and toxicity symptoms. Many other heavy metals like Cu, Zn, Ni, Mn and Fe are essential for plants, acting especially as structural or functional cofactors in proteins, although these essential metals can also cause toxic effects similar to those of toxic metals, if present in excess. Therefore, metal uptake and efflux at the cellular level has to be finely regulated, to maintain certain metal concentrations within the cell or within cellular compartments. The cellular metal homeostasis must be coordinated with the needs of the whole plant. As sessile organisms, which depend strongly on the metal availability in the surrounding soil, plants have developed different strategies to take up essential metals from soil (Marschner, 1995) while preventing toxicity. This requires the coordination of metal uptake with detoxification and storage of metals, including

mechanisms to regulate the solubilization, short- and long-distance transport, chelation, remobilization, subcellular compartmentalization and partitioning to plant organs and to different tissues or cell types.

## **2.2.1 The physiological role of heavy metals in plants**

### **Essential heavy metals in plants**

Plants require a range of mineral nutrients for normal growth and development, also including several heavy metals. Until the year 1920, only 14 elements had been identified as essential. Carbon (C), hydrogen (H), and oxygen (O) had long been known to be major components of carbohydrates and to be required for photosynthesis. Nitrogen (N), phosphorus (P), and potassium (K) were referred to as the primary elements, while calcium (Ca), magnesium (Mg) and sulphur (S) were described as secondary elements. Other elements, called trace or minor elements, included iron (Fe), zinc (Zn), manganese (Mn), copper (Cu) and boron (B). In the 1950s, chlorine (Cl) and molybdenum (Mo) were added to the list of the essential elements. In 1966, silicon (Si), sodium (Na), vanadium (V) and cobalt (Co) were identified as beneficial elements. In 1987, it was shown that nickel (Ni) is also an essential element, and Ni was included in the list (Brown et al, 1987).

Today, most scientists recognize 17 elements as being essential to plants, with another four (V, Co, Si, Na) on the list of beneficial elements. Six of these essential elements are heavy metals, namely Mn, Mo, Zn, Cu, Fe and Ni. When any of these metals are short of supply, a range of deficiency symptoms can appear and growth is reduced (Marschner, 1995).

### **The physiological function of heavy metals in plants**

Essential metals have been acquired during evolution due to their chemical properties, e. g. the redox-activity of Fe and Cu which is fundamental to cellular function, or the Lewis acid strength of Zn (Frausto da Silva and Williams, 2001). This is why about one third of all structurally characterized proteins are metalloproteins (Finney and O'Halloran, 2003).

Heavy metals serve for a range of essential functions in plant. **Manganese**, for example, plays an important role in photosynthesis, where a cluster of Mn atoms forms the catalytic centre for light-induced water oxidation in PS II (photosystem II). Mn is also required as a cofactor in various enzymes, such as the  $\text{Mn}^{2+}$ -dependent superoxide dismutase (MnSOD) (Marschner, 1995, for a review see Pittman, 2005). **Molybdenum** forms together with a pterin compound the molybdenum cofactor (Moco), which is the active site of eukaryotic Mo enzymes. There are four plant enzymes that depend on Mo: nitrate reductase catalyzes the first step in nitrate assimilation, peroxisomal sulfite oxidase detoxifies sulfite, aldehyde oxidase catalyzes the last step of abscisic acid biosynthesis and xanthine dehydrogenase is essential for purine degradation and stress response (Schwarz and Mendel, 2006). **Zinc**, as a third example of essential elements, plays a special role in plants, as  $\text{Zn}^{2+}$  has pronounced Lewis acid characteristics because of its small radius-to-charge ratio, and thus forms strong covalent bonds with S, N and O donors, making it an essential component in thousands of plant proteins (Frausto da Silva and Williams, 2001). As Zn only appears as a divalent cation ( $\text{Zn}^{2+}$ ) in biological systems, it does not participate in redox reactions and does not induce the formation of radicals. Therefore Zn is a structural element in numerous proteins (e. g. zinc finger proteins) or a catalytic element in many hydrolyzing enzymes (Frausto da Silva and Williams, 2001). **Copper** belongs, in contrast to Zn, to the redox active transition metals. Due to its two oxidation states Cu(I) and Cu(II) it is often involved in electron transfer reactions, making it essential for photosynthesis and respiration e. g. in enzymes like plastocyanin and cytochrome c oxidase (Frausto da Silva and Williams, 2001). **Iron** is required for several life-sustaining processes in plants. Similar to Cu, Fe is highly redox active, making it important for different electron transfer processes through its cycling between  $\text{Fe}^{2+}$  and  $\text{Fe}^{3+}$ . Iron is a component of haem proteins (e. g. cytochromes, catalase, and Fe-S proteins such as ferredoxin) and a range of other enzymes, and is essential for chlorophyll production (reviewed in Kim and Guerinot, 2007).

**Nickel** is the most recent candidate that won the status as an essential trace element for plants according to the Agricultural Research Service Plant, Soil and Nutrition in Ithaca (Brown et al., 1987). Nickel is considered as an essential plant nutrient primarily due to

its function as an irreplaceable component of the urea hydrolyzing enzyme urease (Gerendás et al., 1999). The involvement in urea breakdown is the only proven nutritional function of Ni in higher plants. Urease is the only Ni-dependent metalloenzyme identified yet in plants, whereas in bacteria there are several reports on additional Ni-dependent enzymes, like different hydrogenases or methyl coenzyme M reductase (Walsh and Orme-Johnson, 1987). Urease catalyzes the hydrolysis of urea to ammonia and carbon dioxide (Dixon et al., 1975). Thus, the primary role of the plant urease is to allow the use of external or internally generated urea as a nitrogen (N) source (Sirko and Brodzik, 2000). Urea N can be assimilated exclusively by urease in higher plants, the released ammonia is then incorporated into organic compounds mainly by glutamine synthetase. Therefore, the addition of Ni to Murashige and Skoog medium in plant tissue culture was reported to activate the urease activity and to reduce metabolic stress (Witte et al, 2002a).

**Cobalt** is not considered as essential but is beneficial for plants. The term essential mineral element (or mineral nutrient) was proposed by Arnon and Stout (1939). They concluded that certain criteria must be fulfilled for an element to be considered essential, including: 1. A plant must be unable to complete its life cycle in the absence of the mineral element. 2. The function of the element must not be replaceable by another mineral element. Therefore, beneficial elements are those that can compensate for toxic effects of other elements or may replace other mineral nutrients in some cases, for example when the essential nutrient is not available to the plant. Cobalt is considered as being beneficial for plants, because it is required by bacteria for symbiotic nitrogen fixation in legumes (Reisenauer, 1960; Gad, 2006; Delwiche et al., 1961) and in root nodules of nonlegumes (Hallsworth et al., 1965). For certain nonlegumes like *Alnus* and *Myrica*, cobalt is essential when they are nodulated, and if no Cobalt is supplied the plants develop symptoms of nitrogen deficiency, whereas no cobalt requirement was detected in non-nodulated plants (Hewitt and Bond, 1966). Co also has protective effects under conditions of osmotic stress (Li et al., 2005). Bacteria, fungi and algae contain a number of Co-dependent metalloenzymes. For example, methionine aminopeptidase, the enzyme that cleaves the N-terminal methionine from newly translated polypeptides, is Co dependent in animals, yeast and bacteria

(Kobayashi and Shimizu, 1999), but by now there is no known essential function for Co in plants.

### 2.2.2 Heavy metal toxicity

Over the past 200 years emissions of toxic heavy metals have risen tremendously and significantly exceed those from natural sources for practically all metals. Heavy metal contamination of soil results from anthropogenic as well as natural activities. Anthropogenic activities such as mining, manufacturing, smelting operation, municipal waste disposal and fertilization have locally increased the levels of heavy metals in soils up to dangerous levels (Sharma and Agrawal, 2005).

The same above mentioned properties (redox-activity, Lewis acid strength) that make heavy metal ions essential for many biological reactions are also a reason why they can easily be toxic when present in excess. There are three different molecular modes of heavy metal toxicity: (1) Redox-active metal ions in plants can participate in Haber–Weiss and Fenton reactions and thereby trigger the formation of reactive oxygen species (Halliwell and Gutteridge, 1986; 1990; reviewed in Clemens, 2006), (2) uncontrolled high affinity binding to sulphur-, nitrogen- and oxygen-containing functional groups in biological molecules can cause their inactivation or damage (Chrestensen et al., 2000) and (3) heavy metals can displace essential elements from biomolecules, for example the exchange of essential metal ions from the active centres of enzymes (El-Jaoual and Cox, 1998). Point (1) is of special interest for the presented work and will be explained in more detail in the following paragraph.

The induction of the production of ROS (reactive oxygen species) by heavy metals was first described for Fe and later also for other metals, including Cu, Mn, Mo and Ni (Halliwell and Gutteridge, 1986; 1990; Stohs and Bagchi, 1995). The formation of ROS by Fe in the Haber-Weiss cycle and the Fenton reaction was first characterized by Fenton, 1984. Due to the ability of Fe and other metals to readily change their redox state, they can react with O<sub>2</sub> or incompletely reduced oxygen species (such as hydrogen peroxide), leading to the formation of hydroxyl radicals (Cadenas, 1989), which can react with almost all cellular molecules, including DNA, proteins and lipids. Hydroxyl radicals can initiate lipid oxidation, in which firstly a fatty acid radical is formed, which

reacts readily with molecular oxygen, thereby propagating the formation of additional radicals. This leads to an autocatalytic chain reaction in lipid peroxidation, which induces lasting changes in the composition and the integrity of plant membranes, including the plasma membrane and chloroplastic membranes (Ouariti et al., 1997; Schützendübel and Polle, 2002).

Whilst Fe, Cu, Cr, V and Co undergo redox-cycling reactions, for a second group of metals, namely Hg, Cd and Ni, the primary route for their toxicity is depletion of glutathione and bonding to sulfhydryl groups of proteins. The unifying factor for all these metals is the generation of reactive oxygen and nitrogen species. Ni compounds, for example, have been shown to produce ROS through the interactions of Ni ions with protein ligands, such as the imidazole nitrogen of histidine in mammalian cells (Datta et al., 1992). The treatment of rats with Ni results in enhanced lipid peroxidation, decreased glutathione peroxidase activity and increased tissue Fe levels, due to Ni-mediated production of hydroxyl radicals (Athar et al., 1987). It was also shown that in mammalian cell cultures the incubation with soluble Ni salts resulted in an increased oxidant concentration, shown as oxidation of DCFH (2,7-dichlorofluorescein diacetate, a non-fluorescent parent molecule) to DCF (dichlorofluorescein), a fluorescent oxidized product (Huang et al., 1993). Also in higher plants, increased concentrations of metals lead to the production of reactive oxygen species (Baccouch et al., 1998; Briat and Lebrun, 1999; Dat et al., 2000; Noctor and Foyer, 1998; Schützendübel and Polle, 2002). In plants reduced glutathione (GSH) acts as a strong antioxidant that can directly reduce some ROS (Noctor and Foyer, 1998). Total glutathione accumulation also correlates with increased plant tolerance to Ni and with increased resistance to Ni-induced accumulation of ROS in root tips of *Arabidopsis thaliana* (Freeman et al., 2004). The Ni hyperaccumulator *Thlaspi goesingense* is tolerant to Ni, Zn and Co, due to elevated shoot GSH levels. These multiple metal tolerances are mimicked in *Arabidopsis* through heterologous expression of the *Thlaspi goesingense* mitochondrial serine acetyltransferase (TgSATm) which results in elevated GSH accumulation in leaves and enhanced oxidative stress resistance (Freeman et al., 2007). Ni toxicity is of concern for plant grown in soils receiving sewage sludge or industrial byproducts. Ni as well as Co toxicity may also be found in plants grown in soils formed from serpentinite or other ultrabasic rocks (McBride, 1994).

The consequences of unbalanced metal concentrations within plant cells can be severe. Antioxidants (both enzymatic and nonenzymatic) provide protection against metal-mediated free radical attacks. But mechanisms for cellular tolerance to heavy metals appear to be involved primarily in avoiding the build-up of toxic concentrations at sensitive sites within the cell, rather than in radical scavenging or in the development of less sensitive proteins. To avoid an increased production of heavy metal-mediated ROS, plants have developed a range of mechanisms to avoid the accumulation of toxic metal concentrations in the cytoplasm. All plants including *A. thaliana* possess a basic metal tolerance, allowing the adjustment of metal homeostasis to fluctuations in soil metal concentrations and cellular metal influx rates within narrow concentration ranges (Clemens, 2001; Clemens et al., 2002).

### 2.2.3 Heavy metal homeostasis and detoxification

As the physiological range for essential metals, within which plants are unaffected by deficiency or toxicity, is extremely narrow, plants had to develop a tightly controlled metal homeostasis network to adjust to changes in micronutrient concentrations, and also had to develop mechanism for detoxification of heavy metals. These mechanisms include the immobilization of metals in the apoplast, chelation of heavy metals, transport of metals or metal-chelates out of the cell and intracellular sequestration. Additionally, mycorrhizas and particularly ectomycorrhizas that are characteristics of trees and shrubs can be effective in ameliorating the effects of metal toxicity on the host plant (Marschner, 1995; Hartley et al., 1997; reviewed in Hall, 2002). Of particular interest for heavy metal tolerance and homeostasis are transporters for metals or metal-chelates. Compared to other organisms, plants have expanded families of transporters that are involved in the uptake and efflux of metals. The application of genetic and molecular techniques has now identified a range of families of metal transporters that vary in their substrate specificities, expression patterns, and cellular localization to govern metal translocation throughout the plant. These include the heavy metal (or P<sub>1B</sub>-type) ATPases, the natural resistance-associated macrophage proteins (Nramps), the cation diffusion facilitators (CDFs), the ZIP family proteins and others (Hall and Williams, 2003). Some of these transporter gene families are large and comprise several genes. For example, in *Arabidopsis* there are eight P<sub>1B</sub>-ATPases (Mills et al., 2003), six

members of the Nramp family (Williams et al., 2000) and 15 ZIP family transporters (Mäser et al., 2001).

**Heavy metal ATPase family (HMAs):** The superfamily of P-type ATPases use energy from ATP hydrolysis to translocate cations across biological membranes and can be divided into several subfamilies, including the heavy-metal-transporting P<sub>1B</sub>-ATPases, sometimes also referred to as CP<sub>X</sub>-ATPases, due to a conserved intramembranous cysteine-proline-cysteine/histidine/serine sequence that is thought to play a role in translocation (Axelsen and Palmgren, 2001; Williams and Mills, 2005). Phylogenetically, the P<sub>1B</sub>-type ATPases comprise two main groups which seem to correlate with transport specificity either for monovalent cations (Cu<sup>+</sup> or Ag<sup>+</sup>) or the divalent Zn<sup>2+</sup>, Co<sup>2+</sup>, Cd<sup>2+</sup>, Pb<sup>2+</sup> cations (Solioz and Odermatt, 1995; Axelsen and Palmgren, 2001; Mills et al., 2003). From the eight Arabidopsis HMAs, four (HMA1-4) group with the divalent cation transporter class, whereas HMA5-8 encode Cu/Ag monovalent cation transporters (Williams and Mills, 2005; Cobbett et al., 2003). In the last few years functions could be assigned to several members of the HMAs: AtHMA2 and AtHMA4 function in Zn homeostasis and are involved in Zn translocation from root to shoot, possibly by loading of Zn to the xylem (Eren and Argüello, 2004; Hussain et al., 2004; Mills et al., 2005). AtHMA5 was characterized as a root-expressed, Cu-induced transporter and is involved in Cu detoxification in roots in response to high Cu supply (Andres-Colas et al., 2006). Three P<sub>1B</sub>-ATPases are involved in Cu transport in the chloroplast: AtHMA1, AtHMA6 and AtHMA8. HMA1 and HMA6 (PAA1) play a role in Cu transfer across the chloroplast envelope to the stroma (Seigneurin-Berny et al., 2005; Shikanai et al., 2003; Abdel-Ghany et al., 2005) and HMA8 (PAA2) is localized at the thylakoid membrane and delivers Cu to the thylakoid lumen (Shikanai et al., 2003; Abdel-Ghany et al., 2005). AtHMA7 (RAN1) is thought to deliver Cu<sup>+</sup> across post-Golgi membranes to create functional ethylene receptors (Hirayama et al., 1999; Woeste and Kieber, 2000).

**The natural resistance-associated macrophage family (Nramps):** The mammalian Nramp1 was the first gene of this family to be identified. It is found on the endosomal compartment of macrophages, where it determines the sensitivity to bacterial infection

by controlling divalent cation concentrations (namely Fe and Mn) within this compartment (Govoni and Gros, 1998). The mammalian transporter Nramp2 (DCT1, DMT1) functions in the uptake of dietary Fe (Gunshin et al., 1997) and will be further described in chapter 1.5 of this work. Subsequently, homologues of the mammalian Nramps in plants were shown to be capable of divalent cation transport, including Fe (Bereczky et al., 2003; Kaiser et al., 2003). In Arabidopsis the Nramp family comprises six members, which appear to cluster into two sub-families: one includes AtNramps 1 and 6 and the other Nramps 2-5 (Thomine et al., 2000; Mäser et al., 2001). AtNramp1 is able to functionally complement a yeast mutant defective in Fe uptake and overexpression of AtNramp1 in Arabidopsis increases the resistance to toxic Fe levels. This implies the function of AtNramp1 in the control of Fe homeostasis in plants (Curie et al., 2000). AtNramp3 and 4 are closely related, and have a similar tissue-specific expression, regulation by Fe and localize both to the vacuolar membrane, where they function redundantly in the mobilization of Fe from the vacuole, especially during seedling development (Lanquar et al., 2005; Thomine et al., 2003)

**The cation diffusion facilitator family (CDFs):** Members of this family were first identified in bacteria, but can also be found in archaea and eukaryotes, where they encode proton antiporters that efflux heavy metals like Zn, Co or Cd out of the cytoplasm (Paulsen and Saier, 1997; Eide, 1998; Gaither and Eide, 2001). Some of the best characterised members of this family are the ZnT zinc efflux transporters of human and rodents, but in the last few years two Arabidopsis CDFs have been identified and studied. The first member of the CDF family characterized in Arabidopsis was ZAT1 (zinc transporter gene 1), later renamed MTP1 (metal tolerance protein 1) (Delhaize et al., 2003). Overexpression of MTP1 confers Zn tolerance in Arabidopsis (van der Zaal et al., 1999), whereas plants lacking the expression of MTP1 are more sensitive to Zn, due to a function of MTP1 in sequestration of Zn to the vacuole (Kobae et al., 2004; Desbrosses-Fonrouge et al., 2005). Another member of the CDF family in Arabidopsis, AtMTP3, contributes to basic cellular Zn tolerance and controls Zn partitioning, particularly under conditions of high rates of Zn influx into the root symplasm, for example at conditions of Zn oversupply or Fe deficiency (Arrivault et al., 2006). Members of the CDF family are also supposed to be involved in the hyperaccumulation

of metals in species like *Arabidopsis halleri*, a Zn/Cd hyperaccumulator. *A. halleri* contains three MTP1 genes, two MTP1 loci co-segregate with Zn tolerance (Drager et al., 2004). Cross-species microarray revealed an increased expression of MTP1 in shoots of *Arabidopsis halleri* (Becher et al., 2004). Enhanced expression of CDF transporters also determines the metal tolerance of the Ni/Zn hyperaccumulator *Thlaspi goesingense* (Persans et al., 2001). The *T. goesingense* TgMTP1 functions as a Zn exporter at the plasma membrane (Kim et al., 2004). The CDF transporter ShMTP1 of the tropical legume *Stylosanthes hamata* confers Mn<sup>2+</sup> tolerance when expressed in yeast and Arabidopsis (Delhaize et al., 2003).

**The ZIP (ZRT, IRT-like protein) family:** The first member of this family to be identified was IRT1 (iron-regulated transporter 1) in *Arabidopsis*, an iron exporter that is expressed in the roots of Fe deficient plants (Eide et al., 1996). IRT1 is now thought to be the major transporter for high affinity Fe uptake by roots (Connolly et al., 2002; Vert et al., 2002) and will be described in detail in chapter 1.3 of this thesis. Homologues of IRT1, the transporters ZRT1 and ZRT2 (zinc regulated transporter) in yeast, mediate high- (ZRT1) and low- (ZRT2) affinity Zn uptake in *Saccharomyces cerevisiae* (Zhao et al., 1996a, 1996b). Based on these members, the gene family was named ZRT, IRT-like protein (ZIP) family (Eng et al., 1998). By now, more than 100 ZIP homologues have been identified in bacteria, fungi, animals and plants (reviewed in Guerinot, 2000), including 15 genes in Arabidopsis (Mäser et al., 2001). Based on homologies to the yeast *ZRT1* and *ZRT2* genes, three homologous Zn transporter genes from Arabidopsis, the *ZIP1*, *ZIP2* and *ZIP3* genes, were identified. Expression of these closely related genes in yeast confers zinc uptake activities (Grotz et al., 1998). A homologue of the Fe uptake transporter AtIRT1, AtIRT2 (another member of the ZIP-family) is also expressed in root epidermal cells under Fe deficiency and shows Fe and Zn uptake capacity, but cannot substitute for a loss of IRT1 (Vert et al., 2001; Grotz and Guerinot, 2002). A ZIP gene homologue, TcZNT1, from the Zn/Cd-hyperaccumulating plant *Thlaspi caerulescens* was shown to mediate high-affinity Zn uptake and low-affinity Cd uptake when expressed in yeast (Pence et al., 2000). A member of the ZIP family, GmZIP1, has now been identified in soybean (Moreau et al., 2002). By functional complementation of *zrt1 zrt2* yeast cells, GmZIP1 was found to be highly

selective for Zn, while yeast Zn uptake was inhibited by Cd. GmZIP1 was specifically expressed in the nodules and not in roots, stems or leaves, and the protein was localized to the peribacteroid membrane, indicating a possible role in the symbiosis (Moreau et al., 2002; reviewed in Hall and Williams, 2003).

**Other metal transporters:** There is a range of other families of transporters, that also exhibit metal transport activities. For example, members of the YSL family that mediate uptake of metals that are complexed with plant-derived phytosiderophores or nicotianamine, a non-proteinogenic amino acid that serves as a precursor for phytosiderophore synthesis in grasses (Curie et al., 2001), are important for the strategy II Fe uptake. Another protein family that is involved in metal transport, the COPT family of *Arabidopsis*, includes five members (Sancenon et al., 2003), but to date only COPT1 has been characterized in detail. COPT1 is a putative  $\text{Cu}^{2+}$  influx transporter and seems to play a role in Cu transport in pollen and root tips, thereby influencing plant growth and development (Sancenon et al., 2004). The plant tonoplast also contains a number of cation/ $\text{H}^+$ -antiporters. Those involved in the regulation of cytosolic  $\text{Ca}^{2+}$  and  $\text{Na}^+$  concentrations by transport into the vacuole are particularly well characterized (Hirschi, 2001; Maeshima, 2001; Gaxiola et al., 2002), for example the *Arabidopsis thaliana* cation exchangers, CAX1 and CAX2, can both transport  $\text{Ca}^{2+}$  into the vacuole. CAX2 additionally also functions in vacuolar Mn transport (Shigaki et al., 2003), which led to the speculation that other cation/proton antiporters could also be involved in metal homeostasis. A relatively newly identified family of multidrug resistance efflux transporters was named MATE (multidrug and toxic compound extrusion) family and contains at least 56 members in *Arabidopsis* (Li et al., 2002). AtDTX1 (*Arabidopsis thaliana* detoxification 1) is a member of the MATE family and serves as a carrier for a range of toxic compounds and is also capable of the detoxification of  $\text{Cd}^{2+}$  (Li et al., 2002). Another member of this family, FRD3 (ferric reductase defective 3), is thought to have an important role in Fe homeostasis in *Arabidopsis*, although it does not transport Fe directly but mediates the efflux of citrate to the vasculature, thereby being necessary for the efficient translocation of Fe (Rogers and Guerinot, 2002; Durrett et al., 2007). In sorghum, a gene of the MATE family confers aluminium tolerance (Magalhaes et al., 2007).

These data show that by now a wide range of metal transporters has been identified. This is not surprising, because metal uptake, partitioning to certain plant organs and cell types, and metal delivery to metal-requiring proteins in different subcellular localizations, as well as metal storage and remobilization all require the function of metal transporters (Clemens et al., 2002; Krämer et al., 2007). It is striking, that most of the plant gene families are large in comparison to those in other organisms. For example, *Arabidopsis* has six Nramps, but there are only three in yeast and two in mice and humans. Most organisms have only one or two heavy metal ATPases, whereas in *Arabidopsis* there are eight members of this family. Compared to the 15 different ZIP family transporters in *Arabidopsis*, there are only three in yeast. Most metals appear to be substrate for different transporters of the same or different families, and some of the mentioned metal transporters transport more than just one substrate. Some of these genes may be functionally redundant, but the diversity is likely to be required for different reasons: plants need high- and low-affinity transport systems with different substrate specificities to cope with the strongly varying and sometimes rapidly changing metal availability in the soil; homologous transporters could have different subcellular or tissue specific localization, or could be differentially regulated to mediate the adaptation to different stress conditions (Colangelo et al., 2006).

All of the mentioned metal transporting proteins are involved in general homeostasis of metals; some of them could function especially in the cellular tolerance to or detoxification of heavy metals. Roles of heavy metal transporters in detoxification could involve the efflux of metals out of the cell or sequestration to less sensitive compartments like the vacuole. These detoxification mechanisms will be discussed in chapter 5.3 and 5.5. Just recently it was shown that the *Arabidopsis* metal tolerance protein AtMTP3 leads to tolerance to high Zn and Co, when expressed in yeast. *In planta* it seems that AtMTP3 functions in the sequestration of Zn to vacuoles, thereby functioning in the detoxification of Zn under high Zn supply or Fe deficiency (Arrivault et al., 2006). The expression of AtMTP3 is upregulated under Fe-deficient conditions, which shows that there is a crosstalk between Fe and the metal homeostasis in plants. The need to detoxify metals is closely linked to the iron nutritional status and the iron uptake mechanism of plants, which will be discussed in the next two chapters.

## 2.3 Iron uptake in higher plants

Like described previously in this thesis, Fe is an essential nutrient, but can also be toxic in high concentrations: Fe is essential for cellular redox reactions due to its ability to undergo reversible valence changes from  $\text{Fe}^{2+}$  to  $\text{Fe}^{3+}$ . Fe is, for example, required for electron transport processes during respiration and photosynthesis. Based on its high redox reactivity, free cellular Fe can generate hydroxyl radicals in the Fenton reaction. To find the balance between Fe requirement and toxicity, the uptake and distribution of Fe is strictly controlled and highly regulated in all organisms. Fe deficiency poses an agricultural challenge because Fe is one of the nutrients that most often limit plant growth. Fe deficiency leads to symptoms such as interveinal chlorosis in leaves and reduction of crop yields. For optimal growth, plants need to be supplied with Fe in a concentration range between  $10^{-9}$  and  $10^{-4}$  M (Marschner, 1995). Fe is the fourth most abundant element in the earth's crust, but is not readily available to plants. Therefore, Fe deficiency is often caused by the extreme insolubility of  $\text{Fe}^{3+}$  in the soil solution, rather than low amounts of Fe in the soil, especially on calcareous and alkaline soils (Guerinot and Yi, 1994). Thus, Fe deficiency is one of the most widespread nutrient imbalances in agriculture. Plants had to develop Fe acquisition strategies, which allow different plants to cope with the range of Fe availabilities and oxidation states characteristic of their habitats. Therefore, plant strategies to cope with Fe deficiency aim at solubilising  $\text{Fe}^{3+}$  in the rhizosphere to facilitate its uptake by the plant roots.

Plants overcome Fe-deficient growth conditions in one of two ways: Non-grasses activate reduction-based mechanisms (strategy I) when starved for Fe whereas the grasses activate a chelation-based strategy (strategy II). The strategy II response of grasses (Takagi et al., 1984) as well as that of certain species of bacteria and fungi (Guerinot, 1994) relies on the chelation of  $\text{Fe}^{3+}$  by phytosiderophores that are released into the soil. The  $\text{Fe}^{3+}$  complexes are subsequently taken up by specific transporters.

### A closer look on strategy I iron uptake

Dicotyledonous and non-graminaceous plants, including *Arabidopsis thaliana*, use the strategy I response, which consists of the induction of three physiological activities under low Fe conditions (Römheld, 1987): (a) Lowering the pH in the soil solution by

proton release, (b) reduction of ferric to ferrous iron and (c) subsequent uptake of  $\text{Fe}^{2+}$ . Under Fe deficient conditions, strategy I plants extrude protons into the rhizosphere through activation of a specific plasma membrane  $\text{H}^+$ -ATPase in rhizodermal cells. Consequently, Fe solubility increases due to the acidification of the soil solution. In general,  $\text{Fe}^{3+}$  solubility is increased 1000-fold with every unit that the pH is lowered (Olsen et al., 1981). The responsible  $\text{H}^+$ -ATPases are not identified yet, but proton-ATPases of the AHA family (Arabidopsis  $\text{H}^+$ -ATPase) are probably involved in this process, because the expression of certain AHA homologs is upregulated under Fe deficient conditions (Fox and Guerinot, 1998; Waters et al., 2007). Before uptake of Fe, a reduction of  $\text{Fe}^{3+}$  to the more soluble  $\text{Fe}^{2+}$  has to take place. This reduction step was shown to be the limiting step for Fe uptake from soil (Yi and Guerinot, 1996). Fe(III) chelate reductase activity is one of the best studied plasma membrane activities (Moog and Brüggemann, 1994). Root Fe reductase activity can be visualised using strong Fe chelators like BPDS (Bathophenanthroline disulfonate) or ferrozine. These chelators form stable coloured complexes upon binding of reduced ferrous Fe. This colour reaction was used for a forward genetic screen to identify *Arabidopsis* mutants lacking Fe reductase activity (Yi and Guerinot, 1996). The Arabidopsis mutant *frd1* (ferric chelate reductase defective 1) shows no induction of Fe(III) chelate reductase under Fe-deficient conditions and develops severe chlorosis when Fe is limiting (Yi and Guerinot, 1996). The corresponding gene in Arabidopsis, *FRO2*, was first identified based on sequence similarities to human gp91phox (respiratory burst oxidase) and to a yeast Fe(III) chelate reductase. *FRO2* mapped to the same locus as *frd1* and can restore the Fe(III) chelate reductase activity in the *frd1* mutant lines (Robinson et al., 1999; Connolly et al., 2003). *FRO2* is thought to be the main Fe(III) chelate reductase in roots, because it is expressed in epidermal root cells and is upregulated under Fe deficient conditions (Robinson et al., 1999). The *FRO2* gene belongs to a five-member gene family in *Arabidopsis*, the other members of this family are expressed in other tissues than roots (including shoots, flowers, cotyledons and leaf veins), indicating that reduction is also required for the Fe distribution throughout the plant (Wu et al., 2005; Mukherjee et al., 2006). Subsequent to the reduction of ferric to ferrous Fe, free  $\text{Fe}^{2+}$  is taken up by the plant roots by IRT1, a member of the ZIP (ZRT, IRT-like proteins) metal transporter family (further discussed in chapter 1.2.3). The Arabidopsis *IRT1* gene

was cloned by functional complementation of the *fet3fet4* mutant of yeast, a strain that is defective in high- and low-affinity Fe uptake. AtIRT1 is expressed in roots and flowers of Arabidopsis and localizes to the plasma membrane of epidermal root cells (Eide et al., 1996). The Arabidopsis *irt1* mutant exhibits chlorosis and severely impaired growth, unless supplied with high levels of soluble Fe (Vert et al., 2002; Varotto et al., 2002; Henriques et al., 2002). These data clearly demonstrate that IRT1 is the major transporter for high affinity uptake of Fe under Fe deficiency.

The strategy I Fe mobilization responses, including the ferric reductase activity and the Fe uptake, are induced by Fe deficiency. The tomato basic helix-loop-helix transcription factor FER is required for the induction of genes for Fe acquisition under Fe-deficient conditions (Ling et al., 2002; Brumbarova and Bauer, 2005). In Arabidopsis, an ortholog of *LeFER* has been described as a potential Fe-regulated transcription factor gene: The Arabidopsis *FER* homologue *FIT* (previously also named FRU or FIT1) is expressed in the outer cell layers of the roots, like *FRO2* and *IRT1*, and is upregulated under low Fe. The *FIT* gene was found to be necessary for induction of *FRO2* and *IRT1*, showing that FIT is the major regulator for the Fe-deficiency stress response in Arabidopsis (Jakoby et al., 2004). The Arabidopsis H<sup>+</sup>-ATPase gene *AHA7* is also upregulated in response to Fe deficiency and its expression is dependent on *FIT*, implicating that *AHA7* is also a part of the Fe-deficiency response, probably as a proton pump to acidify the soil during conditions of low Fe supply (Colangelo and Guerinot, 2004).

In recent studies, group-Ib bHLH genes were reported to be Fe-deficiency regulated. Four basic helix-loop-helix genes (*bHLH038*, *bHLH039*, *bHLH100* and *bHLH101*) were upregulated by Fe deficiency in roots and leaves of Arabidopsis plants. Induction of the four *bHLH Ib* genes was also found in multiple iron acquisition mutants including *fit* (Wang et al., 2007). Two of these genes (*AtbHLH38* and *AtbHLH39*) interact with FIT in the regulation of the Fe uptake gene expression, and the transcription of *FRO2* and *IRT1* is directly regulated by a complex of FIT/*AtbHLH38* or *AtbHLH39* (Yuan et al., 2008).

The process of Fe acquisition has long been known to lead to an enrichment of other metals in the plant tissue. Therefore, in the next chapter the crosstalk between Fe uptake and heavy metal homeostasis in plants will be further discussed.

## 2.4 Crosstalk between the iron nutritional status and metal homeostasis of higher plants

The upregulation of the Fe uptake system under Fe deficient conditions does not only lead to an increase in Fe uptake capacity of plant roots, but can also cause problems due to an accompanying uptake and increasing tissue concentrations of other metals besides Fe. In pea seedlings grown under Fe-deficient conditions the concentration of many divalent cations including Cu, Mn and Mg increased (Welch et al., 1993) and Cd influx into root cells was enhanced (Cohen et al., 1998). Although IRT1 was originally identified as a Fe transporter and was proven to represent the main Fe<sup>2+</sup> uptake system in strategy I plants, we now know that IRT1 is also able to transport other metals besides Fe. Earlier work on the functional characterization of AtIRT1 in yeast already indicated Zn, Mn, Co and Cd to be additional substrates of IRT1 (Eide et al., 1996; Korshunova et al., 1999). Overexpression of AtIRT1 in Arabidopsis plants resulted in higher accumulation of Zn and Cd under Fe-deficient conditions (Connolly et al., 2002), whereas *irt1* mutant lines accumulate a lower amount of Mn, Zn and Co than wildtype plants (Vert et al., 2002). By heterologous expression in yeast it was shown that single amino acid substitutions in AtIRT1 can lead to changes in the substrate specificity for Fe, Zn, Mn and Cd transport (Rogers et al., 2000). Single amino acid changes led for example to a loss of the Zn transport activity or abolished the Fe and Mn transport function of AtIRT1. Interestingly, none of the mutations resulted in a specificity for Fe.

As the low Fe specificity of AtIRT1 leads to a higher sensitivity of plants towards heavy metals under Fe-deficient growth conditions, plants need to avoid an undesired accumulation of metals by a downregulation of IRT1 under metal stress. High Zn or Cd supply leads to a rapid decline of AtIRT1 protein levels (Connolly et al., 2002). The low metal specificity is a phenomenon that does not only apply to IRT1, but that can be found in other metal transporters, too. Also transporters that are part of the strategy II Fe-uptake system of graminaceous plants like the maize Fe-phytosiderophore transporter YS1 are not specific for Fe (von Wirén et al., 1996; Schaaf et al., 2004). Unspecific Fe transport is not restricted to plants, but was reported for a large number of transporters from other organisms like humans, mouse and yeast. A defect in the high-

affinity Fe transport system FET3/FTR1 increased the metal sensitivity in yeast, due to the broad transition metal specificity of the remaining low affinity Fe transporter FET4 (Li and Kaplan, 1998). The divalent metal transporter-1 (DMT1, previously NRAMP2 or DCT1) in mammals is responsible of the uptake of dietary Fe. The physiological role of DMT1 in mammals will be further discussed in the following chapter. When expressed in oocytes, DMT1 from rats was shown to be a H<sup>+</sup>-coupled transporter of Fe<sup>2+</sup>, but with a broad substrate specificity for other metals, including Zn<sup>2+</sup>, Mn<sup>2+</sup>, Cu<sup>2+</sup>, and Ni<sup>2+</sup> (Gunshin et al., 1997).

Many metal transporters have already been identified, but a large number of candidates for heavy metal transport proteins still have to be analyzed at the biochemical level and within the plant metal homeostasis network. In the search for yet unknown heavy metal transporters in plants, the identification of a new conserved transporter gene family, the IREG family, raised open questions on the function of IREGs in plants.

## 2.5 The IREG gene family

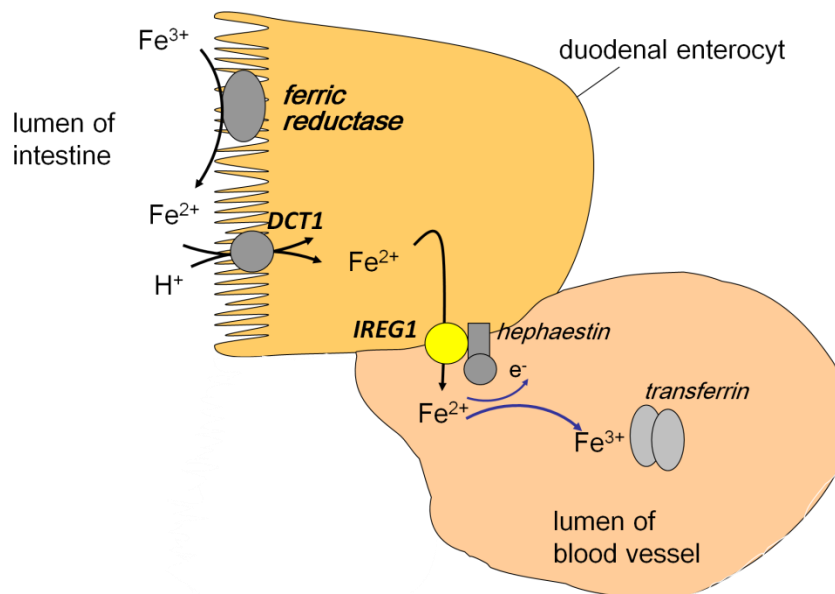
IREG1 (IRON REGULATED GENE 1), also referred to as ferroportin (FPN) or metal transporter protein 1 (MTP1, in vertebrates), was discovered independently by three groups (Abboud and Haile, 2000; Donovan et al., 2000; McKie et al., 2000). Abboud and Haile used an iron-responsive protein (IRP) affinity column to find iron-responsive element (IRE)-containing mRNAs. Thereby, the cDNA of *ferroportin1* / *IREG1* was identified, and named metal transporter protein 1 (MTP1). At the same time, Donovan et al. (2000) examined the severely anaemic zebrafish phenotype *weissherbst* (*weh*), so-called because it appears pale due to a lack of haemoglobin, and identified *ferroportin* (*FPN*) as the gene causing this phenotype. In a third publication, McKie et al. (2000) identified IREG1 as an Fe exporter in mice by using a subtractive cloning approach in hypotransferrinaemic (*hpx*) mice that show anaemic symptoms in spite of highly increased Fe uptake. After these findings, within the last years the role of IREG1 in vertebrates and especially in humans has been intensively studied.

### **The function of IREG1 in dietary iron absorption in vertebrates**

Vertebrates including humans maintain Fe homeostasis mainly through regulation of intestinal Fe absorption, because the capacity to excrete Fe is very limited. The intestinal enterocyte is the key regulatory point for Fe absorption into the body (Roberts et al., 1993). Fe has to cross the apical brush border of duodenal enterocytes, translocate within the cell from the apical to the basolateral surface, and exit to the circulation. In vertebrates dietary ferric Fe is reduced to ferrous Fe by the apical ferric reductase dCytB (McKie et al., 2001). Subsequent to this reduction step ferrous Fe is taken up from the diet to duodenal enterocytes by the divalent metal transporter-1 (DMT1, previously NRAMP2 or DCT1) (Fleming et al., 1997; Gunshin et al., 1997). IREG1 localizes to the basolateral membrane of enterocytes and exports Fe out of the cell into the portal circulation, where it is bound to transferrin, a blood plasma protein for iron delivery, which contains two specific high affinity binding sites for Fe<sup>3+</sup>.

As IREG1 exports Fe<sup>2+</sup> ions, but Fe is bound to transferrin in the oxidized form as Fe<sup>3+</sup>, the loading onto serum transferrin requires a ferroxidase activity, served by the multicopper oxidase hephaestin in the duodenal enterocyte (Vulpe et al., 1999), or by its homologue ceruloplasmin in other cell types (for a review see Hellman and Gitlin, 2002). IREG1 expression is posttranslationally regulated by hepcidin (Nemeth et al., 2004), a 25 aa peptide hormone secreted by hepatocytes in response to Fe loading (Pigeon et al., 2001) and inflammation (Nicolas et al., 2001; Nemeth et al., 2003). Decreased hepcidin levels lead to tissue Fe overload, whereas overproduction of hepcidin causes hypoferremia (Nicolas et al., 2002; Ganz, 2003). Hepcidin binds to IREG1 and induces its internalization and degradation, resulting in decreased Fe export and thereby in cellular Fe retention (Nemeth et al., 2004; Mena et al. 2008). Hepcidin also has the ability to bind Fe (Farnaud et al., 2008), but by now the function of the Fe-binding for hepcidin is not clear. Proposed roles are either a regulatory function of Fe in the maturation of the pro-hepcidin into the active hepcidin, or the Fe-hepcidin complex could be necessary for the interaction between hepcidin and IREG1. *IREG1* is highly expressed in the duodenal mucosa, but could also be detected in other intestinal tissues, where the expression pattern follows the bioavailability of Fe (Frazer et al., 2001; McKie et al., 2000): the expression of *IREG1* is highest in the duodenum, where Fe is highly available due to the acidification by stomach acid, and is lowest in the ileum,

where ferric Fe is likely to form insoluble complexes. *IREG1* is also expressed in reticuloendothelial macrophages of the red pulp of the spleen, of Kupffer cells in the liver and in the bone marrow (Abboud and Haile, 2000; Yang et al., 2002). These cells play an essential role in Fe recycling, pointing to a crucial role of *IREG1* in Fe turnover. *IREG1* is also expressed in the placenta, where it is involved in transfer of Fe between maternal and foetal circulations (Donovan et al., 2000).



**Introductory Figure 1: Model of the IREG1 function in mammals (for a description see the preceding text)**

In summary, *IREG1* can be considered as a universal exporter for Fe in several different tissues in vertebrates. Therefore, alterations in *IREG1* can lead to severe diseases linked to its function in Fe turnover or Fe distribution. In humans, mutations in the coding region of *IREG1* result in an autosomal Fe-overload disease referred to as hemochromatosis type IV. This form is different to other types of hemochromatosis in that it is dominant, requiring only one mutated copy to inherit the disease. Also known as the "ferroportin disease," this condition is typically characterized by high serum ferritin, reduced transferrin saturation and reticuloendothelial macrophage Fe loading (De Domenico et al., 2005). Other types of hereditary hemochromatosis result from inadequate hepcidin production, thereby causing excessive duodenal absorption of Fe and high concentrations of basolateral *IREG1* (Nemeth et al., 2005; Kawabata et al.,

2005; Nicolas et al., 2003). Only recently a discussion was raised, whether IREG1 is able to form oligomers. Evidence for the multimeric structure of IREG1 was presented (De Domenico et al., 2005; reviewed in De Domenico et al., 2006). The dominant heritage of hemochromatosis type IV could indeed be explained, if the functional unit of IREG1 was multimeric. In this case the mutated IREG1 monomer would act as a dominant negative by associating with the wildtype IREG1 monomers, forming a non-functional hetero-oligomer. This hypothesis was supported by experiments, in which IREG1 was tagged with different epitopes (FLAG and GFP) and coexpression of these tagged proteins resulted in a coimmunoprecipitation of both labelled proteins (De Domenico et al., 2005). In contrast to these findings, Gonçalves et al. (2006) could not find any hints for a multimerization of IREG1. In co-transfection experiments mutated and wildtype IREG1 did not co-localize and could not be immunoprecipitated in the same complex. Similar results that also did not support an oligomerization of IREG1 were also obtained by other groups (Drakesmith et al., 2005; Pignatti et al., 2006). In defence of their previous publications, De Domenico et al. showed in different experiments again crosslinking and immunoprecipitation of co-expressed epitope-tagged IREG1 proteins, thereby providing further evidence for a dimerization of IREG1 (De Domenico et al., 2007). These contrasting results led Schimanski et al. to summarize previous publications on IREG1 multimers and to perform additional verifying experiments, concluding that IREG1 is not likely to be active as an oligomer (Schimanski et al., 2008).

Alignment of human, rat, and mouse IREG1 sequences showed a high degree of conservation. IREG1 homologues were also found in other organisms including *Arabidopsis thaliana* (McKie et al., 2000), indicating that IREG1-like proteins are evolutionarily conserved.

## 2.6 Aims of the thesis

Essential transition metals are required in all plant cells for the activities of numerous metal-dependent enzymes and proteins, but can become toxic when present in excess. The maintenance of metal homeostasis in plants depends on membrane transport proteins, which keep whole plant and cellular metal concentrations in the physiological range. Despite a considerable number of metal transporters that have been identified to date, most of their physiological functions remained unclear. A phylogenetic analysis of eukaryote and prokaryote sequences with similarity to the vertebrate Fe exporter IREG1 (IRON-REGULATED GENE 1) showed three homologous genes in *Arabidopsis*, which were named AtIREG1, AtIREG2 and AtIREG3 (Introductory Fig. 2, taken from Schaaf et al., 2006). This phylogenetic analysis also clearly pointed to a separation of a plant cluster from an animal cluster, with particular high sequence conservation among the mammalian sequences (Schaaf et al., 2006). A third cluster comprehends sequences from bacteria, amoeba and nematodes (Introductory Fig. 2).

Until the start of this work, there were no data available on the function of other members of the IREG gene family, except those from zebrafish, humans and mouse. The *Arabidopsis* IREG family members were therefore candidates for yet uncharacterized metal transporters and the main objective of this thesis was to investigate the physiological function of these newly identified transporter family in plants.

In the first chapter of the present thesis, a detailed *in silico* characterization of the three *Arabidopsis* IREG homologues AtIREG1, AtIREG2 and AtIREG3 is presented. Due to the similarity of the three AtIREGs to the vertebrate Fe exporter IREG1, there was a high likelihood that the *Arabidopsis* IREG family members also represent Fe efflux proteins. The mechanism of Fe efflux in plants is not yet clearly understood and by now no Fe exporter has been identified in plants. Therefore, the primary task was to identify the substrate specificity of the AtIREGs and to study whether these transporters also have a Fe transport function. As it has been shown for AtIRT1, in which single amino acid changes can completely alter its substrate specificity, it was anticipated that the



the most likely substrates of AtIREG1 and AtIREG2, transgenic plants were generated that either lack the expression or overexpress one of the two *AtIREG* transporter genes and growth phenotypes of these lines on metal containing medium were investigated. To define the physiological characterization of AtIREG1 and AtIREG2 both proteins were localized at the cellular level and the influence of *AtIREG1* or *AtIREG2* expression on metal transport and distribution in *Arabidopsis* was assessed.

In the next chapter the functional relationship between AtIREG1 and AtIREG2 was studied, employing growth experiments on metal containing medium for a comparative analysis of the metal-dependent phenotype of the transgenic lines with altered expression of AtIREG1 and AtIREG2. To investigate a possible additive function of AtIREG1 and AtIREG2, a double mutant with lacking expression of both genes, *AtIREG1* and *AtIREG2*, has been generated, and Ni-induced production of reactive oxygen species (ROS) was compared to that of the single T-DNA insertion lines.

In the subsequent chapter a potential metal transport function of the third AtIREG gene family member AtIREG3 was investigated by screening of AtIREG3 mutant lines on media with different metal concentrations.

The final chapter summarizes the previously described results and discusses them in the context of previous work on metal transport and metal detoxification strategies in plants. A physiological role has been attributed to AtIREG1 and AtIREG2, and is presented in form of a model that also includes the most relevant data on known metal transporters in plants.

## 3 Materials and Methods

### 3.1 Yeast growth experiments

DNA manipulations were carried out using standard protocols (Sambrook and Russell, 2001). The open reading frame (ORF) of *AtIREG2* was amplified by PCR from an *Arabidopsis thaliana* Col-0 cDNA library (kindly provided by Karin Schumacher, ZMBP, Tübingen, Germany) using the primers 5'-CGGGATCCATGGAGGAGGAAACAGAAAC-3' and 5'-GGCGAGCTCTCATGAAGCAAAAAAGTTGTTC-3'. The *AtIREG1* ORF was cloned in the same way, using the primers 5'-CGGGATCCATGGAGAATGAGACAGAATTG-3' and 5'-GGCGAGCTCTTACACGTTTCCACGAGAAGG-3'. PCR products were A-tailed, cloned into the pGEM-T Easy Vector (Promega, Madison, WI), and subcloned into the yeast expression vector pDR195 (Rentsch et al., 1995) at the NotI restriction site. Yeast cells were transformed by the LiAc method (Gietz et al., 1992) and transformants were selected on uracil-deficient medium containing 1% arginine as nitrogen source and the appropriate supplements. For growth tests, saturated cultures of yeast transformants were spotted in 5-fold serial dilutions onto uracil-deficient YNB medium, containing 0.1% arginine, 3% glucose, 0.01% of each, histidine, leucine, methionine (when appropriate) that were supplemented with the respective metal as indicated.

### 3.2 Transformation of Arabidopsis plants

*Arabidopsis* plants were transformed by floral-dip infiltration using a protocol modified from Clough and Bent (1998). The used *Agrobacterium* strain was *A. tumefaciens* GV3101, carrying a rifampicin resistance gene in its genome, and a gentamycin resistance gene on the Ti-plasmid. Generated binary plasmids (chapter 3.3) were introduced into the *Agrobacterium* strain and selected on 100  $\mu\text{g mL}^{-1}$  rifampicin, 40  $\mu\text{g mL}^{-1}$  gentamycin and 100  $\mu\text{g mL}^{-1}$  spectinomycin. *Agrobacterium* cells were pretransformed with pSoup and were then precultured in selective medium, washed

twice in washing solution (5% sucrose, 10 mM MgSO<sub>4</sub>) and were then diluted to an OD<sub>600</sub> of 0.8 in dipping solution (5% sucrose, 10 mM MgSO<sub>4</sub>, 0.02% Silwet L-77, Lehle seeds, Round Rock, TX, USA). Three week-old flowering Arabidopsis plants were dipped into the Agrobacterium solution. Seeds were harvested and screened on selective half-strength MS agar plates. Resistant plants were transferred to TKS I and grown until harvest of T<sub>1</sub> seeds. T<sub>1</sub> seeds were again sown out on selective plates, and from lines that showed a 3:1 segregation, resistant plants were selected and seeds were amplified on TKS I. T<sub>2</sub> seeds of these plants were screened for segregation on selective plates; homozygous lines were used for further experiments.

### 3.3 Generation of plasmids and transgenic Arabidopsis lines

The cDNA of *AtIRT1* was subcloned from pFL61-*AtIRT1* (kindly provided by C. Curie) into pDR195 at the NotI sites. For transient expression of *AtIREG*-GFP fusion proteins in protoplasts, the *AtIREG1* ORF without a stop codon was amplified using the primers 5'-CGGGATCCATGGAGAATGAGACAGAATTG-3' and 5'-CGGGATCCGCACGTTTCCACGAGAAGGG-3' and the *AtIREG2* ORF without stop codon was amplified with the primers 5'-GGATCCATGGAGGAGGAAACAGAACTAGG-3' and 5'-GGATCCTGAAGCAAAAAAGTTGTTCAAAGG-3'. The PCR product was inserted into the pGEM-T Easy Vector and subcloned at the BamHI sites into the plant transformation vector pCF203 (kindly provided by C. Frankhauser, ETH Zuerich) under control of a CaMV-35S promoter and fused at the 3'-end to a gene encoding GFP. For the generation of Arabidopsis plants overexpressing *AtIREG1* or *AtIREG2*, a modified transformation vector based on pGreenII (Hellens et al., 2000) was used for insertion of the *AtIREG2* ORF from pGEM-T into pGreen0229-35S between the CaMV-35S promoter and CaMV-terminator sequences using the BamHI/PstI sites. The construction of a plant transformation vector for stable expression of promoter:gene-GFP fusions in Arabidopsis was based on the binary vector pTkan, which was derived from pPZP212 (Hajdukiewicz et al, 1994). To generate a new multiple cloning site, the oligonucleotides 5'-

CTAGAGGGCCCGGGACGTCCGCGGAGATCTACGCGTGTCGACTCGAGATAT  
 CCAACTAGTTGGCTGCA-3' and  
 5'-GCCAACTAGTTGGATATCTCGAGTCGACACGCGTAGATCTCCGCGGACGT  
 CCCGGGCCCT- 3' were hybridized and cloned into pTkan at the XbaI/PstI restriction  
 sites resulting in pTkan<sup>+</sup>. *AtIREG1*- and *AtIREG2-GFP* fusions were excised from the  
 vector CF203 by Acc65I and PstI. A blunt end was created at the Acc65I cutting site  
 and subcloned into the PstI/EcoRV restriction sites of pTkan<sup>+</sup>.

A 919-bp *AtIREG1* promoter fragment was amplified from genomic DNA using the  
 primers 5'-CCGCTCGAGCATGTCCTGATCGAGAGAG-3' and  
 5'-TTCTGCAGTTTCTGCTGGAAAGTCTCG -3'. In the same way, a 1794-bp  
*AtIREG2* promoter fragment was amplified with the primers  
 5'-TTCTGCAGTTCTTCTGACTACTTTGATTCTTTC-3' and  
 5'-CCGCTCGAGGGCCGAAGCTCAGGGAGAG-3'. The resulting PCR products  
 were A-tailed, cloned into pGEM-T Easy, digested with NotI and subcloned into the  
 pTkan<sup>+</sup>-*AtIREG*-GFP construct at the Bsp120I restriction site resulting in the plasmids  
 pTkan<sup>+</sup>-*AtIREG2* promoter-*AtIREG2*-GFP and pTkan<sup>+</sup>-*AtIREG1* promoter-*AtIREG1*-  
 GFP.

### 3.4 Isolation and recombination of T-DNA insertion lines

Seeds of the following T-DNA insertion lines were obtained from the SALK institute:

*AtIREG1* T-DNA insertion lines: SALK\_016176 (*ireg1-1*) and SALK\_013005 (*ireg1-2*)

*AtIREG2* T-DNA insertion lines: SALK\_074442 (*ireg2-1*) and SALK\_127071 (*ireg2-2*)

*AtIREG3* T-DNA insertion lines: SALK\_034189 (*ireg3-1*) and SALK\_016772 (*ireg3-2*)

Seeds were sown out on TKS I and genomic DNA was isolated from leaves of these  
 plants. For identifying plants containing a T-DNA insert within the gene of interest and  
 for determining genotypes of plants as heterozygous or homozygous for the T-DNA  
 insertion, PCR reactions with gene specific primers and a T-DNA left border primer  
 were performed.

Gene specific primers for amplification of the wildtype gene:

line	primers
<i>ireg1-1</i>	forward: 5'-TCCCAGTGCCTAGTGGGAATC- 3' reverse: 5'-CTTGATGACTGCACCACCAGC- 3'
<i>ireg1-2</i>	forward: 5'-ATGGAGTGCCAGGTAGGTTTC- 3' reverse: 5'-GGTTCTAGACGGAGGGTTTCC- 3'
<i>ireg2-1</i>	forward: 5'-TTTCCTCGACTTCGATTTGGT- 3' reverse: 5'-CCATCGAGCAAGAAAATAGCC- 3'
<i>ireg2-2</i>	forward: 5'-CGAAAAATTGAAAATCGAACTCAAA- 3' reverse: 5'-TGATCAGACCTTGCACCCCAT- 3'
<i>Ireg3-1</i>	forward: 5'- ACGAATAGAGCGAGCCGTAAG- 3' reverse: 5'- GCTTGTATTGCGTTCAAGCTG- 3'
<i>Ireg3-2</i>	forward: 5'- TCAATGGATCTCTAATATTCCTCG- 3' reverse: 5'- TCTTCTCCAAACTCATGCAGC- 3'

To screen for the T-DNA insertion, PCR was performed with the reverse primer (see above) and the T-DNA left border primer LBb1 (5'-GCGTGGACCGCTTGCTGCAACT-3'). The site of the T-DNA insertion in the *AtIREG1* and *AtIREG2* T-DNA insertion lines was confirmed by cloning the resulting PCR product to pGEM T-EASY, and sequencing this vector construct.

A pTkan<sup>+</sup>- AtIREG2-promoter:AtIREG2-GFP construct (see above) was used for complementation of the *ireg2-1* T-DNA insertion line. Homozygous plants were identified in the T2 generation based on segregation analysis on 50 µg mL<sup>-1</sup> kanamycin.

### 3.5 Localization experiments

For subcellular localization, *Arabidopsis* protoplasts were transformed as described previously (Liu et al., 2003). Transformed protoplasts were analyzed by confocal laser scanning microscopy (TCP-SP Leica, Bensheim, Germany). Localization experiments with *ireg2-1* recomplemented lines (see above) were conducted with homozygous T2 plants using an inverted fluorescence microscope equipped with an ApoTome (Zeiss Axiovert 200 M, Jena, Germany). Plant roots were stained with 25  $\mu$ M FM4-64 (Molecular Probes) for 5 min and shortly rinsed in ultra pure water before observation under the microscope.

### 3.6 Plant culture and growth conditions

#### 3.6.1 *Arabidopsis* growth tests on agar

*Arabidopsis* seeds were surface sterilized using a solution of 70% ethanol and 0.05% Triton X100. 1 mL of this solution was added to 100  $\mu$ L seeds and then shaken at room temperature for 20 min at 1400 rpm. The supernatant was aspirated, seeds were washed two times with 100% ethanol and left to dry for at least 4 h. For growth tests on agar plates containing different micronutrient or heavy metal concentrations, seeds of wildtype and transgenic plants were germinated under long day conditions in a growth chamber on half-strength Murashige and Skoog (MS) medium (Duchefa, Haarlem, NL), 1% sucrose, solidified with 0.7% Difco agar (Becton Dickinson). After 7 d seedlings with comparable root and shoot development were transferred to vertical plates supplemented with metals at indicated concentrations. Plants were continued to grow for 14 d for the determination of root length and root and shoot fresh weight and photographs were taken of representative plates. For growth tests on urea containing medium, the medium was autoclaved without a nitrogen source. Sterile filtrated urea solution was added to the medium directly before pouring of plates (when the temperature of the medium was below 60 °C).

### 3.6.2 Hydroponic culture

For hydroponic culture *Arabidopsis* seeds (ecotype Columbia-0) were germinated on glass wool moistened with tap water and precultured in the dark for 4 d. Further plant growth conditions have been described by Loqué et al. (2005). The nutrient solution was renewed weekly during the first 3 weeks, and every 3 d afterwards. Plants were grown under non-sterile conditions in a growth cabinet under the following growth conditions: 10 /14 h light / dark; light intensity  $280 \mu\text{mol m}^{-2} \text{s}^{-2}$ ; temperature 22 / 18°C day / night; humidity 60%.

For the analysis of metal accumulation in *Arabidopsis* plants, 4 – 5 week old plants were set for 3 to 10 days (depending on experiment and metal concentration) on nutrient solution containing metals at indicated concentrations. Nutrient solution was renewed every 2 d. All plants were harvested at the same time, approx. 5 h after onset of light. Before harvest, for removal of metals bound in the root apoplast, roots were washed for 20 min with 1 mM EDTA pH 6.0. Roots and shoots were separated, 3 plants were pooled per replicate. Whole roots and shoots were digested by heating in a microwave oven with concentrated  $\text{HNO}_3$  and  $\text{H}_2\text{O}_2$ , and metal concentrations were determined using inductively coupled plasma mass spectrometry (ICP-MS).

Metal efflux analysis from wildtype and *AtIREG1* T-DNA insertion lines was performed with 40 d old hydroponically grown plants, that were transferred for 4 d to a nutrient solution supplied with 10  $\mu\text{M}$  Ni or Co. Roots were washed for 20 min with 1 mM EDTA pH 6.0 and single plants were placed on 4.5 mL diluted (1:10) standard nutrient solution. After 8 h plants were removed and Ni or Co concentrations in this solution were measured by ICP-MS.

For collection of xylem exudates, in the evening before the xylem exudate collection the air humidity in the growth chamber was increased to 75% and the plants were transferred to nutrient solution supplemented with Ni. After onset of lights, shoots were cut off above the hypocotyl and exudates were collected in tubes for 3 h and stored at -20°C until measurement. For one replicate exudates of five plants were pooled. To measure metals in xylem exudates, the exudates were diluted with 1%  $\text{HNO}_3$  and metal determination was performed via ICP-MS. Iron in xylem exudates was measured using

atomic absorption spectrometry. All values were normalized over potassium concentration in the exudates, which was obtained on the basis of flame photometry.

### 3.7 RNA gel blot analysis

Roots and shoots of hydroponically grown plants were shock frozen directly after harvest and the plant material was grinded. Total RNA was isolated by Trizol (Invitrogen, Carlsbad, CA) extraction. 20 µg total RNA was denatured and resolved by electrophoresis on MOPS-formaldehyde agarose gels. After blotting to a Hybond N<sup>+</sup> nylon membrane (Amersham), RNA was crosslinked to the membrane by incubation at 80°C for 2h. The ORFs of *AtIREG1*, *AtIREG2* and *AtIRT1* were excised from vectors containing the respective ORF and were used as a probe for hybridization to total RNA. Probes were labelled with <sup>32</sup>P-dCTP using the Megaprime Labeling Kit (Amersham) and hybridized to the membrane at 42°C in 50% (v/v) formamide, 1% (w/v) sarkosyl, 5x SSC, and 100 µg mL<sup>-1</sup> yeast t-RNA. Membranes were washed repeatedly in 2x SSC, 0.1% (w/v) SDS and finally in 0.2x SSC, 0.1% (w/v) SDS at 42°C for 40 min and were exposed for 1 – 14 d at -70°C to X-ray films. Ethidiumbromide-stained gels were used as a RNA loading control.

### 3.8 Reverse transcription (RT)-PCR

To analyse *AtIREG1* gene expression by semi-quantitative reverse transcription-PCR, total RNA was isolated from leaf and root material of hydroponically grown plants using the Trizol RNA extraction kit (Invitrogen, Carlsbad, CA). 1 µg of total RNA was reverse transcribed into cDNA using oligo dT primers provided with the SuperScript II Reverse Transcriptase Kit (Invitrogen, Carlsbad, CA) and 10% of the resulting cDNA was used as a template in each PCR reaction. *AtIREG1* was amplified with the specific primers 5'-ATGGAGAATGAGACAGAATTGAG-3' and 5'-CAGTCTCGTTCGATCAGAATG-3'. *Actin8* served as a control and was amplified using the primers 5'-GCCAGATCTTCATCGTCGTG-3' and 5'-TCTCCAGCGAATCCAGCCTT-3'. Annealing temperature was optimized and

cycle number was adjusted, so that PCR products were analysed in the exponential phase of amplification, generally after 40 – 50 cycles (details are given in chapter 4.2.1). PCR products were separated by agarose gel electrophoresis and stained with ethidiumbromide.

### 3.9 Vacuole isolation from Arabidopsis leaves

For the isolation of vacuoles a modification of a protocol kindly provided by Oliver Trentmann (University of Kaiserslautern) was used. Wildtype and transgenic plants were grown in hydroponic culture under short day conditions. Plant age was between 6 and 8 weeks, depending on plant size. For the isolation fully grown but not senescent leaves were used. For each sample 5 g leaves were harvested in the morning before the onset of light.

*Preparation of protoplasts:* The lower side of 5 g Arabidopsis leaf material was rubbed with sandpaper 600 and the leaves were placed with the rubbed side on 20 mL digestion buffer containing 500 mM sorbitol, 1mM CaCl<sub>2</sub>, 10 mM MES-KOH pH 5.6, 0.1% pectinase (Fluka, from *Rhizopus* sp.), 0.1% Macerozyme R-10 (Duchefa) and 1% cellulase Onozuka R-10 (Duchefa). Leaves were digested for 5 h in the dark at 28 °C with manual shaking every 30 min, until the leaves were fully digested.

*Purification of protoplasts:* The content of the petri dish was filtered through a 125 µm and a 60 µm filter into two 15 mL Falcon tubes. 1 mL 100% Percoll was added to the bottom of each Falcon tube and centrifuged for 7 min at 250 g (using a swing-out rotor). The supernatant was removed, one more mL 100% Percoll was added and the protoplasts were resuspended carefully. A density gradient with three layers was used to purify the protoplasts. Over the 2 mL protoplast solution 2 mL 35% Percoll and 1 mL 5% Percoll were layered and centrifuged for 7 min at 250 g (swing-out rotor). Intact protoplasts were located between the 35% and the 5% Percoll layer and could be collected with a cut blue pipette tip. 1 mL per Falcon tube was collected, and the two preparations that derived from the same leaf material were pooled.

*Isolation and purification of vacuoles:* Lysis buffer (200 mM sorbitol, 10% Ficoll 400, 20 mM EDTA (free acid), 20 mM HEPES pH 8.0, 0.1% BSA, 1mM DTT) was preheated in a 30°C water bath. 2 mL of the protoplast preparation was mixed with 4 mL prewarmed lysis buffer, incubated in a 30°C water bath and inverted every minute for 8 – 12 minutes. Lysis was checked under the microscope and was stopped, when nearly all protoplasts were lysed and vacuoles were visible. Samples were put on ice to stop the lysis and cooled down for 10 min. A density gradient was used to purify the vacuoles. 6 mL of lysed protoplasts were covered with a layer of 2 mL of a mix of lysis and glycinebetaine buffer (400 mM betaine, 30 mM K-gluconate, 20 mM HEPES pH 7.2, 0.1% BSA, 1 mM DTT). Over this 1 mL of betaine buffer was layered and samples were centrifuged for 7 min at 250 g (in a swing out rotor). Vacuoles could be collected between the 2 mL mix and the 1 mL betaine buffer. Between 200 and 500 µL interphase including the vacuoles was collected. Vacuoles were counted using a microscopic counting chamber. Ni measurements were done by Günther Weber (ISAS Dortmund) using adsorptive stripping voltammetry (chapter 4.3.6).

### **3.10 Visualization of ROS (reactive oxygen species) formation in Arabidopsis**

ROS formation in Arabidopsis roots was visualized by detection of fluorescence derived from the oxidation of H<sub>2</sub>DCFDA (2', 7' - dichlorodihydrofluorecein diacetate, Molecular Probes, Eugene, OR). Upon oxidation, H<sub>2</sub>DCFDA becomes the highly fluorescent 2', 7'-dichlorofluorescein. The presence of the derived fluorescence was determined in roots of 10 d old *Arabidopsis thaliana* seedlings which were grown on half-strength MS agar plates with or without 40 µM Ni. Seedlings were stained for 15 minutes in a 10 µM H<sub>2</sub>DCFDA-solution, rinsed twice in deionized water and the detection of ROS was performed using an ApoTome imaging system in an inverted fluorescence microscope (Zeiss Axiovert 200 M, Jena, Germany).

## 4 Results

### 4.1 *In silico* analysis of the IREG gene family in Arabidopsis

As described in chapter 1.6 there are several eukaryote and prokaryote genes with similarity to the vertebrate IREG1 Fe exporters, including three homologous genes in *Arabidopsis* (*AtIREG1*, *AtIREG2* and *AtIREG3*, see Introductory Fig. 2).

The *AtIREG1* gene (At2g38460) has a genomic length of 2575 bp including seven exons and 6 introns. The coding region has a length of 1575 bp, encoding a protein (accession number AAC28758) with a length of 524 amino acids and a molecular weight of 58.20 kDa. *AtIREG2* (At5g03570) has a genomic length of 2909 bp with 8 exons and 7 introns. The corresponding ORF (open reading frame) comprises 1539 bp encoding for a protein (accession number CAB83320) with a molecular weight of 57.09 kDa, consisting of 512 amino acids. *AtIREG3* (At5g26820) has a genomic length of 3487 bp including 12 exons and 11 introns. The corresponding protein (accession number AAL32684) with a length of 598 amino acids is encoded by an ORF of 1797 bp.

The phylogenetic analysis of several IREG1 homologues shown in form of a phylogenetic tree in chapter 1.6 (Introductory Fig. 2) clearly pointed to a separation of a plant cluster from an animal cluster, with particular high sequence conservation among the mammalian sequences. *AtIREG1* and *AtIREG2* seem to be very closely related and fall in one cluster, together with one rice gene. *AtIREG3* groups into another cluster that mainly comprises genes of invertebrate species (*Dictyostelium discoideum* and *Caenorhabditis elegans*), but seems to have a plant subcluster including *AtIREG3* and one additional rice gene. To have a closer look at the relation among the three Arabidopsis IREGs and to the well characterized IREGs from mouse, rat, zebrafish and humans, the amino acid sequences of these proteins (protein sequences obtained from <http://www.arabidopsis.org/> and <http://www.ebi.ac.uk/embl/>) were compared and revealed the following similarities (Table 1):

	1	2	3	4	5	6	7	
1		84.6	20.2	32.4	31.9	31.0	32.4	1 AtIREG1
2			21.6	31.5	31.0	30.5	32.4	2 AtIREG2
3				22.8	22.1	24.6	22.5	3 AtIREG3
4					95.0	67.8	89.1	4 Rattus norvegicus IREG1
5						69.4	90.0	5 Mus musculus IREG1
6							67.8	6 Danio rerio IREG1
7								7 Homo sapiens IREG1
	1	2	3	4	5	6	7	

**Table 1: Identity of the amino acid sequences of AtIREG-related proteins.**

Alignment was performed with the MegAlign tool (Jotun Hein method) provided by the DNASTar software package. Identities are given in percent.

A comparison of the Arabidopsis IREGs with each other shows, that AtIREG1 and AtIREG2 share the highest similarity (84.6%), whereas AtIREG3 only has a similarity of around 20% to both other AtIREGs. The similarity of AtIREG1 and AtIREG2 to the vertebrate homologues from rat, mouse, zebrafish and humans is about 30%, whereas AtIREG3 only shares 20% similarity to the vertebrate IREGs. To compare the three Arabidopsis IREG proteins more detailed at amino acid level, an alignment of At2g38460 (AtIREG1), At5g03570 (AtIREG2) and At5g26820 (AtIREG3) was made (Fig. 2), showing the high similarity of AtIREG1 and AtIREG2, which share a high conservation and identical amino acids over a big part of the protein. The amino acid divergence of AtIREG3 expresses in particular in the N-terminal region of the protein, which is longer in the AtIREG3 protein. Nevertheless, the overall structure of the three IREGs has similarities in the number and arrangement of the predicted transmembrane domains (Figure 1). Hydrophobic regions that are likely to form membrane spanning structures are distributed in a similar manner in all three proteins, especially in the C-terminal half of the proteins.

```

At2g38460 -----
At5g03570 -----
At5g26820 MVSVMALVRHSPSPDFLHFHFPVDRSRFLSPVAFSSVRYHRFHSCRWLSLRSSPSCSRRLNSFSSRCSITNTDVCHEFVTT
eq -----
At2g38460 -----MENETELRVVHQEEQQREE-----GEDESQPQNPPALRRRFVIYLYVGYFLAR
At5g03570 -----MEEETETRVFLSNEQHQQE-----EEEEEE-----PSLPRSMVISLYLYGFLAR
At5g26820 DDEIHEDLLTPIEDHSIPIVHLDTNISVTESLTLLTECTYVDTVLTALPVLSEEEQTVIAATPAHPEGLYLYVYASCLVGN
eq -----*-----*-----*-----*-----*-----**-----
At2g38460 WSARTWEFSVALYMIHLWPNSELLAAIYGAIESGSTAIFGPIVQWVEGMDYVVKVLRLLWLLFQNLSTIAGGAVIKLLLV
At5g03570 WGARTWEFSVALYMIYLPNSLFLTAMYGVVESGSATLFGPIVQGMIDGMSYVKVLRLLWLVTONLSFIVAGGAVALLVV
At5g26820 LVEQLWNFAWPSAIAMLYP-SLLPVAVMGFVTKLAI IAGGPVVGKFM DYSPRVPTYISLNVIQAAAQVLSAGMI IHA YTV
eq -----*-----*-----*-----*-----*-----**-----*-----*-----*-----*-----
At2g38460 SDLKSRNLPVFAILVLTNLAGAIGVLTSTL AGLTILIERDWAVVMSEGHPPAVLTKMNSVIRGIDLSSKLLSPVITGLIIS
At5g03570 PDLKSQNFVVFATLVVLTNLGAIGVLTSTL AGLTVLIERDWVVMSEGHSPAVLTRMNSVIRGIDLSSKLLSPVITGLIIS
At5g26820 PSTSASSILLQPWFFALL-FAGAI D SLCG IASGVAIERDWVWVLLAGINRPIALAQANAVLHRI D L LCEIAGT M L F G I L L S
eq -----*-----*-----*-----*-----*-----*-----*-----*-----*-----*-----*-----
At2g38460 FVSLKASAITFAAWATITAWVEYWLFI SVYSGVPAITRSNERRILRSRTKQVEGRDAPVSVSIVPGTEEGYTG NPPSR TG
At5g03570 FVSLRASAITFAAWATI TVWIEYWLFI SVYNGVPAI VQSDERRSLRSSQSAEETDSASSFYVPLLHEEESYRNTQSRSR
At5g26820 ----IFDIGMETIKLGWKEYIQPVLPASL AYVLLYFNIVLTPGSLMTAFLTQRCVNPSVIGGFSGLCVAVMGVAATFLSA
eq -----***-----*-----*-----*-----*-----*-----*-----*-----*-----*-----
At2g38460 ILVILDRMSKSSFVGAWRIFYNQEVVLPVGS LALLFF-TVLSFGT LMTATLQWEGIPT Y I I G I G R G I S A T V G L A A T L V Y P
At5g03570 ILRILRISSESSFVSAWRNYLNQEI VLPVGS LALLFF-TVLSFGT LMTATLEWKGIP T Y I I G I G R G I S A G V G L A A T V L Y P
At5g26820 ----IFDIGMETIKLGWKEYIQPVLPASL AYVLLYFNIVLTPGSLMTAFLTQRCVNPSVIGGFSGLCVAVMGVAATFLSA
eq -----*-----*-----*-----*-----*-----*-----*-----*-----*-----*-----*-----
At2g38460 LMQSRLSTLRTGLSFWFSQW SCLLVCGVSIWVK--KDKIASYMLMAGVAASRLGLWMPDLAVIQMQDLVSESDRCVVG G
At5g03570 LMQSRISPLRTGVSWFSQW TCLLVCGVSIWVE--KEKIASYMLMAGVAASRLGLWMPDLAVIQMQDLVPESDRCVVG G
At5g26820 NLVKRVGILKAGAVGLFFQASLLAVAVAVYCSSSLSHKSP LFFLSMIVLSRLGHMSYGVVGAQILQGTGIPSSKANLIGA
eq -----*-----*-----*-----*-----*-----*-----*-----*-----*-----*-----*-----
At2g38460 VQNSLQSALDLMAYLLGIIVSNPKDFWILT LISFSTVSLAGMLYTIHLYRIRNHIFHLEKIPLLKNCIFKLLP SRGNV
At5g03570 VQNSLQSALDLMANLLGIIVSNPKDFWMLT LISFATVSLAGILYTIHLYRIRKHLFHLEKIPLLNNFFAS-----
At5g26820 TEISVASLAESLMLGVAIAANDASHFGFLAVLSLLSVVAASLIFCRLLRNPTDEQRRLFSFDPLSN-----
eq -----*-----*-----*-----*-----*-----*-----*-----*-----*-----*-----*-----

```

**Figure 1: Amino acid alignment of AtIREG1, AtIREG2 and AtIREG3.**

Amino acid sequences of At2g38460 (AtIREG1), At5g03570 (AtIREG2) and At5g26820 (AtIREG3) were aligned (using the tools provided on <http://www.ch.embnet.org/>). Putative transmembrane domains are labelled in red letters. Asterisks (\*) label amino acids that are the same in all three aligned proteins.

A further comparison of the relative position of the transmembrane domains of AtIREG1, AtIREG2 and AtIREG3 was performed with different publicly available prediction tools. The plant membrane protein database <http://aramemnon.botanik.uni-koeln.de/> (employing several different prediction algorithms) predicts AtIREG2 and 3 to have 11 membrane spanning alpha helices, whereas AtIREG1 has only 10. Analysis with the TMHMM algorithm (available under <http://www.cbs.dtu.dk/services/TMHMM/>) resulted in a prediction of 11 transmembrane domains in AtIREG3, whereas AtIREG1 and AtIREG2 are both predicted to have 8 transmembrane helices. The N- and C-termini of all three proteins were predicted to protrude into the intracellular space (<http://www.cbs.dtu.dk/services/TMHMM/>).

### **Prediction of the subcellular localization**

The PSORT database (<http://psort.nibb.ac.jp/form.html>) gave no clear prediction for the subcellular localization of the Arabidopsis IREGs. All three proteins (AtIREG1, AtIREG2 and AtIREG3) are predicted to localize to the plasma membrane (with a probability of 60 %). An extension of the PSORT program is WoLF PSORT (<http://wolfsort.org/>, described in Horton et al., 2006), which makes predictions based on known sorting signal motifs and correlative sequence features. Predictions for AtIREG1 are: plasma membrane 9.0, vacuole 3.0, endoplasmic reticulum (ER) 1.0. For AtIREG2 and 3 the predictions are less clear (with values less than 6.0). The plant membrane protein database (<http://aramemnon.botanik.uni-koeln.de/>) gave no prediction for AtIREG1 and AtIREG2, but AtIREG3 was strongly predicted to localize to the chloroplast. Searches for chloroplastic subcellular location (<http://www.cbs.dtu.dk/services/ChloroP/>) revealed a chloroplast transit peptide sequence within the AtIREG3 protein. Additionally, computer predictions based on the proteomic analysis of the plastid envelope gave a very high probability for plastid localization of the AtIREG3 protein (Koo and Ohlrogge, 2002; Ferro et al., 2002). Different other prediction tools were used, which all gave no clear hint for the subcellular localization of the Arabidopsis IREG proteins.

### **Gene expression data obtained from publicly available microarray data**

The expression of the *AtIREG* genes was analyzed with Genevestigator (<https://www.genevestigator.ethz.ch/>), which provides a number of tools to visualize the expression of genes across microarrays or categories. Different meta-profile analysis tools are available that process average values for the expression across space (anatomy), time (development) and environmental or genetic factors (stimulus and mutation). The expression of *AtIREG1* (At2g38460) seemed to be similar in different plant organs and growth stages. There was also no clear difference in its expression among the available treatments (e.g. hormonal, abiotic stresses, light and pathogens). The available data on *AtIREG1* expression was checked in a number of other databases. The finding that *AtIREG1* seems to be constitutively expressed in all organs and under all conditions that were tested by now was supported by the AtGenExpress

Visualization Tool (<http://jsp.weigelworld.org/expviz/expviz.jsp>), in which also no factor triggering a change in *AtIREG1* expression was found. Another tool that summarizes the results of several Arabidopsis microarray experiments is the Arabidopsis eFP browser (<http://www.bar.utoronto.ca/efp/cgi-bin/efpWeb.cgi>), which provides a visualization of expression levels in different growth stages, organs and under different growth conditions. For *AtIREG1* this tool shows a low and similar expression in all plant organs, with slightly higher expression in seeds. The only interesting finding was an experiment published in the Stanford microarray database (<http://genome-www5.stanford.edu/>) indicating that *AtIREG1* gene expression was regulated in response to the plant Fe nutritional status (ExptID 9549 and 7114), a finding that will be scrutinized in the following chapter of the present thesis. For *AtIREG2* (At5g03570) the function *gene atlas* in Genevestigator - which provides data on gene expression in different plant organs – shows a high expression of *AtIREG2* in roots and radicles. The same result was obtained by a search in the AtGenExpress Visualization Tool, where *AtIREG2* was also expressed higher in roots than in all other plant organs. Additionally, *AtIREG2* seems to be highly expressed in germinating plants and the expression level decreases after start of flowering. Use of the Arabidopsis eFP browser database also showed a high expression in radicles and roots of vegetative plants, but the root expression levels goes down in flowering plants. For *AtIREG3* (At5g26820) the obtained data gives no clear hints on a certain expression pattern. According to Genevestigator *AtIREG3* is expressed at the same level in all plant organs and treatments, except of a higher expression in pollen. Also the AtGenExpress Visualization Tool and the Arabidopsis eFP browser point to an unaltered expression of *AtIREG3* in all samples (different developmental stages and treatments).

### **Cell-type specific expression**

The publication “A Gene Expression Map of the Arabidopsis Root” (Birnbaum et al., 2003) allows searching for the expression of a certain gene of interest in different Arabidopsis root cell types. The employed approach is based on a couple of transcriptome analyses of different root cell types and tissues and along a developmental gradient by using transgenic lines expressing green fluorescent protein (GFP) in five specific root cell types (stele, endodermis, endodermis plus cortex,

epidermal atrichoblast cells and lateral root cap). Different cell types were isolated and sorted from plants of three developmental stages. Developmental stage I includes cells from root tips, cells of stage II were isolated from the zone of longitudinal expansion (about 0.15 mm from the root tip) and stage III includes cells from the root hair zone (0.45 to 2 mm from the root tip). Thus, 15 different zones of the root were mapped that correspond to different cell types and tissues at progressive developmental stages. Information on *AtIREG2* was not included in this publication, as the sample was lost during processing. A comparison of the data on *AtIREG1* and *AtIREG3* shows that both genes were expressed at relatively low levels. The expression level of *AtIREG1* was similar in all analyzed cell types, but was always increased approximately 1.5-fold in the third developmental stage compared to stage I and II. *AtIREG3* expression was lower in stage II compared to the other two stages in all cell types, and expression was highest in the endodermis and cortex, lower in stelar cells and the lateral root cap, and lowest in endodermal cells.

## 4.2 AtIREG1

### 4.2.1 Expression of AtIREG1

In a first experiment, *AtIREG1* mRNA levels were examined in wildtype plants. Database searches (see chapter 2.1) pointed to an induction of *AtIREG1* under Fe-deficient growth conditions. Therefore, wildtype Arabidopsis plants were grown hydroponically first under Fe-sufficient conditions. For the Fe deficiency treatment, plants were starved for Fe for 10 days before half of the deficient plants were resupplied with Fe. Corresponding root and shoot samples were used for RNA extraction to perform a northern blot analysis (Fig. 2.2).

Expression levels of *AtIREG1* were extremely low and *AtIREG1* transcripts could only be detected if the film used to detect the radioactivity was exposed to the gel for at least 2 weeks, which then led to a strong background (Fig. 2). Due to the strong background signal an interpretation of the northern blots was difficult, but the expression of *AtIREG1* was clearly higher in root compared to shoot samples and no induction of *AtIREG1* under Fe-deficient conditions could be detected (Fig. 2).

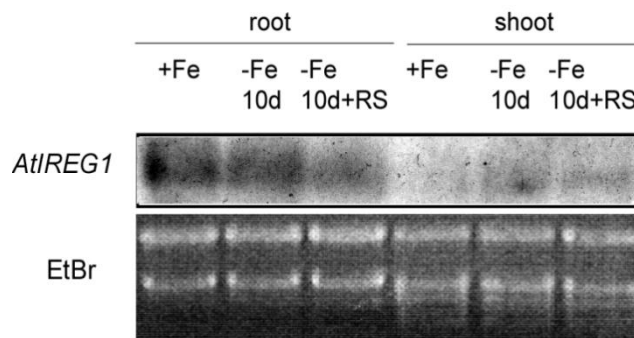


**Figure 2: Iron-dependent expression of *AtIREG1* in roots and shoots of wildtype *Arabidopsis* plants.**

RNA gel blot analysis was performed to determine *AtIREG1* expression in roots and shoots from hydroponically grown plants that were precultured for 5 weeks in presence of 50  $\mu$ M Fe(III)-EDTA and starved for 10 days for iron, before resupply (RS) with 50  $\mu$ M Fe(III)-EDTA for 24 h. Total RNA from roots (*left*) or shoots (*right*) were used for hybridization to the complete ORF of *AtIREG1*. EtBr-stained gel blots are shown as loading control.

Because of the low quality of the RNA gel blots, RT-PCR was used as an alternative method to analyze gene expression of *AtIREG1*. One  $\mu$ g of total RNA was used for cDNA synthesis. Due to the amplification in the PCR reaction, RT-PCR is more sensitive but can also be error-prone. Therefore, several optimization reactions were performed to verify the specificity of the used PCR primers, to optimize the PCR cycle number and to prove the success and comparability of cDNA synthesis from root and shoot RNA samples, and from different *Arabidopsis* lines. To verify the specificity of the used primers samples from wildtype and an *AtIREG1* overexpressing line were used (Fig. 3). Overexpression of *AtIREG1* (which was previously also confirmed by northern blotting, Fig. 6) led to stronger bands in the RT-PCR gel, showing that the used primers were clearly specific to *AtIREG1*. The same primers were also used for PCR reactions on cDNA samples from *35S::AtIREG2* lines, to verify eventual binding of the primers to both homologues. These lines showed bands with intensities similar to that of bands obtained from wildtype samples (data not shown), leading to the conclusion that the primers bind specifically to *AtIREG1* and not to *AtIREG2*. *AtIREG1* transcript could be detected in wildtype root and shoot samples only at high PCR cycle numbers, a clear band was only visible after 45 reaction cycles. This points to a low expression level of *AtIREG1*, which goes along with the preceding RNA gel blot experiments (Fig. 2) in

which the detection of *AtIREG1* was difficult due to its low expression. Even though higher cycle numbers increase the error rate in PCR reactions, up to 60 cycles were performed without obtaining secondary bands (data not shown). In wildtype plants, a band was visible after 40 PCR cycles and the band strength was saturated after 50 cycles. For the following experiments 40 to 50 PCR cycles were used.

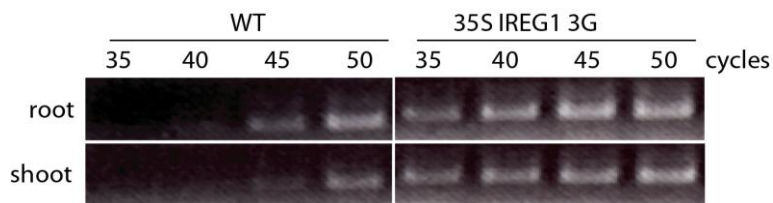


**Figure 3: Setup of RT-PCR conditions to detect *AtIREG1* expression in Arabidopsis RNA extracts.** RT-PCR was performed to determine *AtIREG1* expression in roots and shoots from hydroponically grown plants. cDNA was synthesized from total RNA of root and shoot samples of wildtype (WT, left) and an *AtIREG1* overexpressing line (35S IREG1 3G, right) and used for the PCR reaction. Samples were taken after 35, 40, 45 and 50 PCR cycles.

RT-PCR conditions to determine the expression of the Arabidopsis housekeeping gene *Actin8* (*AtACT8*) were established to use *Actin8* as a reference for further RT-PCR experiments. To verify the lack of *AtIREG1* expression in the *AtIREG1* T-DNA insertion lines *ireg1-1* and *ireg1-2*, RT-PCR was performed and samples were taken after 40, 45 and 50 PCR cycles (Fig. 4). An *AtIREG1* overexpressing line was included in the experiment as a positive control for the template RNA.

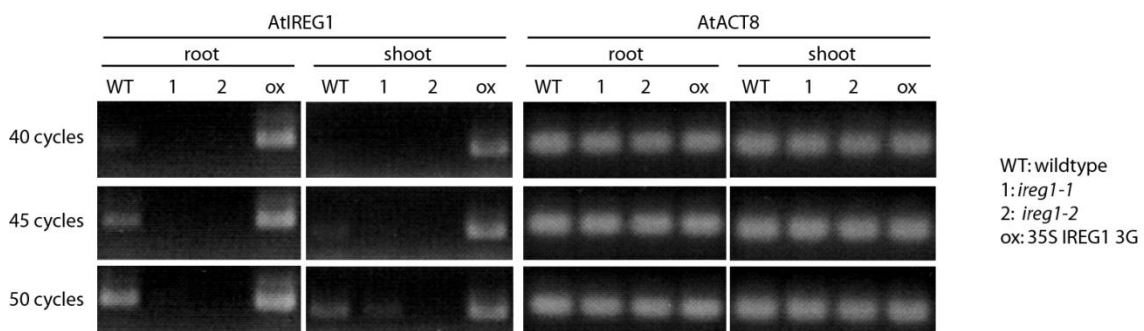


**Figure 4: Expression of *AtIREG1* is higher in roots and can not be detected in *ireg1* lines.**

RT-PCR was performed to determine *AtIREG1* and *AtACT8* expression in roots and shoots from hydroponically grown plants. cDNA was synthesized from total RNA of wildtype (WT), two independent *AtIREG1* T-DNA insertion lines (1: *ireg1-1*, 2: *ireg1-2*) and one *AtIREG1* overexpressing line (ox: 35S IREG1 3G). Samples were taken after 40, 45 and 50 PCR cycles.

The expression of *AtIREG1* in wildtype plants was higher in roots than in shoots, which goes along with the RNA gel blot results (Fig. 2) and the previously shown RT-PCR experiment (Fig. 3). No expression of *AtIREG1* could be detected in roots and shoots of the T-DNA insertion lines *ireg1-1* and *ireg1-2*. In shoot samples of *ireg1-1* after 50 PCR cycles a weak band appeared which could be due to a contamination of the PCR reaction or during gel loading. To verify the outcome of the RNA gel blot experiment shown in Fig. 2 cDNA from roots and shoots of wildtype plants cultured under Fe-sufficient or Fe-deficient conditions was used for RT-PCR (Fig. 5).

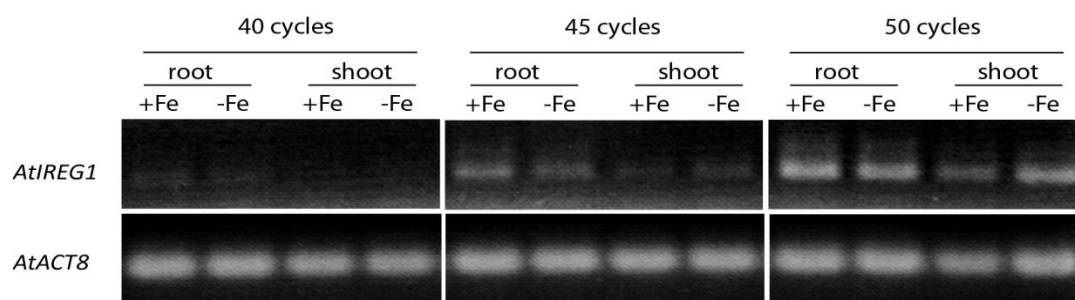


**Figure 5: Expression of *AtIREG1* is not upregulated under iron deficiency.**

RT-PCR was performed to determine *AtIREG1* expression in roots and shoots from hydroponically grown plants. cDNA was synthesized from total RNA of root and shoot samples from hydroponically grown wildtype (Col 0) Arabidopsis plants that were precultured for 5 weeks in the presence of 50 $\mu$ M Fe(III)-EDTA and starved for 10 days for iron (- Fe) or were continuously grown under Fe sufficient conditions (+ Fe). *Actin8* (*AtACT8*) was used as a control.

Higher *AtIREG1* expression was detected in roots than in shoots of plants grown under Fe-sufficient as well as Fe-deficient conditions (Fig. 5). The expression of *AtIREG1* was slightly lower in Fe-deficient Arabidopsis roots than in roots of plants grown with adequate Fe supply. In shoots the signal was stronger in samples of plants grown under low Fe nutrition, but as the *Actin8* band in the same sample was also slightly weaker, the experiment needs to be repeated before drawing a final conclusion.

## 4.2.2 Characterization of the growth phenotype of *AtIREG1* overexpressing Arabidopsis lines

To investigate the putative function of *AtIREG1* *in planta*, transgenic Arabidopsis lines were generated that express *AtIREG1* under the control of the constitutive 35S promoter. Three independent homozygous lines (2F, 3G and 5E) were examined in the T2 generation by RNA gel blot analysis (Fig. 6A). *AtIREG1* was highly overexpressed in both roots and shoots of the line 3G. Line 5E showed a lower expression of *AtIREG1* than line 3G, but still the expression of *AtIREG1* was highly increased compared to the wildtype expression level. The third 35S::*AtIREG1* line 2F showed an increased expression of *AtIREG1* in roots, but no (or much lower) overexpression in shoots (Fig. 6A).

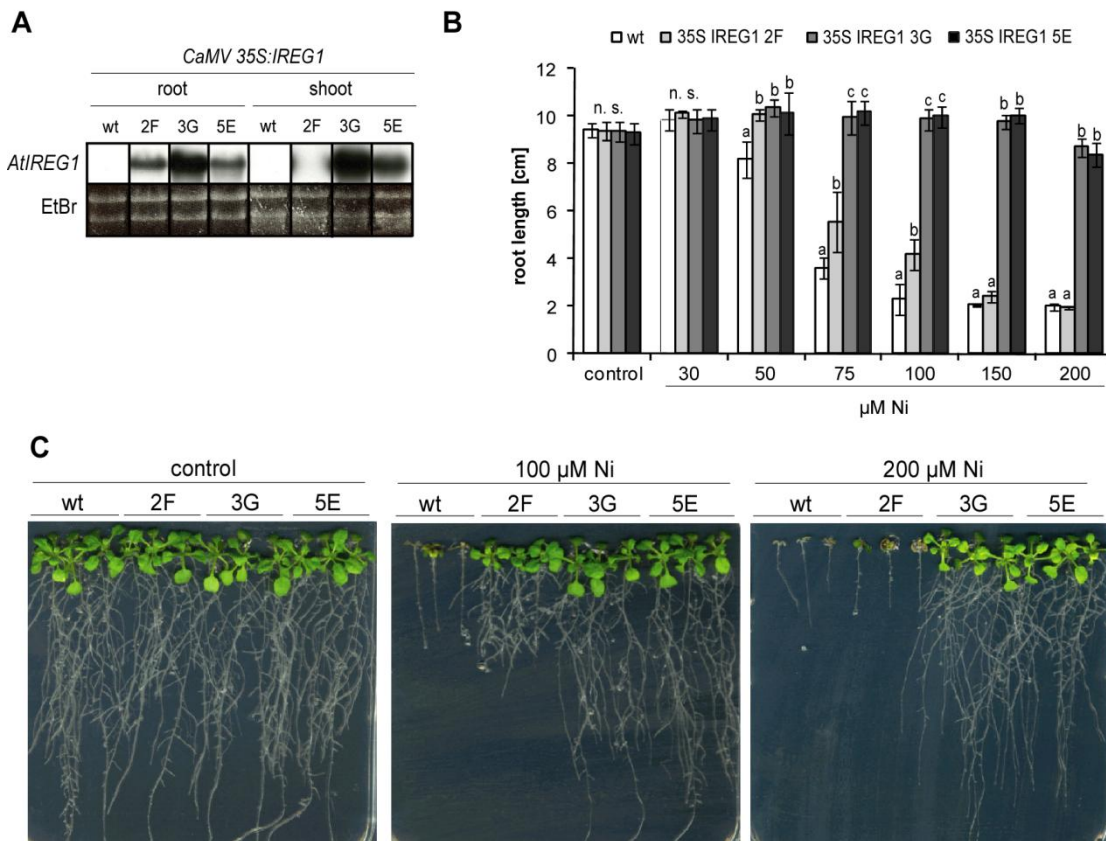


**Figure 6: Overexpression of *AtIREG1* increases nickel tolerance in Arabidopsis.**

A, RNA gel blot analysis of *AtIREG1* expression in roots of wildtype and 35S-*AtIREG1* plants (lines 2F, 3G, 5E), which were cultured for 40 days under Fe-sufficient conditions. The corresponding EtBr-stained rRNA is shown as a loading control. B, primary root length of 21-day-old wildtype and 35S-*AtIREG1* plants precultured for 7 days on half strength MS agar plates and then for 2 weeks on half strength MS agar plates with elevated supply of Ni. Significant differences at  $p < 0.01$  are indicated by different letters (n.s.: not significant),  $n = 4$ , 3 plants per replicate. C, Phenotype of the same lines, pictures of representative plates are shown.

To investigate the growth phenotype of *AtIREG1* overexpressing lines on Ni containing medium, seeds were germinated and plants were precultured on agar plates without Ni. After seven days plants of comparable root length and shoot development were transferred to vertical agar plates supplemented with 30 to 200  $\mu\text{M}$  Ni and were cultured for two more weeks (Fig. 6C). Primary root length (Fig. 6B), and root, shoot and total fresh weight (Fig. 7A-C) were determined. The root/shoot-ratio (Fig. 7D) was calculated based on root and shoot fresh weight. Wildtype plants underwent a severe reduction in root length at concentrations higher than 50  $\mu\text{M}$  Ni and a loss of biomass at concentrations above 75  $\mu\text{M}$  Ni. In contrast, the gain of primary root length and biomass was unaffected in *AtIREG1* overexpressing lines 3G and 5E even at 200  $\mu\text{M}$  Ni (Fig. 6D and 7A-C). Line 2F, which had a lower expression level of *AtIREG1* in roots compared to the other two overexpressing lines, showed an intermediate response with higher root length than wildtype plants at concentrations of 75 and 100  $\mu\text{M}$  Ni, but the same reduction of root elongation like wildtype plants at concentrations higher than 100  $\mu\text{M}$  Ni.

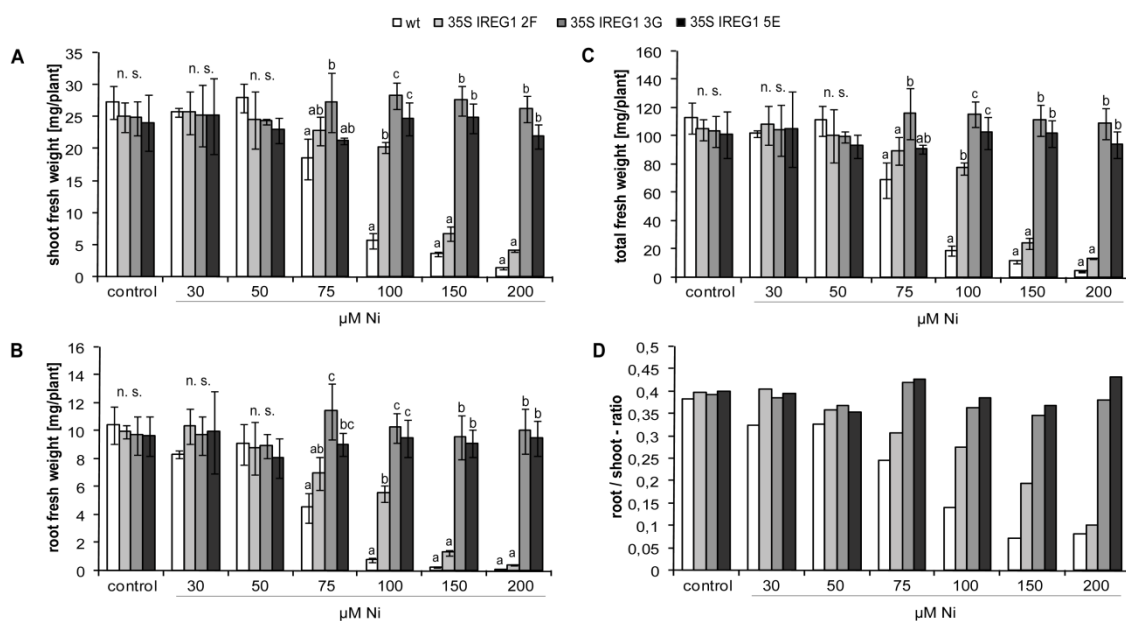


**Figure 7: Overexpression of *AtIREG1* leads to higher fresh weight production in Arabidopsis plants grown under elevated nickel concentrations**

21-day-old wildtype and *35S::AtIREG1* plants (lines 2F, 3G and 5E) were precultured for 7 days on half strength MS agar plates and then for 2 weeks on half strength MS agar plates with elevated supply of Ni. The following measures were taken: A, shoot fresh weight, B, root fresh weight C, total fresh weight (root and shoot) and D, root / shoot-ratio (based on fresh weight). Significant differences at  $p < 0.01$  are indicated by different letters (n.s.: not significant),  $n = 4$ , 3 plants per replicate.

An increased Ni tolerance of *AtIREG1* overexpressing lines became also obvious in terms of biomass production (Fig. 7): At 100  $\mu\text{M}$  Ni and above root and shoot fresh weight production was severely reduced in wildtype plants, whereas the lines 3G and 5E were still unaffected up to 200  $\mu\text{M}$  Ni supply. Again the line 2F again showed an intermediate phenotype, with an almost complete growth arrest at 150  $\mu\text{M}$  Ni. Similar results were obtained when the same lines are grown on plates containing different concentrations of Co (50 to 500  $\mu\text{M}$ , Fig. 8 and 9), but compared to the phenotype of *35S::IREG1* lines on Ni, the effect of Co on the differences between wildtype and *AtIREG1* overexpressing lines were smaller.

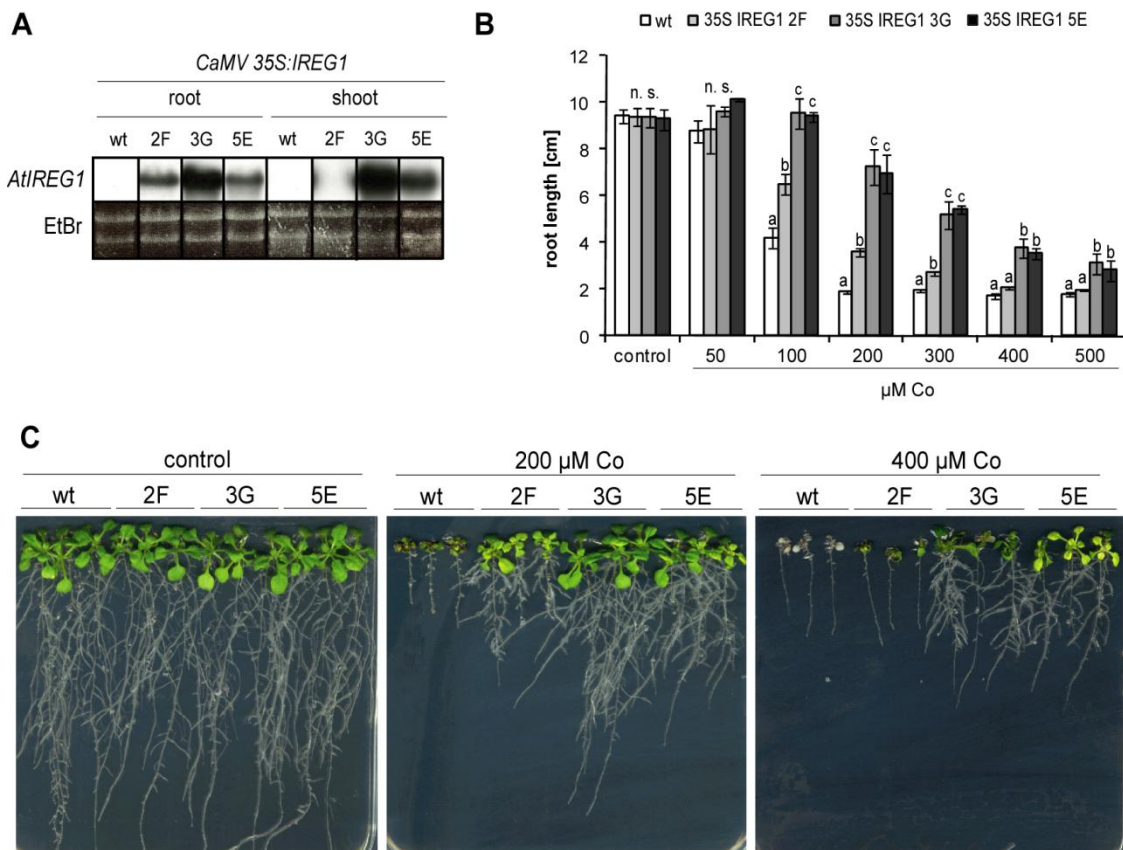


**Figure 8: Overexpression of *AtIREG1* increases cobalt tolerance in Arabidopsis.**

**A**, RNA gel blot analysis of *AtIREG1* expression in roots of wildtype and *35S::AtIREG1* plants (lines 2F, 3G, 5E), which were cultured for 40 days under Fe-sufficient conditions. The corresponding EtBr-stained rRNA is shown as a loading control. **B**, primary root length of 21-day-old wild type and *35S-AtIREG1* plants precultured for 7 days on half strength MS agar plates and then for 2 weeks on half strength MS agar plates with elevated supply of Co. Significant differences at  $p < 0.01$  are indicated by different letters (n.s.: not significant),  $n = 4$ , 3 plants per replicate. **C**, Phenotype of the same lines, pictures of representative plates are shown.

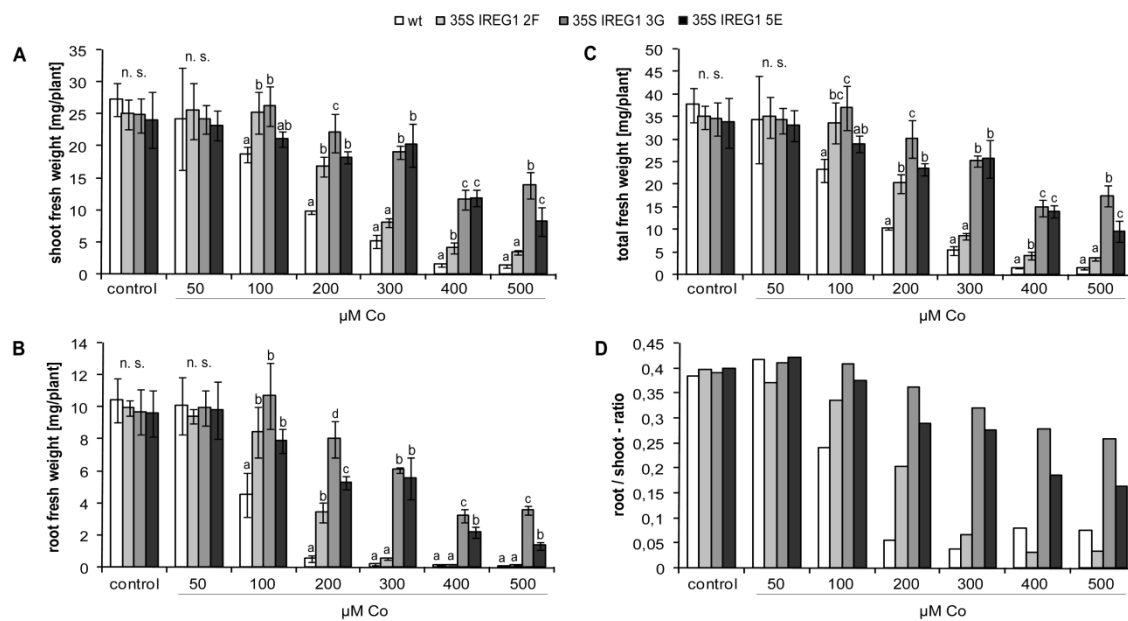


**Figure 9: Overexpression of *AtIREG1* leads to higher fresh weight production in Arabidopsis plants grown under elevated cobalt concentrations.**

21-day-old wildtype and *35S::AtIREG1* plants (lines 2F, 3G and 5E) were precultured for 7 days on half strength MS agar plates and then for 2 weeks on half strength MS agar plates with elevated supply of Co. The following measures were taken: A, shoot fresh weight, B, root fresh weight, C, total fresh weight (root and shoot) and D, root / shoot-ratio (based on fresh weight). Significant differences at  $p < 0.01$  are indicated by different letters (n.s.: not significant),  $n = 4$ , 3 plants per replicate.

The root/shoot-ratio of *35S::IREG1* lines was higher than that of wildtype plants at concentrations above  $75 \mu\text{M Ni}$  or  $100 \mu\text{M Co}$ , because in wildtype plants root biomass production was more affected than shoot biomass production by elevated metal concentrations. In *AtIREG1* overexpressing lines differences between root and shoot growth appeared at higher metal concentrations than in wildtype. *35S::IREG1* lines show no alteration in root/shoot-ratio up to  $200 \mu\text{M Ni}$  (Fig. 7D), whereas the root/shoot-ratio of the same lines is slowly decreasing at Co concentrations higher than  $100 \mu\text{M}$  (Fig. 9D). The line 2F with a lower level of overexpression showed ratios between those of wildtype plants and the two strong overexpressor lines 3G and 5E, supporting the notion that the root/shoot-ratio is a sensitive measure for metal tolerance as it is closely correlated with the level of *AtIREG1* gene expression.

### 4.2.3 Characterization of the growth phenotype of *AtIREG1* T-DNA insertion lines

Two independent T-DNA insertion lines (SALK\_016176 and SALK\_013005) were obtained from the SALK collection (Alonso et al., 2003) and named *ireg1-1* and *ireg1-2*, respectively. One of the lines carries a T-DNA insertion in the 5'-UTR, the other line in the second exon (Fig. 10). Homozygosity was verified by segregation and PCR analysis and plants from the T3 generation were used for further experiments.

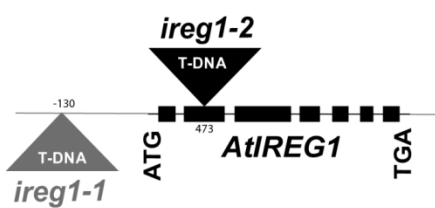


**Figure 10: Scheme of the T-DNA integration sites in *ireg1-1* (SALK\_016176) and *ireg1-2* (SALK\_013005).** The location of the T-DNA insertions is indicated by triangles. The insertion in *ireg1-1* is located 130 bp upstream of the transcription start, the insertion in *ireg1-2* is located 473 bp downstream of the transcription start in the second exon.

Expression of *AtIREG1* could not be detected by RT-PCR in both T-DNA insertion lines (*ireg1-1* and *ireg1-2*, Fig. 4 and 11A). Under normal growth conditions in soil, on plates or in hydroponic culture *ireg1-1* and *ireg1-2* showed no growth differences compared to wildtype plants. However, when seeds of transgenic lines were germinated on agar plates, that were supplemented with different metals (Ni, Co, Mn, Zn, Cu, Fe in concentrations from low to toxic) a conditional phenotype of the T-DNA insertion lines was detected in plants grown on Ni- or Co-supplemented medium (data not shown). On the other tested metals visual differences could not be detected, irrespective of whether root elongation, root branching, chlorophyll content or shoot development (number and size of leaves) was determined. To further analyze and quantify the phenotype of the T-DNA insertions lines on Ni, seeds of wildtype, *ireg1-1* and *ireg1-2* plants were germinated on agar plates with standard half strength MS medium. After 7 days plants of comparable shoot development and root length were transferred to vertically oriented square agar plates supplemented with Ni at concentrations from 20 to 100  $\mu$ M (Fig. 11). *AtIREG1* T-DNA insertion lines were more sensitive to high Ni concentrations in the medium than wildtype plants (Fig. 11C). At a concentration of 60  $\mu$ M Ni primary root length of wildtype plants was only slightly affected, whereas the root length of *ireg1-1* and *ireg1-2* was decreased to 50% compared to the control treatment without supplemented Ni (Fig. 11B).

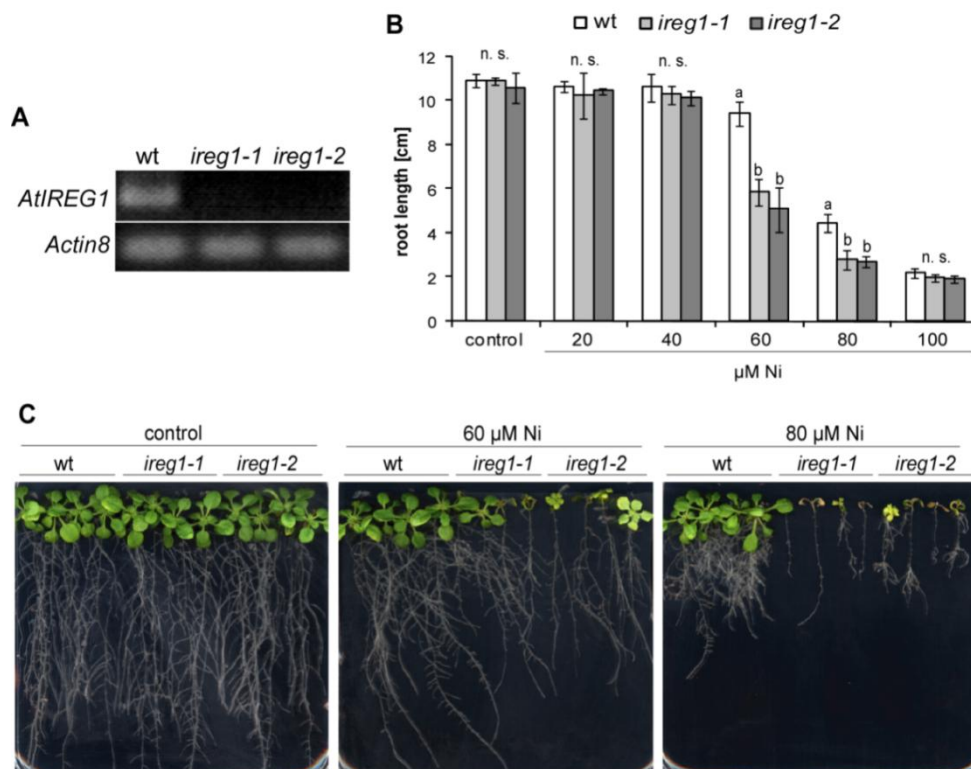


**Figure 11: Loss of *AtIREG1* increases nickel sensitivity in *Arabidopsis*.**

**A**, RT-PCR of *AtIREG1* expression in roots of wildtype and *AtIREG1* T-DNA insertion lines (lines *ireg1-1* and *ireg1-2*) which were cultured for 40 days under Fe-sufficient conditions. The corresponding RT-PCR of *Actin8* is shown as a control. **B**, primary root length of 21-day-old wild type and *AtIREG1* T-DNA insertion lines precultured for 7 days on half strength MS agar plates and then for 2 weeks on half-strength MS agar plates with elevated supply of Ni. Significant differences at  $p < 0.01$  are indicated by different letters (n.s.: not significant),  $n = 4$ , 4 plants per replicate. **C**, Phenotype of the same lines, pictures of representative plates are shown.

Visually, *AtIREG1* T-DNA insertion lines did not only show a decrease in root length, but also less root and shoot biomass than wildtype plants, when grown on Ni concentrations of 60  $\mu\text{M}$  or higher (Fig. 11C). Quantification of fresh weight (Fig. 12) showed a decrease in both root and shoot biomass of the T-DNA insertions lines compared to wildtype plants at Ni concentrations above 60  $\mu\text{M}$ . No clear differences in the root/shoot-ratio (based on fresh weight) were determined, because root and shoot growth were affected to a similar extent in the T-DNA insertion lines. For example, at a concentration of 60  $\mu\text{M}$  Ni root and shoot fresh weight were decreased by approximately 60 % relative to the control.

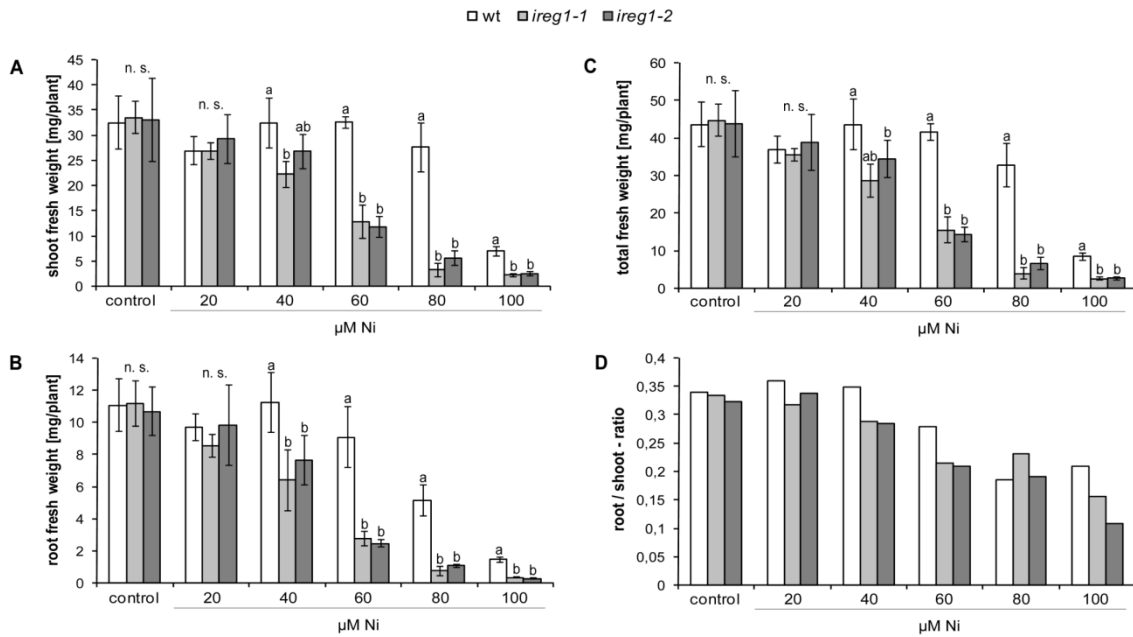


**Figure 12: Loss of *AtIREG1* leads to reduced fresh weight in Arabidopsis under elevated nickel supply.**

21-day-old wildtype and *AtIREG1* T-DNA insertion lines (*ireg1-1* and *ireg1-2*) were precultured for 7 days on half strength MS agar plates and then for 2 weeks on half strength MS agar plates with elevated supply of Ni. The following measures were taken: A, shoot fresh weight, B, root fresh weight C, total fresh weight (root and shoot) and D, root/shoot-ratio. Root/shoot-ratio is based on fresh weight. Significant differences at  $p < 0.01$  are indicated by different letters (n.s.: not significant),  $n = 4$ , 4 plants per replicate.

*AtIREG1* T-DNA insertion lines also showed differences compared to wildtype plants when grown on agar plates supplemented with Co, but primary root length (Fig. 13B) was affected to a lower extent than in the experiments with Ni (Fig. 11B). A significant difference between wildtype and *AtIREG1* T-DNA insertion lines could only be found at a concentration of 75  $\mu\text{M Co}$ , but not on plates supplemented with higher or lower Co concentrations. When *ireg1-1* and *ireg1-2* plants are grown on plates containing 150  $\mu\text{M Co}$  (Fig. 13C), the primary root length of the *AtIREG1* T-DNA insertion lines was comparable to that of wildtype plants, but *ireg1-1* and *ireg1-2* showed a lower number and a decreased length of lateral roots. The increased Co sensitivity of *AtIREG1* T-DNA insertion lines compared to wildtype plants also expressed in a stronger chlorosis of transgenic lines. Leaves of *ireg1-1* and *ireg1-2* were more chlorotic when grown on plates supplemented with 75  $\mu\text{M Co}$ , while leaves of wildtype plants on the same plates remained green (Fig. 13C, 75  $\mu\text{M Co}$ ).

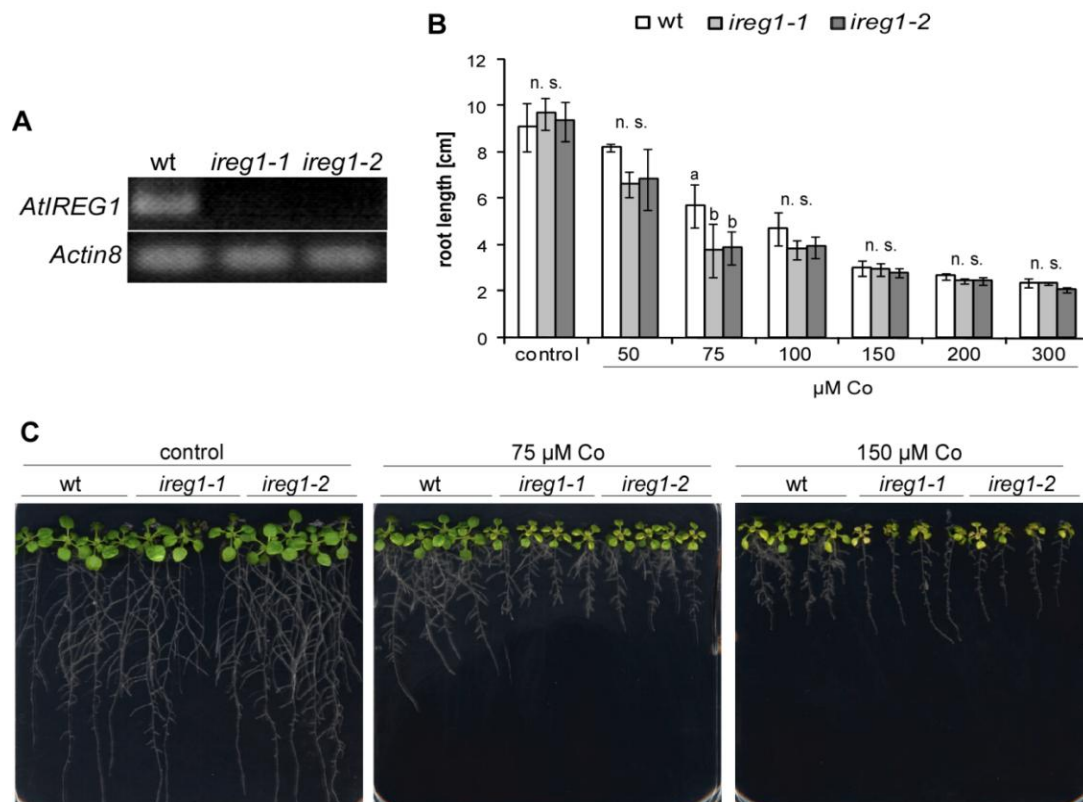


**Figure 13: Loss of *AtIREG1* increases cobalt sensitivity in Arabidopsis.**

**A**, RT-PCR of *AtIREG1* expression in roots of wildtype and *AtIREG1* T-DNA insertion lines (lines *ireg1-1* and *ireg1-2*) which were cultured for 40 days under iron-sufficient conditions. The corresponding RT-PCR of *Actin8* is shown as a control. **B**, primary root length of 21-day-old wild type and *AtIREG1* T-DNA insertion lines precultured for 7 days on half strength MS agar plates and then for 2 weeks on half strength MS agar plates with elevated supply of Co. Significant differences at  $p < 0.01$  are indicated by different letters (n.s.: not significant),  $n = 4$ , 4 plants per replicate. **C**, Phenotype of the same lines, pictures of representative plates are shown.

When the fresh weight of wildtype, *ireg1-1* and *ireg1-2* plants was quantified at a Co supplementation of 150 μM (Fig. 14), root biomass of *AtIREG1* T-DNA insertions lines was only 50 % of that of wildtype plants. Significant decreases in shoot fresh weight of *ireg1-1* and *ireg1-2* were found at 200 and 300 μM Co. At 150 μM Co root/shoot-ratio was lower in *AtIREG1* T-DNA insertions lines, but this effect was reversed at concentrations of 200 μM Co or higher, where wildtype plants had a lower root/shoot-ratio than the two transgenic lines. This is due to the fact that root fresh weight was affected already at lower Co supply than shoot fresh weight.

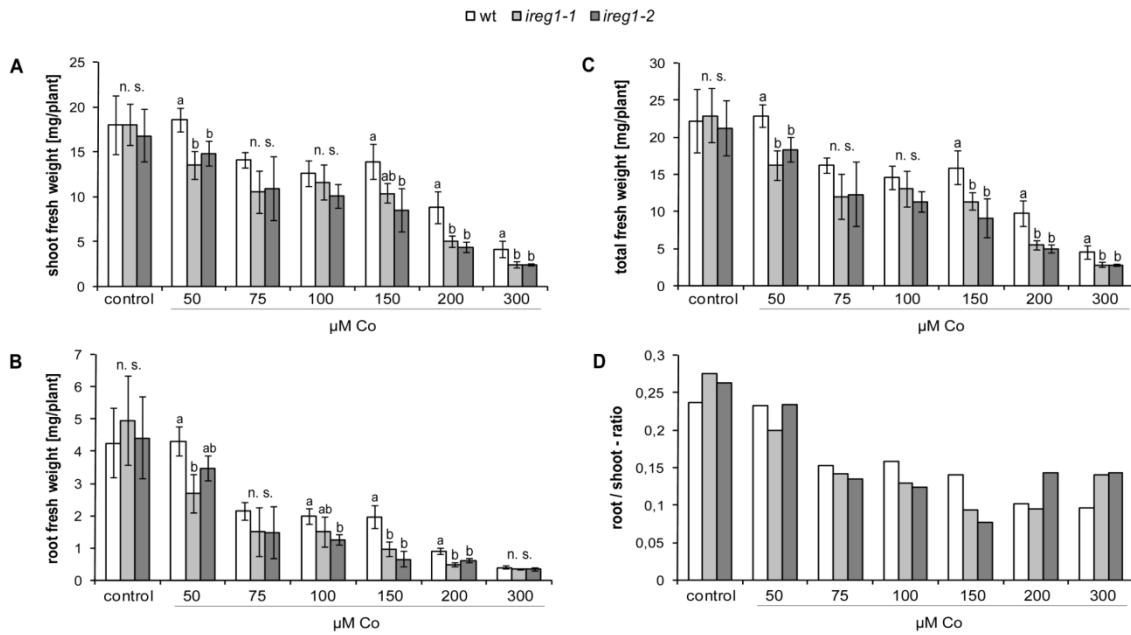


**Figure 14: Loss of *AtIREG1* leads to reduced fresh weight in Arabidopsis under elevated cobalt supply.**

21-day-old wildtype and *AtIREG1* T-DNA insertion lines (*ireg1-1* and *ireg1-2*) were precultured for 7 days on half strength MS agar plates and then for 2 weeks on half strength MS agar plates with elevated supply of Co. The following measures were taken: A, shoot fresh weight, B, root fresh weight C, total fresh weight (root and shoot) and D, root/shoot-ratio. Root/shoot-ratio is based on fresh weight. Significant differences at  $p < 0.01$  are indicated by different letters (n.s.: not significant),  $n = 4$ , 4 plants per replicate.

### Iron dependency of the nickel tolerance of *AtIREG1* T-DNA insertion lines

In the following experiments the question was addressed whether the increased Ni sensitivity of *AtIREG1* T-DNA insertion lines is affected by the Fe nutritional status of the plants. *Ireg1-1*, *ireg1-2* and wildtype plants were precultured on Fe-sufficient medium and then transferred to Fe-sufficient or Fe-deficient medium. Preculture on Fe-sufficient medium was necessary to provide a basic Fe supply to the seedlings to avoid a complete arrest of plant growth already a few days after germination. Plants grown on Fe-deficient medium showed symptoms of Fe deficiency, but no differences in plant development. Agar plates with Fe-deficient and Fe-sufficient medium were then supplemented with increasing concentrations of Ni to determine root length (Fig. 15) and fresh weight (Fig. 16).

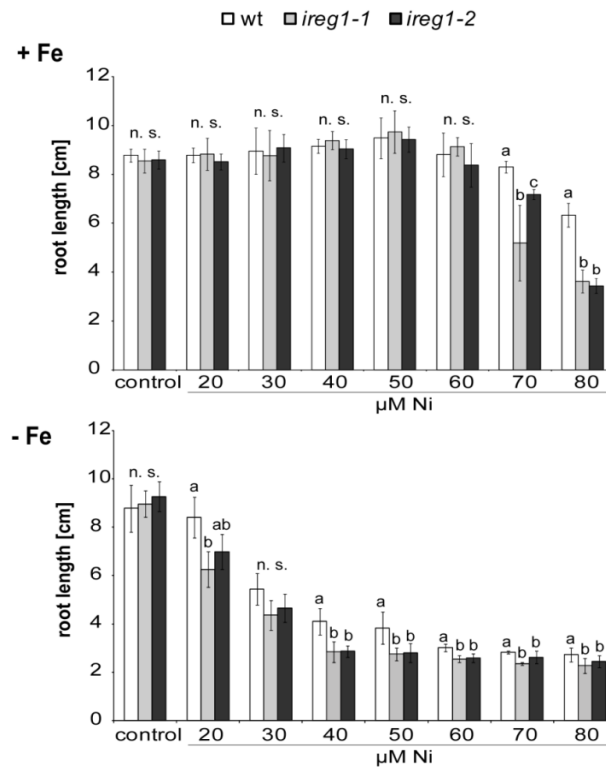


**Figure 15: Nickel sensitivity of *AtIREGI* T-DNA insertion lines is not dependent on iron supply.**

Quantitative analysis of primary root length of wildtype and *AtIREGI* T-DNA insertion lines (*ireg1-1* and *ireg1-2*) precultured for 7 days on Fe-adequate (75 µM Fe-EDTA) half strength MS agar plates and then for 2 weeks on Fe-adequate (75 µM Fe-EDTA, upper graph) or Fe-deficient half strength MS agar plates (lower graph) supplied with different concentrations of Ni. Significant differences at  $p < 0.01$  are indicated by different letters (n.s.: not significant),  $n = 4$ , 4 plants per replicate.

Wildtype plants and the two T-DNA insertion lines *ireg1-1* and *ireg1-2* showed a similar primary root length and no differences to the control plants up to Ni concentrations of 60 µM, as long as Fe supply was adequate (+Fe treatment in Fig. 15). When the same lines were grown on Fe-deficient medium, a reduction in primary root length could be detected at a much lower Ni concentrations and also differences of the transgenic lines compared to wildtype plants were found at lower Ni concentrations (40 µM) relative to Fe-sufficient plants. This goes along with the long known phenomenon that plants grown under Fe-deficient growth conditions are more sensitive to Ni, due to an increased Ni uptake. This effect will be discussed later (chapter 5.5). The differences in primary root length of wildtype plants compared to *AtIREGI* T-DNA insertion lines were lower on Fe-deficient medium. The primary root length of *ireg1-1* and *ireg1-2* accounted for approx. 60 % of the wildtype root length on Fe-sufficient medium supplied with 80 µM Ni. The largest difference in root length between wildtype and

*AtIREG1* T-DNA insertion lines was found on Fe-deficient agar plates supplemented with 40  $\mu\text{M}$  Ni where the root length of *ireg1-1* and *ireg1-2* plants was only 25 % of that of wildtype plants.

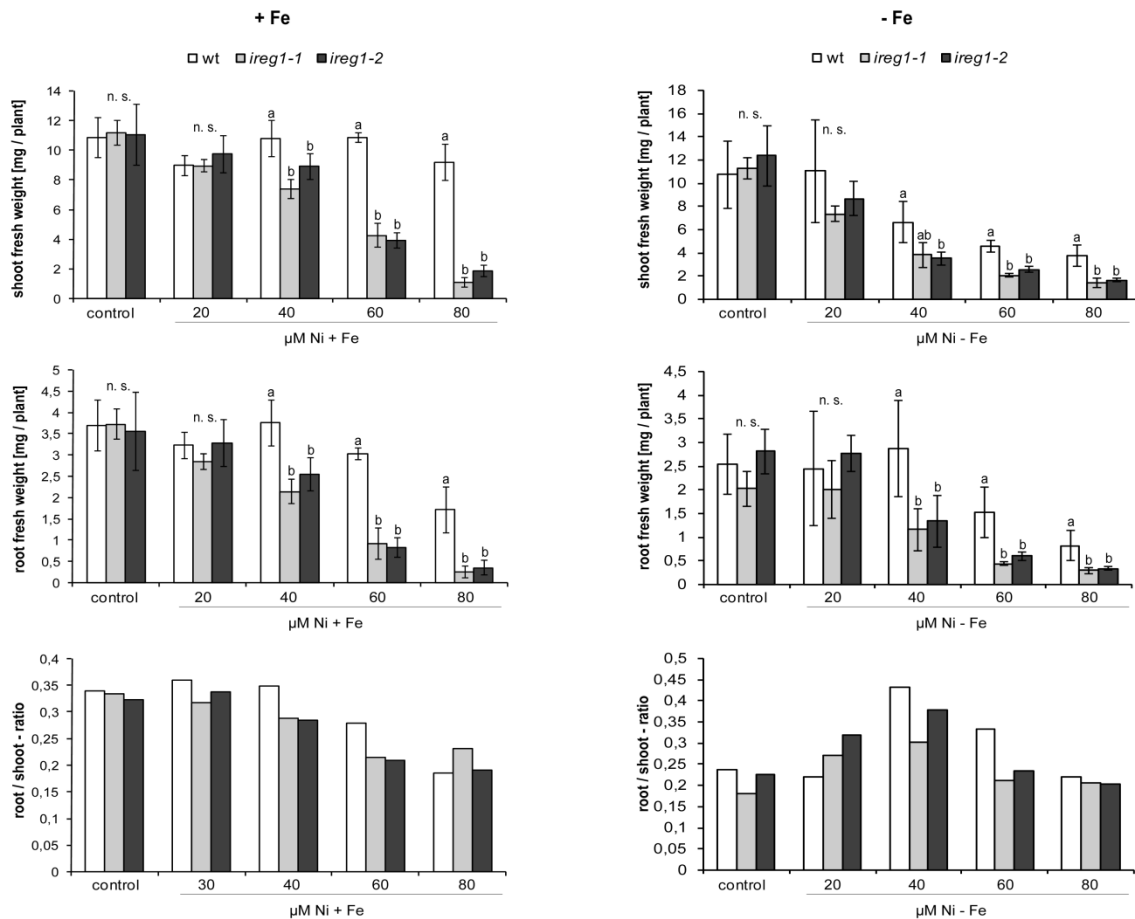


**Figure 16: Nickel sensitivity of *AtIREG1* T-DNA insertion lines is not dependent on iron supply.**

Quantitative analysis of root and shoot fresh weight of wildtype and *AtIREG1* T-DNA insertion lines (lines *ireg1-1* and *ireg1-2*) precultured for 7 days on Fe-adequate (75  $\mu\text{M}$  Fe-EDTA) half strength MS agar plates and then for 2 weeks on Fe-adequate (75  $\mu\text{M}$  Fe-EDTA, left) or Fe-deficient half strength MS agar (right) supplied with different concentrations of Ni. Significant differences at  $p < 0.01$  are indicated by different letters (n.s.: not significant),  $n = 4$ , 4 plants per replicate.

In the same lines and treatments also root and shoot fresh weights as well as the root/shoot-ratio were determined (Fig. 16). Again, the same conclusions could be drawn from the analysis of primary root length: Ni sensitivity appeared at lower Ni concentrations in all lines when grown on Fe-deficient medium. A comparison of the shoot fresh weight clearly showed that the Ni-induced decrease in fresh weight of *AtIREG1* T-DNA insertion lines compared to wildtype plants was not higher under Fe-deficient conditions. While the shoot biomass of *ireg1-1* and *ireg1-2* decreased to

10 - 15% of that of the wildtype at 80  $\mu\text{M}$  Ni under Fe-sufficient growth conditions, the strongest effect on Fe-deficient medium (also at 80  $\mu\text{M}$  Ni) only caused a reduction to 35% of the shoot biomass of the wildtype. A similar pattern was also found in the root biomass, indicating that the impact of AtIREG1-mediated Ni sensitivity does not increase (or does probably even decrease) with Fe deficiency. A comparison of root/shoot-ratio did not provide additional information. On agar plates supplied with adequate Fe the root/shoot-ratio decreased steadily with increasing Ni concentrations, whereas on Fe-deficient growth medium it was higher at 40  $\mu\text{M}$  Ni compared to all other Ni concentrations.

#### 4.2.4 Localization of AtIREG1 proteins and *AtIREG1* expression in Arabidopsis

Before the start of the work presented in this thesis, previous experiments had been undertaken by Gabriel Schaaf (University of Hohenheim, Stuttgart) to examine the intracellular localization of AtIREG1 *in planta*. A GFP cDNA was fused to the 3'-end of AtIREG1 and set under control of a 35S promoter. The construct was used for transient expression in *Arabidopsis thaliana* protoplasts derived from suspension cell cultures.

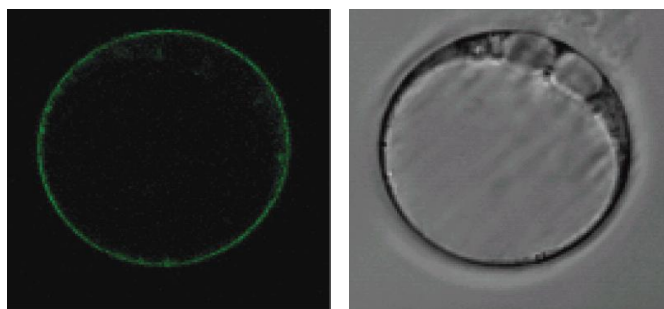


**Figure 17: Plasma membrane localization of GFP-fused AtIREG1.**

*Left*, GFP-derived fluorescence from protoplasts transformed with pCF203-AtIREG1-GFP. *Right*, phase contrast view. Protoplasts derived from a dark-adapted *Arabidopsis* cell suspension culture and were assayed by confocal laser scanning microscopy. Pictures kindly provided by Gabriel Schaaf (University of Hohenheim, Stuttgart).

By confocal laser scanning microscopy, AtIREG1-dependent green fluorescence was observed along the border of the protoplast, indicating plasma membrane localization (Fig. 17, only one representative picture is shown). To verify this result *in planta*, Arabidopsis wildtype plants were transformed with the same construct. Unfortunately, no GFP signal could be detected in the selected lines. The construct was then re-sequenced, but the 35S promoter, as well as the *AtIREG1* ORF and the *GFP* cDNA were confirmed in the correct orientation and sequence. To test the functionality of the AtIREG1-GFP fusion protein derived from the described construct, the *AtIREG1-GFP* cassette was re-cloned and set under the control of the native *AtIREG1* promoter. *Ireg1-1* plants lacking the expression of *AtIREG1* were transformed and transformants were selected and grown together with wildtype and *ireg1-1* plants on Ni-supplemented plates. *Ireg1-1* plants were more sensitive to Ni than wildtype plants (Fig. 11). Transformation of *ireg1-1* with the 35S-AtIREG1-GFP fusion construct resulted in a complementation of the Ni-sensitive phenotype and restored the wildtype phenotype (data not shown). This growth phenotype confirmed functionality of the AtIREG1-GFP fusion. However, no GFP-derived fluorescence could be detected microscopically in these lines, rising doubts whether the protein was correctly fused to GFP, although the same construct was already successfully used for protoplast transformation (Fig. 17). Due to time constraints the detection of GFP in these lines (either by detection of an altered transcript length by northern blotting or by detection of the GFP protein using a specific antibody) could not be carried out before completion of the present thesis. Another explanation might be a low expression level of *AtIREG1*, or an expression that was restricted to a certain tissue or cell type in Arabidopsis, which is more difficult to detect by fluorescence or confocal microscopy.

To determine the cell-type specific promoter activity of the *AtIREG1* promoter, the native *AtIREG1* promoter was fused with a *GFP* or a *GUS* (beta-glucuronidase) cDNA for transformation of Arabidopsis plants. However, also in these lines no GFP signal or GUS staining was detected, possibly due to the low expression level of *AtIREG1*. The design and validation of a specific antibody against AtIREG1, that could be used for immunohistochemical detection of AtIREG1 was not successful.

## 4.2.5 Influence of *AtIREG1* expression level on nickel and cobalt transport and distribution *in planta*

### 4.2.5.1 Nickel and cobalt accumulation in dependency on *AtIREG1* expression level

As the phenotype of transgenic lines either lacking the expression of *AtIREG1* or overexpressing *AtIREG1* pointed to a function of *AtIREG1* in Ni and Co transport, the accumulation of these two metals in dependence of *AtIREG1* was assessed. For this purpose, wildtype plants, two *AtIREG1* T-DNA insertion lines (*ireg1-1* and *ireg1-2*) and two *AtIREG1* overexpressing lines (35S IREG1 3G and 5E) were precultured on nutrient solution for 5 weeks, continued to grow on nutrient solution supplemented with 10 or 30  $\mu\text{M}$  Ni or Co for 5 days and metal concentrations in roots and shoots were determined (Fig. 18). Germination of line 35S IREG1 5E was not optimal which resulted in a decreased number of plants, so that this line could only be analysed in the 10  $\mu\text{M}$  Ni and 10  $\mu\text{M}$  Co treatments.

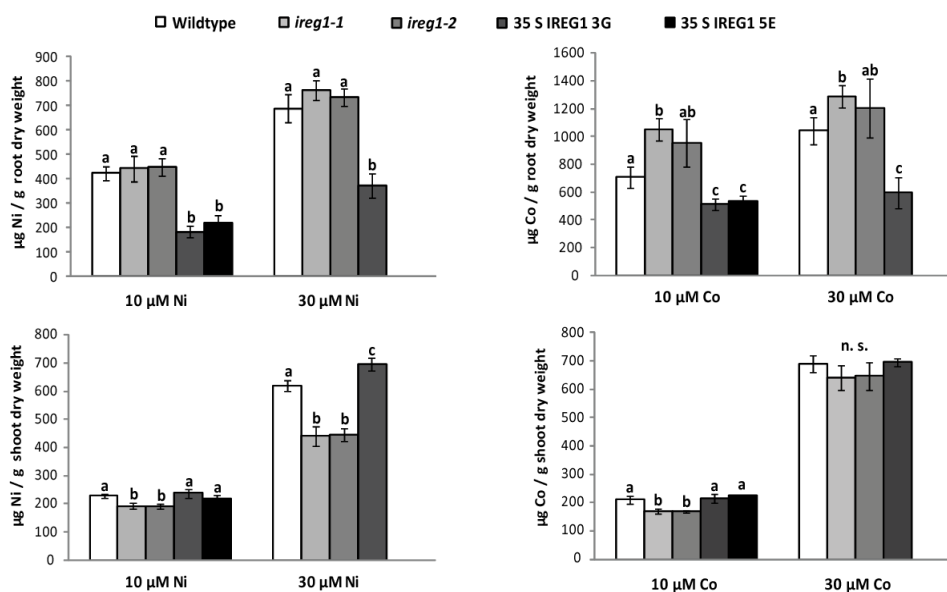


**Figure 18: Changes in *AtIREG1* expression affects nickel and cobalt concentrations in Arabidopsis.** Concentrations of Ni (left) and Co (right) in roots (upper graphs) and shoots (lower graphs) of 42 d old wildtype, *AtIREG1* T-DNA insertion lines (*ireg1-1* and *ireg1-2*) and the *AtIREG1*-overexpressing lines 3G and 5E, which were cultured for 5 days on nutrient solution supplied with 10 or 30  $\mu\text{M}$  Ni. Significant differences at  $p < 0.01$  are indicated by different letters (n.s.: not significant),  $n = 4$ , 3 plants per replicate.

Concentrations of both Ni and Co were lower in roots of *AtIREG1* overexpressing lines compared to those of wildtype plants (Fig. 18). In shoots the concentration of Ni was lower in *AtIREG1* T-DNA insertion lines than in the wildtype. This was also the case for Co, but to a lower extent and only visible in the low Co (10  $\mu\text{M}$ ) treatment. Thus, under exposure to elevated Ni concentrations *AtIREG1* appeared to decrease root but increase shoot concentrations of Ni. Values were also calculated for the accumulation of Ni and Co in these samples ( $\mu\text{g}$  metal per plant, data not shown), which resulted in the same pattern and same significances.

#### 4.2.5.2 Metal concentrations in Arabidopsis xylem exudates in dependency on *AtIREG1* expression

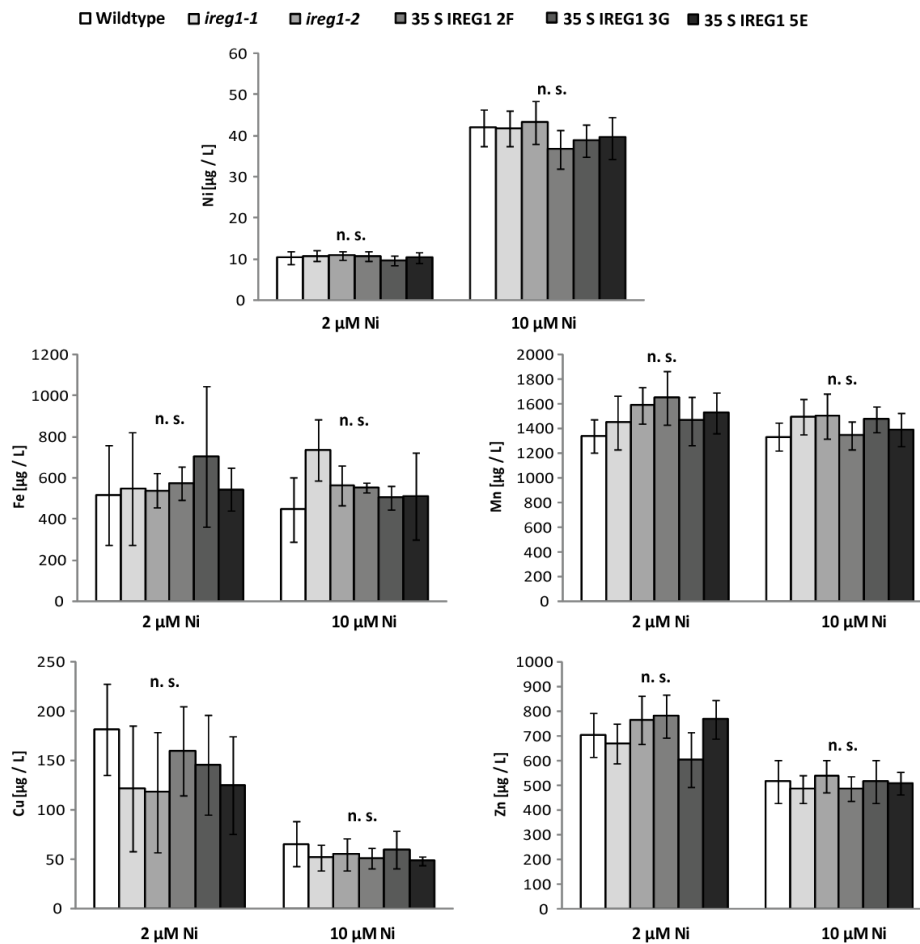


**Figure 19: Changes in *AtIREG1* expression do not affect metal concentrations in Arabidopsis xylem exudate.**

Concentrations of Ni, Fe, Mn, Cu and Zn in xylem sap of wildtype, *AtIREG1* T-DNA insertion lines (*ireg1-1* and *ireg1-2*) and the *AtIREG1*-overexpressing lines 2F, 3G and 5E, which were set on nutrient solution supplied with 2 or 10  $\mu\text{M}$  Ni 14 h before collection of xylem exudate. Exudate was collected for 3 h. No significant differences were detected (n.s.: not significant),  $n = 5$ , 5 plants per replicate.

The observation that loss of *AtIREG1* caused decreased Ni concentrations in shoots, whereas overexpression of *AtIREG1* lowered Ni concentration in roots could be due to a Ni loading function of *AtIREG1* into the xylem. Therefore, hydroponically grown *Arabidopsis* plants were placed on nutrient solution supplemented with 2 or 10  $\mu\text{M}$  Ni 14 hours before collection of xylem sap. Directly after onset of light xylem exudates were collected for 3 h. Potassium concentrations in the xylem sap were used to normalize the values of metal concentrations in xylem exudates. Ni, Fe, Mn, Cu and Zn concentrations were measured in xylem exudates of wildtype, two *AtIREG1* T-DNA insertion lines (*ireg1-1* and *ireg1-2*) and three *AtIREG1* overexpressing lines (35S IREG1 2F, 3G and 5E). No significant differences between lines could be found (Fig. 19). A fivefold higher Ni concentration in the medium resulted in approximately fourfold higher Ni concentrations in xylem exudates. Fe and Mn concentrations were similar in plants grown on nutrient solution supplemented with either 2 or 10  $\mu\text{M}$  Ni. Concentrations of Cu and Zn were higher in the 10  $\mu\text{M}$  Ni treatment than in the 2  $\mu\text{M}$  Ni treatment. Root and shoot fresh and dry weight of the used plants was determined, no significant differences were found (data not shown).

#### 4.2.5.3 Root metal efflux

To test whether a loss of *AtIREG1* can cause changes in the efflux of Ni and Co from *Arabidopsis* roots, wildtype and *AtIREG1* T-DNA insertion lines were grown in hydroponic culture and cultured for four days on nutrient solution supplied with 10  $\mu\text{M}$  Ni or 10  $\mu\text{M}$  Co. Roots of those Ni- or Co-loaded plants were washed to remove apoplastic metals, and plants were transferred to diluted nutrient solution for 8 hours, in which Ni and Co concentrations were measured (Fig. 20). No significant differences were found in Ni efflux between wildtype plants and *AtIREG1* T-DNA insertion lines, but in tendency Ni efflux from roots of *ireg1-1* and *ireg1-2* plants was higher. Line *ireg1-1* showed a significantly higher efflux of Co than the wildtype, but this observation could not be reproduced in line *ireg1-2*.

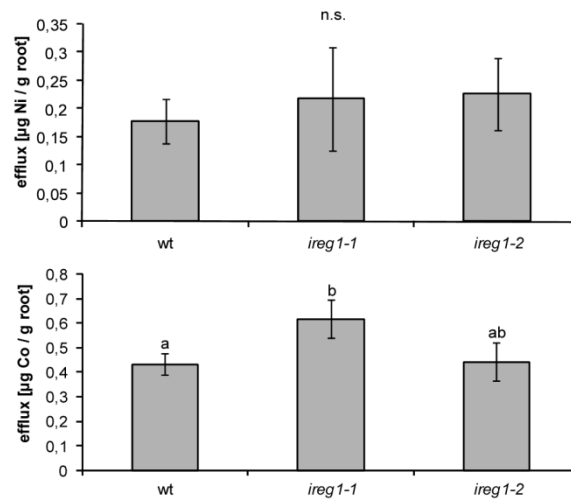


**Figure 20: Loss of AtIREG1 does not clearly influence Ni and Co efflux from Arabidopsis roots.**

40 d old wildtype and *AtIREG1* T-DNA insertion lines (*ireg1-1* and *ireg1-2*) that were grown in hydroponic culture were cultured for 4 d on nutrient solution supplied with 10 µM Ni or 10 µM Co. After washing of roots single plants were transferred to 4.5 mL 1:10 diluted nutrient solution. After 8 h Ni or Co concentrations in this solution was detected. Significant differences at  $p < 0.01$  are indicated by different letters (n.s.: not significant),  $n = 4$ , 1 plant per replicate.

A significant higher efflux of Co but not of Ni in *ireg1-1* goes along with the results of the accumulation experiments (Fig. 18). *AtIREG1* T-DNA insertion lines showed no significant differences in the Ni concentration in root tissue, but line *ireg1-1* accumulated more Co in roots than the wildtype.

#### 4.2.5.4 Urease as a means to assess nickel availability in the cytoplasm

As different approaches to localize AtIREG1 protein at the subcellular level were not successful (see chapter 4.2.4), a physiological approach was undertaken to confirm the plasma membrane localization of AtIREG1. Phenotypes of *AtIREG1* T-DNA insertion lines and overexpressing lines pointed to a Ni transport function of AtIREG1 (chapter 4.4.2 and 4.4.3). Ni is an irreplaceable component of the urea hydrolyzing enzyme urease, which is a soluble enzyme that is active in the cytoplasm and allows the use of urea as a nitrogen (N) source. Urea N can be assimilated exclusively by urease in higher plants, the released ammonia is then incorporated into organic compounds mainly by glutamine synthetase. Thus, urease activity might be used as a bioindicator for Ni availability in the cytoplasm. If AtIREG1 mediates export of Ni from the cytoplasm it

should also influence the activity of urease and thereby the growth of plants on urea as a sole nitrogen source.

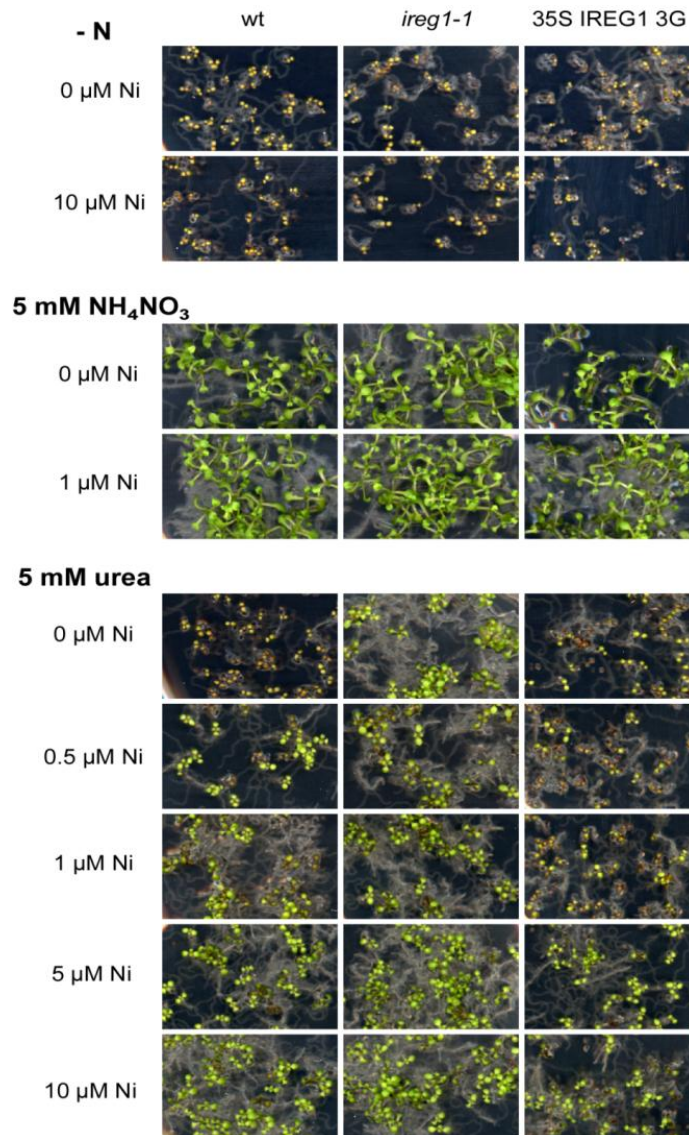


**Figure 21: Nickel transport via *AtIREG1* decreases nickel availability for urea hydrolysis.**

Phenotype of wildtype, an *AtIREG1* T-DNA insertion line (*ireg1-1*) and an *AtIREG1* overexpressing line (35S IREG1 3G), germinated and grown for 9 days on medium without N source (-N), 5 mM  $\text{NH}_4\text{NO}_3$  or 5 mM urea, supplemented with different concentrations of Ni.

To test this hypothesis, in a first screening wildtype, an *AtIREG1* T-DNA insertion line and an *AtIREG1* overexpressing line were germinated on agar plates supplemented with different concentrations of Ni and urea as the sole nitrogen source (Fig. 21). As controls agar plates with ammonium nitrate were used to verify an equal growth of lines under

standard N supply, and agar plates without N supply were used as controls to examine the phenotypes of lines under N deficiency. This first test showed clear growth differences when plants were germinated on urea containing medium without additional addition of Ni (Fig. 21). When no additional Ni was added to the plates, wildtype plants showed a growth similar to that without N supply, indicating that these plants could not use the provided urea as a nitrogen source due to the low availability of Ni in the medium. Traces of Ni in these plates most likely derived from the chemicals used to prepare the half-strength MS (Murashige & Skoog) agar plates. However, these traces of Ni were apparently sufficient to enable growth of the *AtIREGI* T-DNA insertion line *ireg1-1* (Fig. 21), which showed better shoot development, greener leaves and longer roots, similar to the growth of wildtype plants on 1  $\mu\text{M}$  Ni. In accordance with these findings, the *AtIREGI* overexpressing line grew worse than the wildtype and still showed strong symptoms of N deficiency (brown plants and reduced growth) up to concentrations of 1  $\mu\text{M}$  Ni. All lines showed similar germination rates and comparable growth on ammonium nitrate.

To quantify these results another experiment was set up. Wildtype and transgenic lines were precultured on plates with ammonium nitrate and after seven days plants were transferred to medium with urea as the only nitrogen source and with addition of different Ni concentrations (Fig. 22). Root length of all lines was similar (data not shown), but significant differences were determined in shoot and root fresh weights. On urea medium supplemented with 0.5  $\mu\text{M}$  Ni the *AtIREGI* T-DNA insertion lines showed a better developed root system with more extended root branching, longer lateral roots and more root hairs than the wildtype (Fig. 22B). Differences among these lines were even more pronounced regarding the root fresh weight. At concentrations of 0.25, 0.5 and 1  $\mu\text{M}$  Ni the *AtIREGI* T-DNA insertions lines showed a significantly higher root fresh weight than wildtype plants, but the wildtype caught up at a concentration of 5  $\mu\text{M}$  Ni.

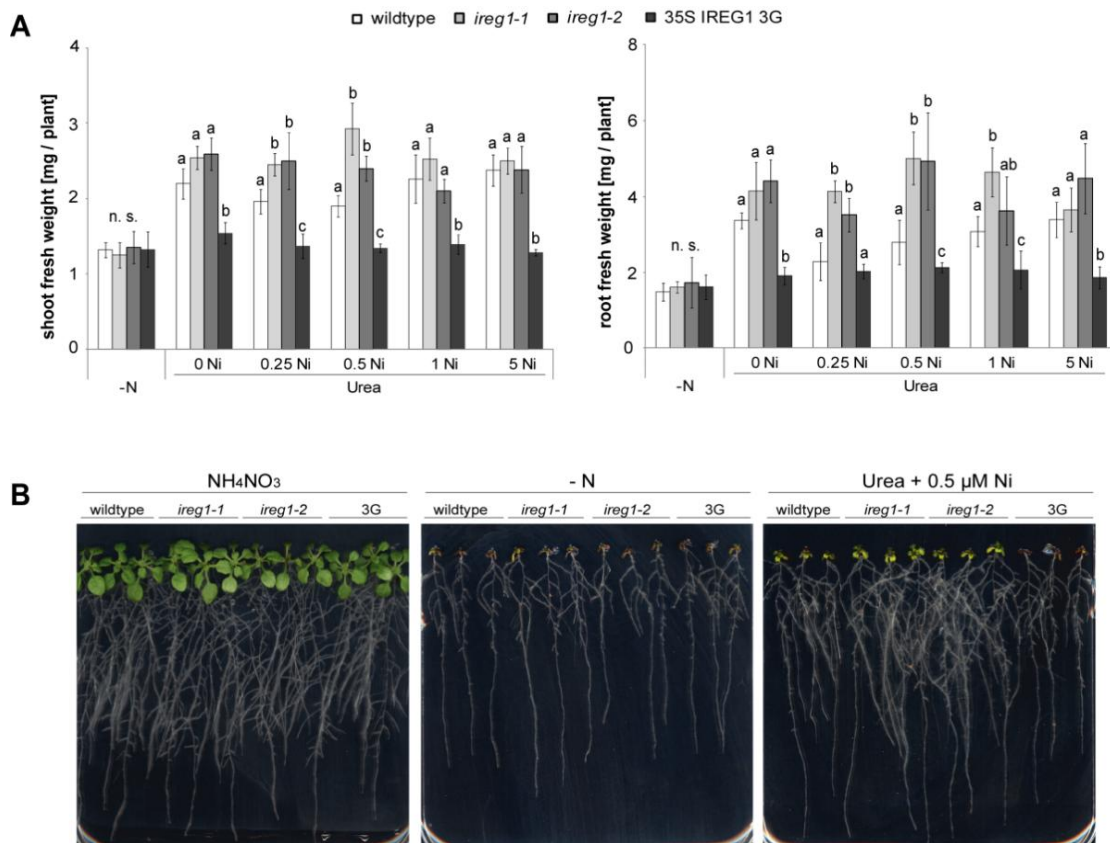


**Figure 22: Nickel transport via *AtIREG1* decreases nickel-availability for urea hydrolysis.**

*A*, root and shoot fresh weight of 21-day-old wild type, *AtIREG1* T-DNA insertion lines (*ireg1-1* and *ireg1-2*) and an *AtIREG1* overexpressing line (3S IREG1 3G) precultured for 7 days on half strength MS agar plates and then for 2 weeks on half strength MS agar plates with either no nitrogen source or with 5 mM urea as a sole nitrogen source, supplemented with different Ni concentrations. Significant differences at  $p < 0.01$  are indicated by different letters (n.s.: not significant),  $n = 4$ , 3 plants per replicate. *B*, Phenotype of the same lines, pictures of representative plates are shown. Plants grown on 5 mM NH<sub>4</sub>NO<sub>3</sub> were used as a control (left).

With addition of Ni up to 5  $\mu$ M the *AtIREG1* overexpressing lines still showed root and shoot fresh weight comparable to that of plants grown in the absence of N, indicating that in this line Ni availability for the urease was inadequate due to the overexpression of *AtIREG1*. To verify this, the experiment was repeated using Ni concentrations of up to 80  $\mu$ M to investigate whether a higher Ni supply can compensate the *AtIREG1*-mediated loss of Ni availability for the urease (Fig. 23). Indeed, the *AtIREG1* overexpressing line partially restored root growth when plates were supplemented with 40  $\mu$ M Ni, but as much as 80  $\mu$ M external Ni supply was needed to fully restore root and shoot growth.

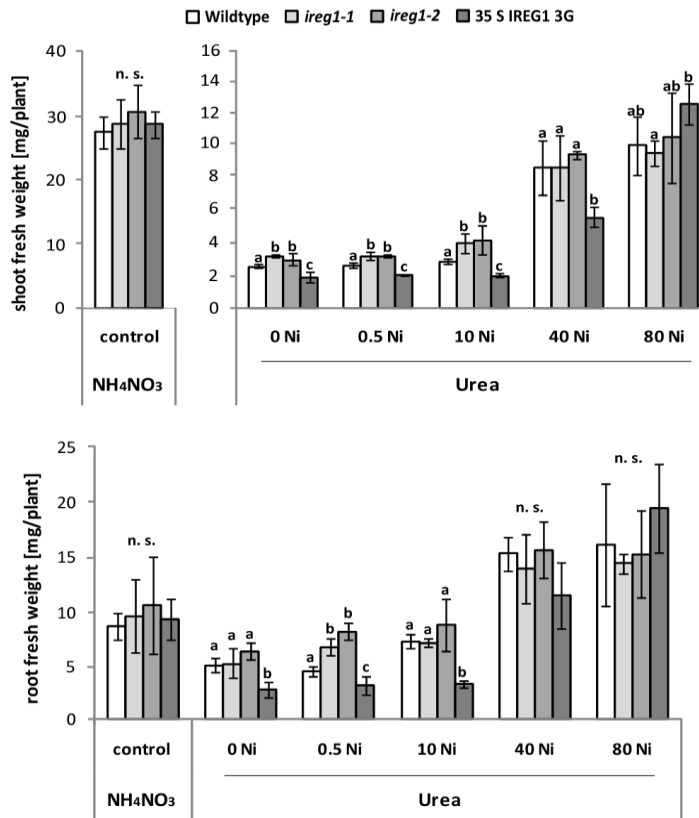


**Figure 23: Nickel supply can compensate for the *AtIREG1*-mediated loss of nickel availability for urea hydrolysis.**

Root and shoot fresh weight of 21-day-old wild type, *AtIREG1* T-DNA insertion lines (*ireg1-1* and *ireg1-2*) and an *AtIREG1* overexpressing line (35S IREG1 3G) precultured for 7 days on half strength MS agar plates and then for 2 weeks on half strength MS agar plates with either 5 mM urea or  $\text{NH}_4\text{NO}_3$  as nitrogen source, supplemented with different Ni concentrations. Significant differences at  $p < 0.01$  are indicated by different letters (n.s.: not significant),  $n = 4$ , 3 plants per replicate.

The next experiment was designed to verify whether the *AtIREG1*-mediated loss of Ni availability for the urease is the cause for the impaired growth of the *AtIREG1* overexpressing line on medium with urea as the sole nitrogen source. For that purpose, transgenic lines with a different level of *AtIREG1* gene expression were used (Fig. 24A). All three overexpressing lines showed the same growth reduction compared to wildtype plants at 0 or 0.5  $\mu\text{M}$  Ni concentrations in the medium (Fig. 24B).

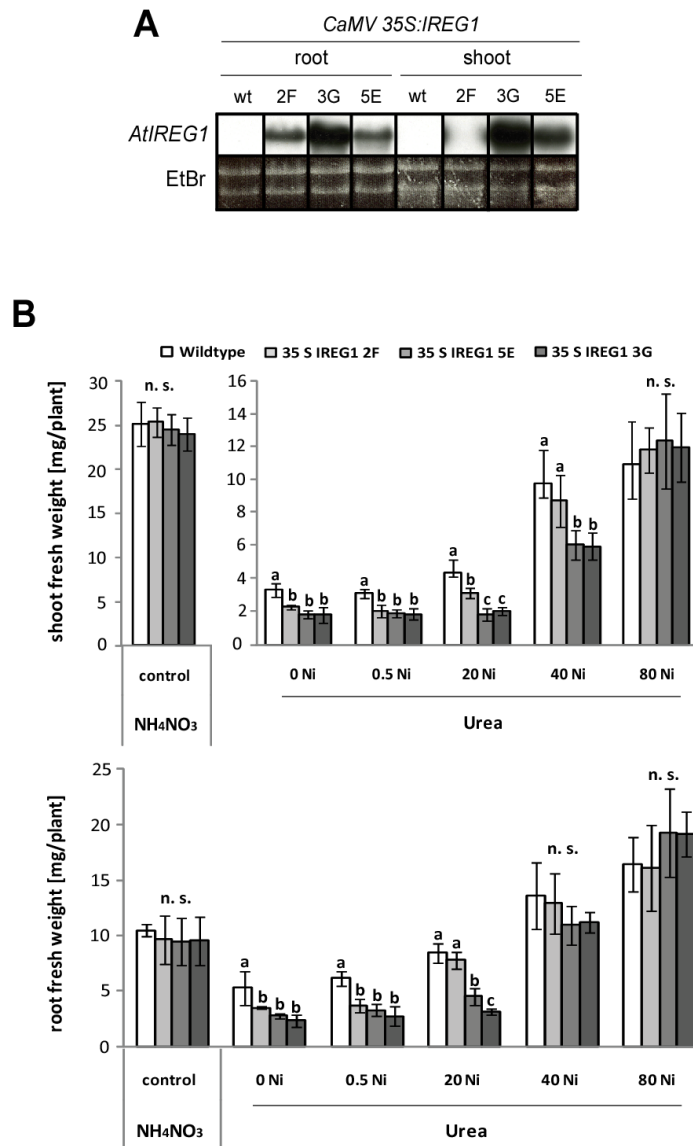


**Figure 24: Decrease of nickel-availability for the urease follows the expression level of *AtIREG1*.**

A, RNA gel blot analysis of *AtIREG1* expression in roots of wildtype and 35S-*AtIREG1* plants (lines 2F, 3G, 5E), which were cultured for 40 days under Fe-sufficient conditions. The corresponding EtBr-stained rRNA is shown as a loading control. B, Root and shoot fresh weight of 21-day-old wild type, and *AtIREG1* overexpressing lines (35S IREG1 2F, 3G and 5E) precultured for 7 days on half strength MS agar plates and then for 2 weeks on half strength MS agar plates with either no nitrogen source or with 5 mM urea as a sole nitrogen source, supplemented with different Ni concentrations. Significant differences at  $p < 0.01$  are indicated by different letters (n.s.: not significant),  $n = 4$ , 3 plants per replicate.

At higher Ni concentrations, the growth depression followed the expression level of *AtIREG1*: The line 2F with the lowest level of overexpression showed an intermediate phenotype (especially at 20  $\mu\text{M}$  Ni). At higher Ni concentrations all three overexpressing lines showed root and shoot fresh weights comparable to that of wildtype plants (Fig. 24B).

A further experiment was performed to prove that urease activity is influenced by the *AtIREG1*-mediated loss of Ni. For this reason wildtype, two *AtIREG1* T-DNA insertion lines and one *AtIREG1* overexpressing line were cultured on plates with urea as the sole nitrogen source and were supplemented with either 0.5 or 5  $\mu\text{M}$  Ni. Agar plates with ammonium nitrate were used as control (Fig. 25). For the measurement of urease activity soluble proteins were extracted from homogenized root and shoot samples. After addition of urea the generation of  $\text{NH}_4^+$  was measured by HPLC at different time points. From the resulting curve urease activity was calculated and specific urease activity was assessed by relating the values to the protein concentration in the extracts.

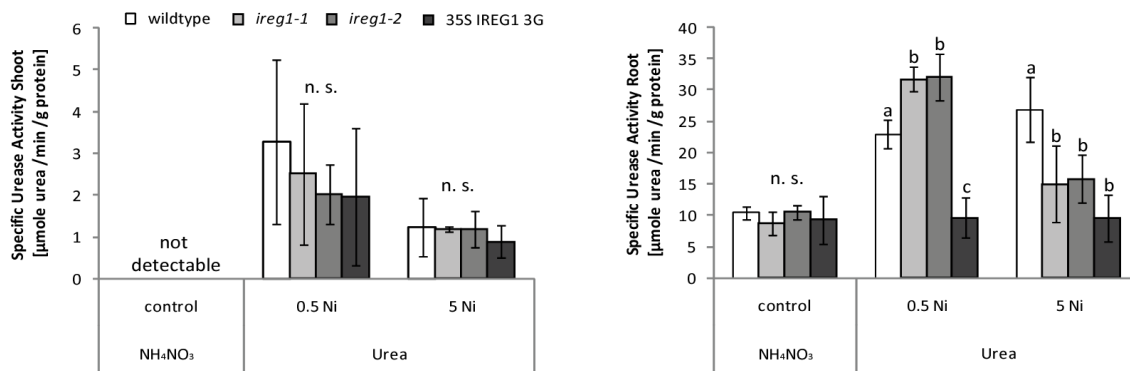


**Figure 25: Enhanced nickel transport via *AtIREG1* decreases urease activity.**

Specific urease activity in roots and shoots of wildtype, *AtIREG1* T-DNA insertion lines (*ireg1-1* and *ireg1-2*) and an *AtIREG1* overexpressing line (35S IREG1 3G). Plants were precultured for 7 days on half strength MS agar plates and then for 2 weeks on half strength MS agar plates with either 5 mM  $\text{NH}_4\text{NO}_3$  or 5 mM urea as nitrogen source and supplemented with different Ni concentrations. Soluble protein was extracted from samples, urea was added to the extract and the  $\text{NH}_4^+$  release over time was measured by HPLC. Significant differences at  $p < 0.01$  are indicated by different letters (n.s.: not significant),  $n = 3$ , 10 plants per replicate.

In all lines and treatments, urease activity was lower in shoots than in roots. In plants grown on  $\text{NH}_4\text{NO}_3$ , urease activity in shoots was below the detection limit. In shoots, no differences were found in urease activity in dependency of the *AtIREG1* expression level, but urease activity in roots of plants grown with urea and 0.5  $\mu\text{M}$  Ni (Fig. 25, right diagram) correlated tightly with the growth phenotype of the same lines (Fig. 22A). Addition of 5  $\mu\text{M}$  Ni to plates with urea as the sole nitrogen source resulted in a strong decrease of urease activity in *AtIREG1* T-DNA insertion lines compared to wildtype plants, although root and shoot fresh weight production of *AtIREG1* T-DNA insertion lines and wildtype plants was similar under these growth conditions (Fig. 22A).

## 4.3 AtIREG2

### 4.3.1 Yeast experiments

Because of the homology of AtIREG2 to vertebrate Fe exporters, we assumed an Fe export function. Before start of the work presented in this thesis, this hypothesis was tested by Gabriel Schaaf (University of Hohenheim, Stuttgart) by expression of *AtIREG2* in yeast as a heterologous expression system. The results gave no hint that *AtIREG2* might alleviate Fe toxicity in Fe-sensitive yeast strains. Neither the *AFT1up* strain, which exhibits a constitutive overexpression of genes involved in Fe acquisition, nor *ccc1*, a mutant suffering from a lower capacity to transport Fe into the vacuole, grew better on high Fe medium when expressing *AtIREG2* (data not shown). To test an iron import function *AtIREG2* was expressed in the Fe uptake-defective yeast mutant *fet3fet4* for a growth complementation test on 4–10  $\mu\text{M}$  Fe(III). Growth of *AtIREG2* transformants, however, did not differ significantly from that of control transformants (data not shown). In general, plant Fe transporters discriminate poorly between Fe and other metals (see chapter 2.4). We therefore decided to screen for a heavy metal transport function of *AtIREG2* employing yeast mutants with increased heavy metal sensitivities.

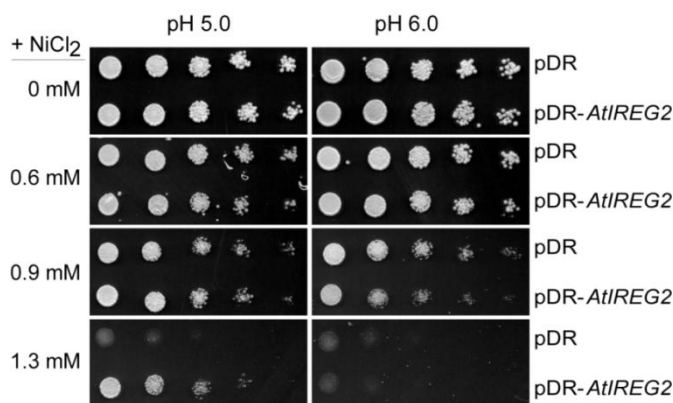


**Figure 26: AtIREG2 mediates tolerance to nickel in yeast.**

Yeast *cot1* cells were transformed with the empty vector pDR195 or with pDR195-*AtIREG2*. Single colonies were cultured in selective media for 48 h and adjusted to an optical density of 1.0 before spotting 5-fold dilutions on uracil-free YNB medium or medium supplemented with NiCl<sub>2</sub>. The pH was adjusted to pH 5 or 6 by 50mM MES/TRIS.

*AtIREG2* mediated a complementation of the Ni sensitivity of yeast *cot1* cells at a pH of 5, but the effect could not be observed at a pH of 6 or higher, pointing to a pH-dependent contribution of *AtIREG2* to Ni tolerance (Fig. 26).

### 4.3.2 Expression of *AtIREG2*

*AtIREG2* mRNA levels were examined in wildtype plants, grown hydroponically first under Fe sufficient conditions. For the Fe deficiency treatment, plants were starved for Fe for 10 days before half of the deficient plants were resupplied with Fe. Corresponding root and shoot samples were used for RNA extraction to perform a northern blot analysis (Fig. 27). Expression of *AtIRT1*, the transporter mainly responsible for Fe uptake in Arabidopsis (see chapter 2.3) was used as a control, because *AtIRT1* is known to be upregulated in Fe deficient plants. *AtIREG2* showed the same pattern of expression as the Fe transporter gene *AtIRT1*: The expression was higher in roots than in shoots, as transcript levels of *AtIREG2* in roots were upregulated under Fe deficiency and downregulated after resupply of Fe (Fig. 27).

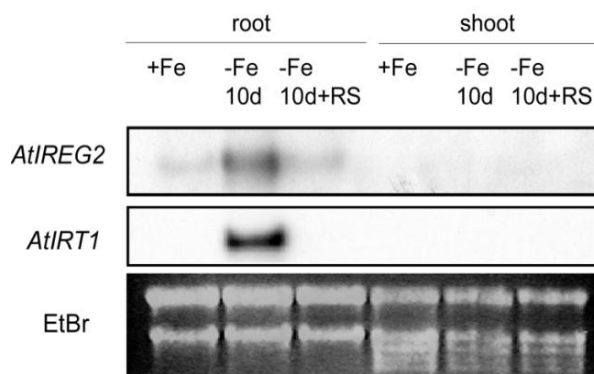


**Figure 27: *AtIREG2* is upregulated under iron deficiency.**

RNA gel blot analysis was performed to determine *AtIREG2* and *AtIRT1* expression in roots from hydroponically grown plants that were precultured for 5 weeks in presence of 50  $\mu$ M Fe(III)-EDTA and starved for 10 days for Fe, before resupply (RS) with 50  $\mu$ M Fe(III)-EDTA for 24 h. Total RNA from roots (left) or shoots (right) were used for hybridization to the complete ORF of *AtIREG2* or *AtIRT1*. EtBr-stained gel blots are shown as loading control.

As the results from heterologous expression of *AtIREG2* in yeast did not give any hint for a Fe transport function of *AtIREG2*, the regulation of *AtIREG2* expression by different metals (Co, Cd and Ni) was tested in RNA gel blot analyses (Fig. 28), but no differences in *AtIREG2* transcript level could be observed after 6 h, 30 h or 54 h culture with the corresponding metals.

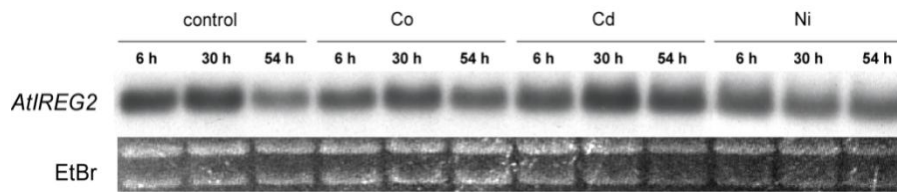


**Figure 28: *AtIREG2* expression is not regulated by cobalt, cadmium or nickel.**

RNA gel blot analysis was performed to determine *AtIREG2* expression in roots from hydroponically grown plants that were precultured for 5 weeks in Arabidopsis nutrient solution and were then cultured with Co, Cd or Ni for 6, 30 or 54 h. Total RNA from roots was used for hybridization to the complete ORF of *AtIREG2*. EtBr-stained gel blots are shown as loading control.

### 4.3.3 Characterization of the growth phenotype of *AtIREG2* overexpressing Arabidopsis lines

Based on the enhanced tolerance to Ni of yeast cells transformed with *AtIREG2* (Fig. 26), we investigated whether overexpression of *AtIREG2* also increases tolerance to elevated concentrations of this metal *in planta*. Transgenic plants expressing *AtIREG2* under control of the constitutive 35S promoter were generated and four independent homozygous lines were examined in the T2 generation. RNA gel blot analysis using plants grown under Fe-sufficient conditions showed that *AtIREG2* was highly expressed in roots of the lines 1, 4, and 10, while mRNA levels in line 7 were only slightly increased relative to the wildtype expression level (Fig. 29A). When grown on agar plates with 100 or 200  $\mu\text{M}$  Ni, wildtype seedlings experienced a severe loss of biomass (Fig. 29B). In contrast, the gain of fresh weight by the *AtIREG2* overexpressor lines 1, 4, and 10 was unaffected even at 200  $\mu\text{M}$  Ni. In agreement with its lower expression level of *AtIREG2*, line 7 showed an intermediate response with higher fresh weight than the wildtype at 100  $\mu\text{M}$  Ni but a similar reduction in fresh weight as wildtype plants at 200  $\mu\text{M}$  Ni. As *AtIREG1* overexpressing lines also showed higher tolerance to Co besides Ni (Fig. 6 and 8), the experiment was repeated with Co but no significant differences could be found (Fig. 29C).

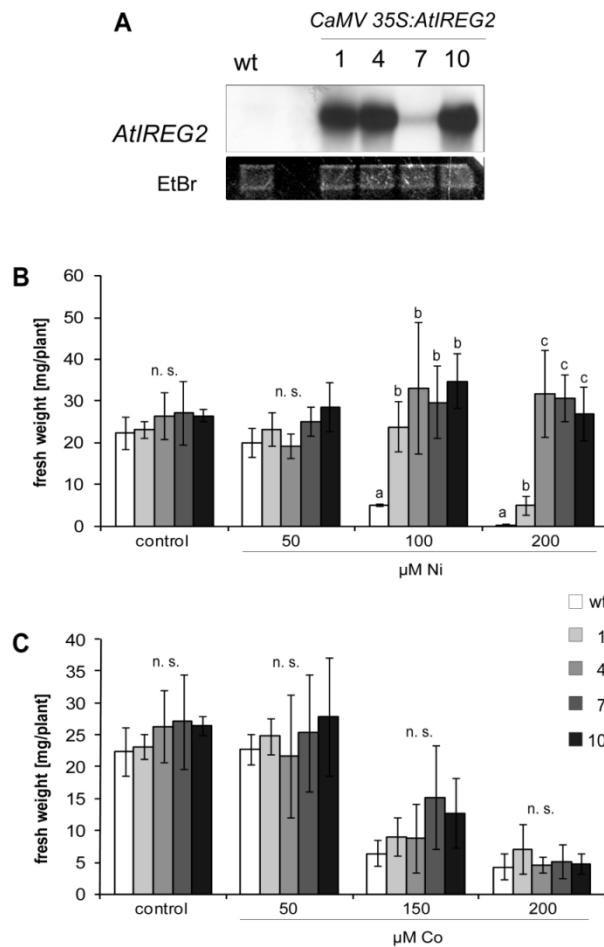


**Figure 29: Overexpression of *AtIREG2* increases nickel but not cobalt tolerance in Arabidopsis.**

*A*, RNA gel blot analysis of *AtIREG2* expression in roots of wildtype and 35S::*AtIREG2* plants (lines 1, 4, 7 and 10), which were cultured for 40 days under Fe-sufficient conditions. The corresponding EtBr-stained rRNA is shown as a loading control. *B* and *C*, fresh weight of 21-day-old wildtype and 35S-*AtIREG1* plants precultured for 7 days on half strength MS agar plates and then for 2 weeks on half strength MS agar plates with elevated supply of Ni (*B*) or Co (*C*). Significant differences at  $p < 0.01$  are indicated by different letters (n.s.: not significant),  $n = 4$ , 3 plants per replicate.

The differential growth response of 35S::*AtIREG2* lines on Ni-containing plates, which was due to the different expression levels of *AtIREG2*, was also reflected in the growth phenotype when plants were directly germinated on agar plates supplemented with Ni. Wildtype plants showed a severe growth repression and germinated poorly above 100  $\mu\text{M Ni}$ , whereas lines 1, 4, and 10 developed cotyledons even up to 500  $\mu\text{M Ni}$  (Appendix 5).

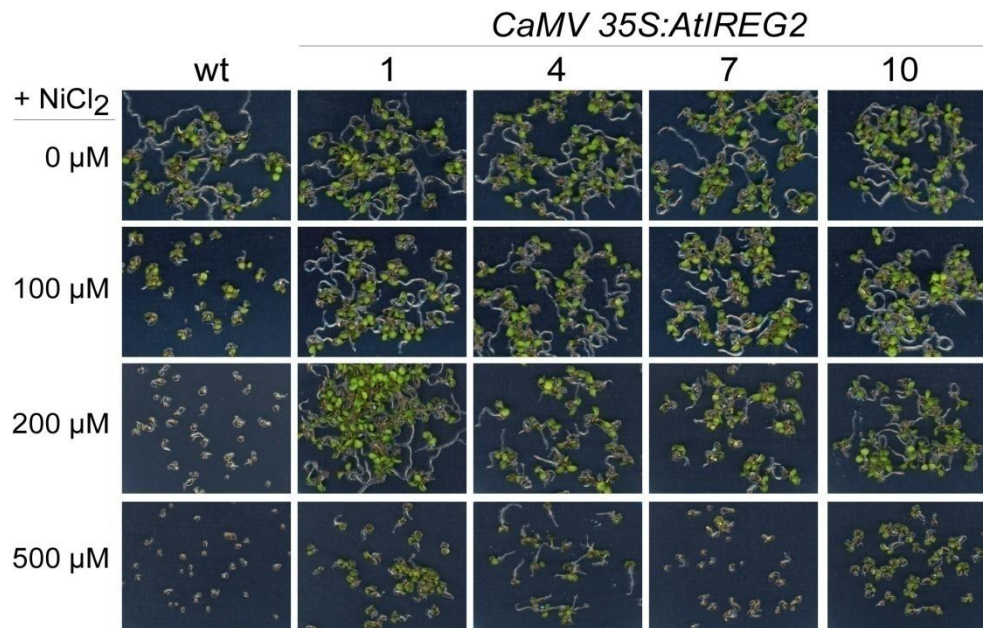


**Figure 30: Overexpression of *AtIREG2* increases nickel tolerance in Arabidopsis.**

Phenotype of 7-day-old wildtype and 35S-*AtIREG2* plants (lines 1, 4, 7 and 10) on half strength MS agar plates supplemented with elevated concentrations of Ni.

A phenotypic analysis of the same lines germinated on agar with elevated concentrations of cadmium, cobalt, manganese, zinc, or iron did not yield any significant differences related to the level of *AtIREG2* gene expression (data not shown).

#### 4.3.4 Characterization of the growth phenotype of *AtIREG2* T-DNA insertion lines

Two lines were obtained from the SALK collection (Alonso et al., 2003; SALK\_074442 and SALK\_217071) and were further named *ireg2-1* and *ireg2-2* in the present thesis.



**Figure 31: Scheme of the T-DNA integration sites in *ireg2-1* (SALK\_074442) and *ireg2-2* (SALK\_127071).**

The location of the T-DNA insertions is indicated by triangles. Both insertions are located 200 bp upstream of the transcription start.

Both lines carried an insertion in the 5'-UTR of the *AtIREG2* gene (Fig. 31). Homozygous plants were selected by segregation and PCR analyses from the T3 generation. In both lines Fe deficiency-induced expression of *AtIREG2* in roots (like shown in Fig. 27) could not be detected in RNA gel blot analyses (Fig. 32A), but the plants did not exhibit any visible phenotype on soil, plates or in hydroponic culture when grown under standard growth conditions.

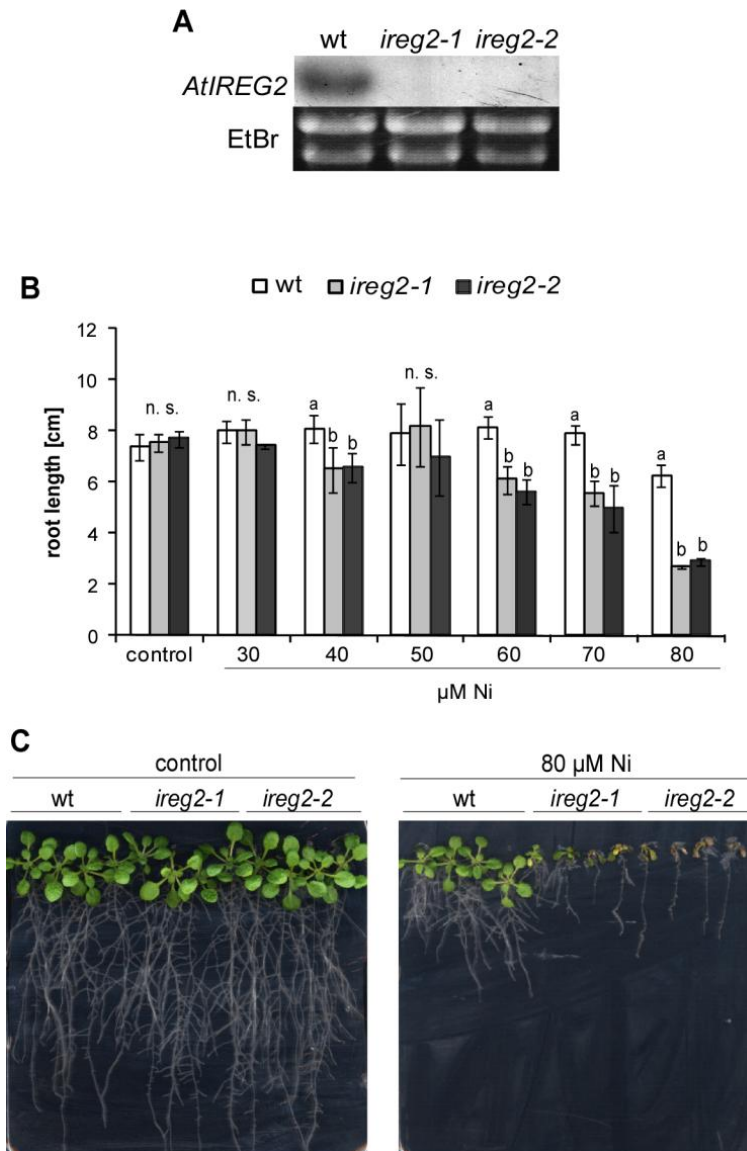


**Figure 32: Loss of *AtIREG2* increases nickel sensitivity in Arabidopsis.**

**A**, RNA gel blot analysis of *AtIREG2* expression in roots of iron-deficient wild type, *ireg2-1* and *ireg2-2*. The corresponding EtBr-stained rRNA is shown as a loading control. **B**, primary root length of 21-day-old wildtype and *AtIREG1* T-DNA insertion lines (*ireg2-1* and *ireg2-2*) precultured for 7 days on half strength MS agar plates and then for 2 weeks on half strength MS agar plates with elevated supply of Ni. Significant differences at  $p < 0.01$  are indicated by different letters (n.s.: not significant),  $n = 4$ , 4 plants per replicate. **C**, Phenotype of the same lines, pictures of representative plates are shown.

A detailed screening was performed on agar plates, supplemented with different concentrations of metals (Fe, Cu, Ni, Co, Zn and Mn), to find out whether a loss of *AtIREG2* can lead to an increased metal sensitivity (data not shown, but part of the results of this screening are found in Fig. 48 and 49). Different growth of *AtIREG2* T-DNA insertion lines compared to wildtype plants was only found on Ni containing plates. Therefore, experiments were set up to quantify the growth on Ni supplemented agar plates. Wildtype and *AtIREG2* T-DNA insertion lines were germinated and cultured on plates without metal supply for seven days. Plants with similar number of leaves, size of leaves and root length were transferred to vertical agar plates supplemented with different concentrations of Ni. *AtIREG2* T-DNA insertion lines clearly showed a conditional phenotype (Fig. 32C) with symptoms of chlorosis and lower shoot and root development than wildtype plants at Ni concentrations of 60  $\mu\text{M}$  or higher.

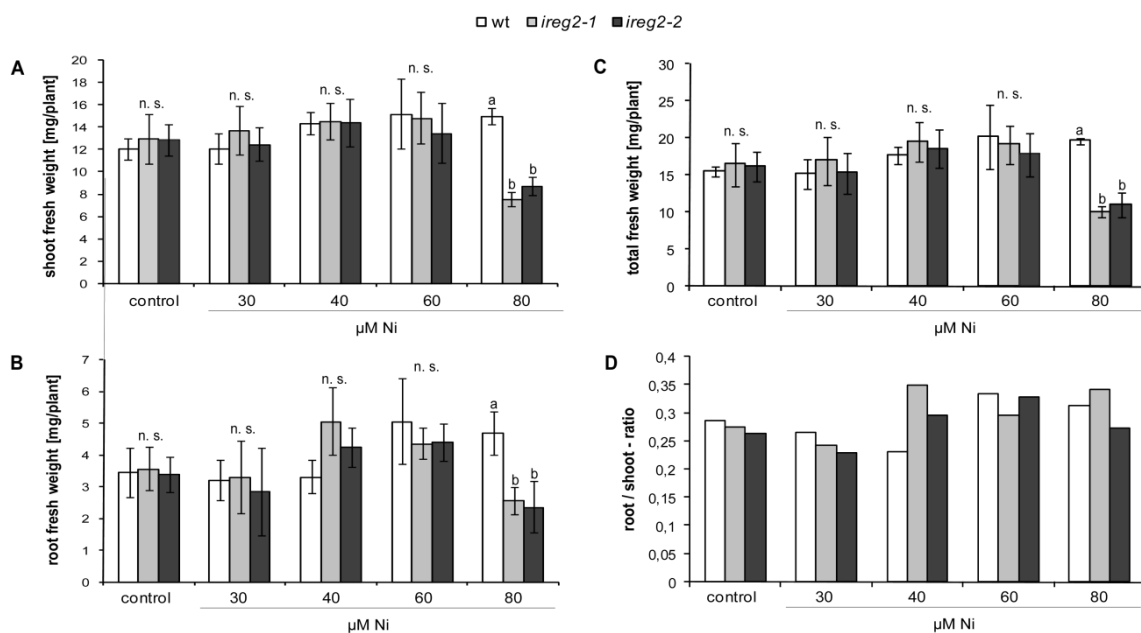


**Figure 33: Loss of *AtIREG2* leads to reduced fresh weight in Arabidopsis under elevated nickel supply.**

21-day-old wildtype and *AtIREG2* T-DNA insertion lines (*ireg2-1* and *ireg2-2*) were precultured for 7 days on half-strength MS agar plates and then for 2 weeks on half strength MS agar plates with elevated supply of Ni. The following measures were taken: A, shoot fresh weight, B, root fresh weight C, total fresh weight (root and shoot) and D, root / shoot-ratio was determined. Root / shoot-ratio was calculated based on fresh weight. Significant differences at  $p < 0.01$  are indicated by different letters (n.s.: not significant),  $n = 4$ , 4 plants per replicate.

When the length of the primary roots of the different lines were compared (Fig. 32B), *AtIREG2* T-DNA insertion lines showed a decrease in root length compared to the wildtype at concentrations of 60, 70 and 80  $\mu\text{M}$  Ni. *AtIREG2* T-DNA insertion lines also developed less root and shoot fresh weight than wildtype plants at 80  $\mu\text{M}$  Ni (Fig. 33). The root/shoot-ratio was not different between *AtIREG2* T-DNA insertion lines and the wildtype, as Ni toxicity affected root and shoot biomass to the same extent.

Detailed experiments with the same experimental setup were also performed with Co instead of Ni. Although first screening experiments with direct germination of wildtype and transgenic lines on Co containing medium did not reveal any growth differences in *AtIREG2* mutant lines (data not shown), Co was used for more detailed experiments because of the phenotype that transgenic *AtIREG1* lines showed when grown on Co containing medium (chapter 4.2.2 and 4.2.3).

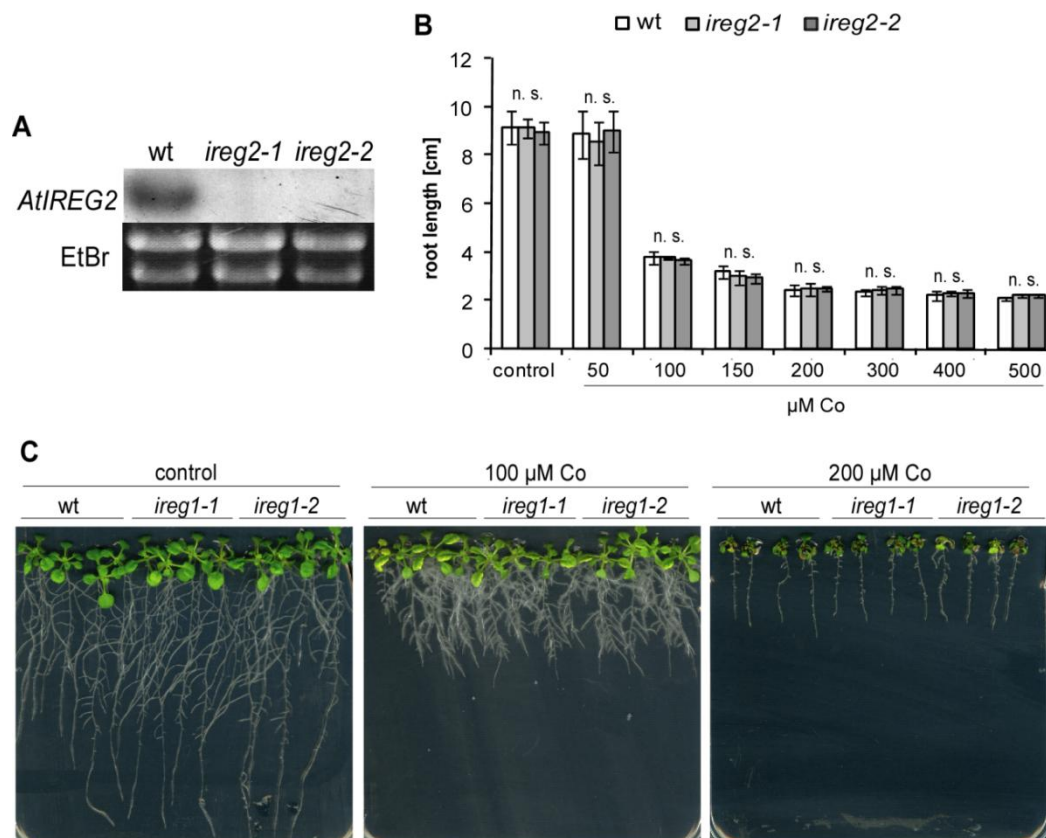


**Figure 34: Loss of *AtIREG2* does not influence plant growth on cobalt.**

A, RNA gel blot analysis of *AtIREG2* expression in roots of Fe-deficient wildtype, *ireg2-1* and *ireg2-2*. The corresponding EtBr-stained rRNA is shown as a loading control. B, primary root length of 21-day-old wild type and *AtIREG2* T-DNA insertion lines (*ireg2-1* and *ireg2-2*) precultured for 7 days on half strength MS agar plates and then for 2 weeks on half strength MS agar plates with elevated supply of Co. No significant differences were found (n.s.: not significant), n = 4, 4 plants per replicate. C, Phenotype of the same lines, pictures of representative plates are shown.

In agreement with the results of the previous experiments, loss of *AtIREG2* did not lead to increased Co sensitivity. Transgenic lines and wildtype plants showed similar symptoms of chlorosis at concentrations of 100  $\mu\text{M}$  Co or higher, and root and shoot development was the same (Fig. 34C). Quantitative analysis proved that there was no altered root length (Fig. 34) nor differences in root or shoot fresh weight (Fig. 35) in lines with lacking *AtIREG2* expression. As a consequence, the root/shoot-ratio was not different in *ireg2-1* and *ireg2-2* compared to the wildtype (Fig. 35D).

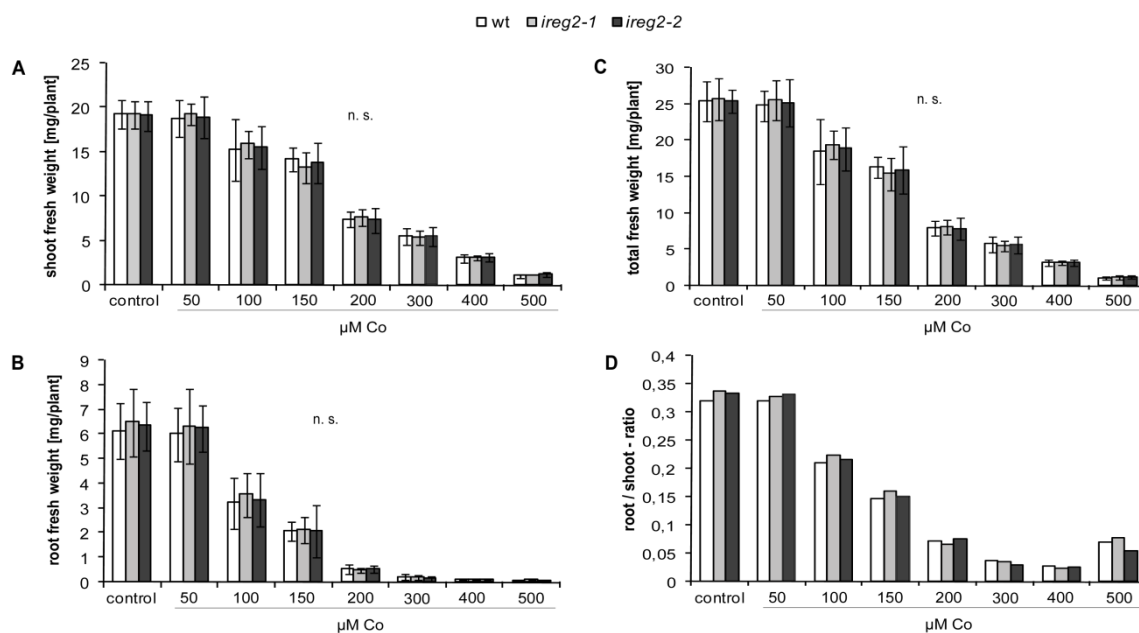


**Figure 35: Loss of *AtIREG2* does not influence Arabidopsis fresh weight under elevated cobalt supply.**

21-day-old wildtype and *AtIREG2* T-DNA insertion lines (*ireg2-1* and *ireg2-2*) were precultured for 7 days on half strength MS agar plates and then for 2 weeks on half strength MS agar plates with elevated supply of Co. The following measures were taken: A, shoot fresh weight, B, root fresh weight, C, total fresh weight (root and shoot) and D, root / shoot-ratio was determined. Root/shoot-ratio was calculated based on fresh weight. No significant differences were found (n.s.: not significant), n = 4, 4 plants per replicate.

### Complementation of *AtIREG2* T-DNA insertion lines

A complementation of the *ireg2* T-DNA insertion line was required, because sequencing of the insertion sites and neighbouring sequences in the two *AtIREG2* T-DNA insertion lines revealed that the insertion in both lines is located at the same site (Fig. 31). Therefore, *ireg2-1* and *ireg2-2* are most likely no independent insertion lines, but derive from the same T-DNA insertion event. Retransformation of *ireg2-1* plants

was performed with an *AtIREG2*-promoter-*AtIREG2*-GFP construct to confirm that the observed phenotype is indeed caused by loss-of-function of *AtIREG2*. We selected homozygous recomplemented lines from the T2 generation, and verified the presence of *AtIREG2*-GFP transcript by RNA gel blot analysis, resulting in high levels of *AtIREG2*-GFP mRNA (Fig. 36A).

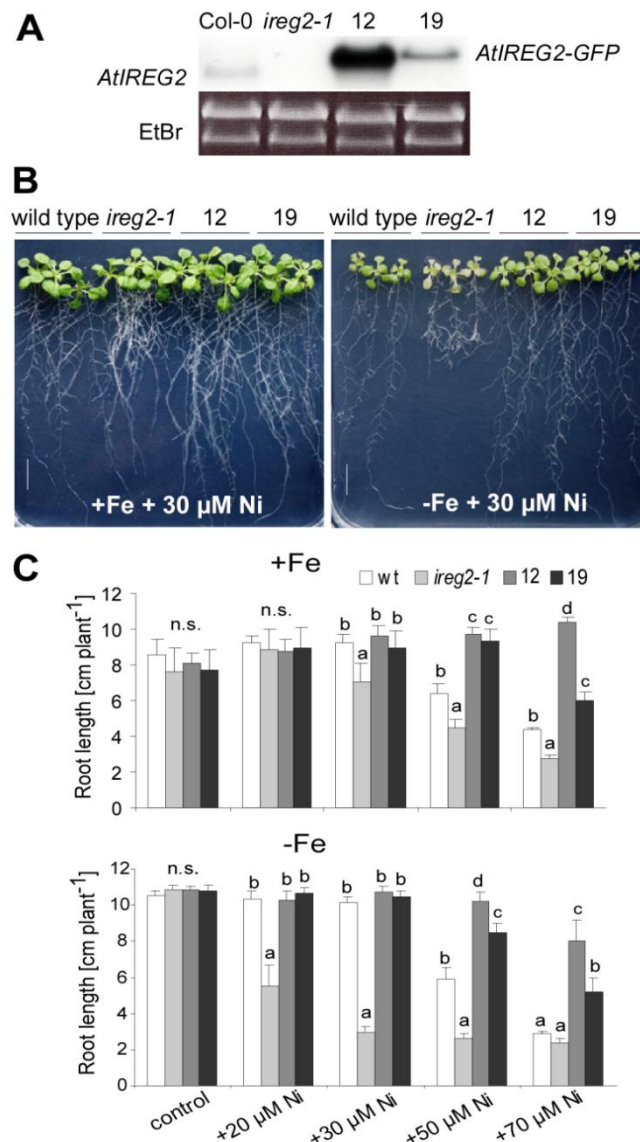


**Figure 36: Retransformation of *ireg2-1* with *AtIREG2* restores tolerance to elevated nickel concentrations.**

A, RNA gel blot analysis of *AtIREG2* expression in roots of wild type, *ireg2-1*, and *ireg2-1* plants retransformed with a *AtIREG2*-promoter-*AtIREG2*-GFP fusion construct (lines 12 and 19). The corresponding EtBr-stained rRNA is shown as a loading control. B, Fe-dependent phenotype of the same lines precultured for 8 days on Fe adequate (75 μM Fe-EDTA) half strength MS agar plates and then for 2 weeks on Fe-adequate (75 μM Fe-EDTA) or Fe-deficient half strength MS agar supplied with 30 μM nickel. Bar, 1 cm. C, quantitative analysis of primary root length after plant cultivation like that described in B with increasing supply of Ni. Significant differences at  $p < 0.05$  are indicated by different letters, n.s.: not significant,  $n = 4$ , 3 plants per replicate.

Wildtype, *ireg2-1* and recomplemented lines were grown on Ni-supplied agar under different Fe regimes. The *ireg2-1* insertion lines grew similar to the wildtype on Fe-sufficient medium supplemented with up to 30  $\mu\text{M}$  Ni (Fig. 36B), while *ireg2-1* plants produced significantly less biomass (data not shown) or root growth at or above 30  $\mu\text{M}$  Ni (Fig. 36C). Under Fe deficient growth conditions, however, growth repression of the *ireg2-1* insertion line was severe in as little as 20  $\mu\text{M}$  Ni, emphasizing that Ni sensitivity increases with Fe deficiency. In comparison, complemented *ireg2-1* insertion lines (lines 12 and 19) were less sensitive to Ni at high Ni supplies and the complemented lines were even less sensitive than the wildtype.

### Iron dependency of the nickel sensitivity of *AtIREG2* T-DNA insertion lines

As described above, loss of *AtIREG2* caused increased Ni sensitivity in a Fe-dependent manner and Ni sensitivity increased with Fe deficiency. To further prove and characterize this effect, additional experiments using both *AtIREG2* T-DNA insertion lines were performed. Plants were germinated and precultured on Fe sufficient agar plates, and were then transferred to plates with or without Fe at increasing Ni supply.

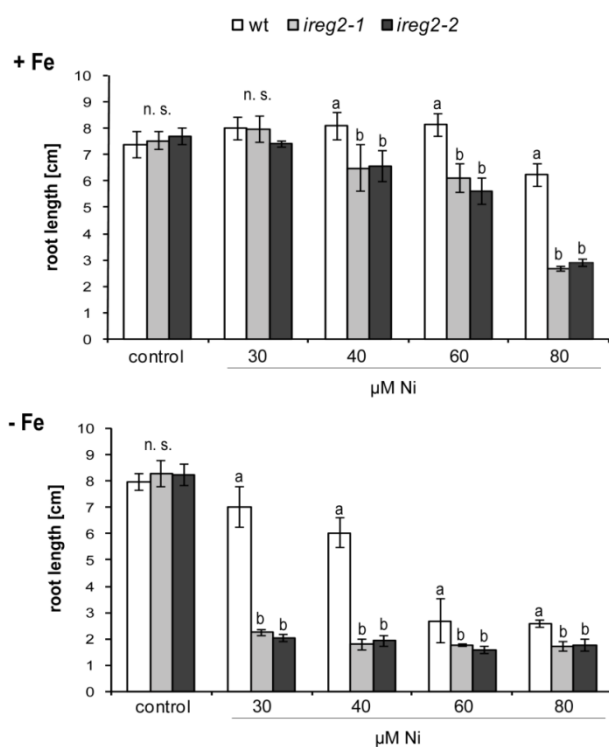


**Figure 37: *AtIREG2* mediates nickel tolerance in an iron-dependent manner.**

Quantitative analysis of primary root length of wildtype and *AtIREG2* T-DNA insertion lines (*ireg2-1* and *ireg2-2*) precultured for 7 days on Fe adequate (75  $\mu\text{M}$  Fe-EDTA) half strength MS agar plates and then for 2 weeks on Fe-adequate (+Fe) or Fe-deficient (-Fe) half strength MS agar supplied with different Ni concentrations. Significant differences at  $p < 0.01$  are indicated by different letters (n.s.: not significant),  $n = 4$ , 3 plants per replicate.

In agreement with the results obtained before (Fig. 36), the Ni-dependent growth depression of *AtIREG2* T-DNA insertion lines was more severe under Fe deficiency (Fig. 37 and 38). Again, effects of Ni toxicity appeared at lower Ni concentrations when plants were grown under Fe-deficient conditions. An assessment of the root length (Fig. 37) yielded large differences in root fresh weight between Fe-deficient and Fe-sufficient plants (Fig. 38, middle diagrams).

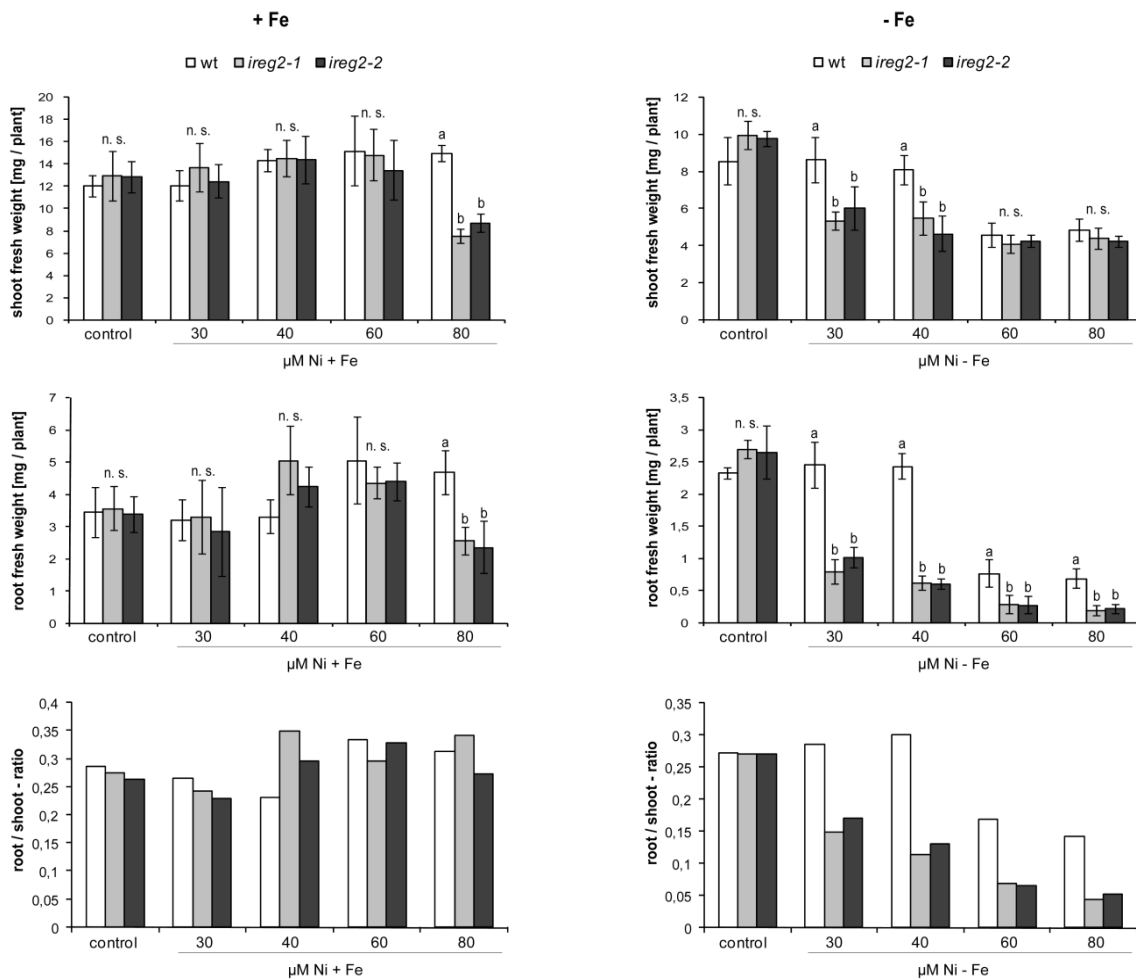


**Figure 38: *AtIREG2* mediates nickel tolerance in an iron-dependent manner .**

Quantitative analysis of root and shoot fresh weight and root/shoot-ratio of wildtype and *AtIREG2* T-DNA insertion lines (*ireg2-1* and *ireg2-2*) precultured for 7 days on Fe adequate (75 µM Fe-EDTA) half strength MS agar plates and then for 2 weeks on Fe-adequate (+Fe, left) or Fe-deficient (-Fe, right) half strength MS agar supplied with different Ni concentrations. Significant differences at  $p < 0.01$  are indicated by different letters (n.s.: not significant),  $n = 4$ , 3 plants per replicate.

*AtIREG2* T-DNA insertion lines developed significantly less root biomass than wildtype plants on Fe sufficient medium supplemented with 80  $\mu\text{M}$  Ni, but the difference between wildtype and *ireg2* lines was much more pronounced when the same lines were cultured under Fe-deficient growth conditions. Under Fe-sufficient conditions root fresh weight of *AtIREG2* T-DNA insertion lines accounted for approximately 50 to 60% of wildtype root fresh weight, when grown on agar plates supplemented with 80  $\mu\text{M}$  Ni. Larger differences between wildtype and transgenic lines were not observed at even higher Ni concentrations, because wildtype plants showed a strong growth depression at concentrations of 90  $\mu\text{M}$  Ni or higher (data not shown). Under Fe deficient growth conditions, *AtIREG2* T-DNA insertion lines produced only 30 to 40% root biomass compared to the wildtype at concentrations of 30 and 40  $\mu\text{M}$  Ni. This also expressed in decreased root/shoot-ratios of *AtIREG2* T-DNA insertion lines cultured under Fe deficient growth conditions, which could not be found in plants provided with adequate Fe (Fig. 38, lower diagrams).

#### 4.3.5 Intracellular localization of *AtIREG2* *in planta*

To examine the intracellular localization of *AtIREG2* *in planta*, a *GFP* cDNA was fused to the 3'-end of *AtIREG2* and the fusion construct was placed under control of a 35S promoter for transient expression in *Arabidopsis thaliana* protoplasts derived from a suspension cell culture. As observed by confocal laser scanning microscopy, *AtIREG2*-dependent green fluorescence appeared as ring-shaped structures (Fig. 39A). A comparison to the transmission view and merging both images allowed identification of these globular compartments as vacuoles. Even in fully differentiated cells with large vacuoles, a small cytoplasmic region including organellar structures separated the *AtIREG2*-dependent fluorescence from the plasma membrane, clearly indicating tonoplast localization (Fig. 39A). In contrast, fluorescence derived from GFP alone localized to the cytoplasm and to the nucleus. In an independent approach, transgenic *Arabidopsis* lines expressing an *AtIREG2-GFP* construct under control of a 1.8-kb fragment of the endogenous *AtIREG2* promoter were analyzed (Fig. 39B). In root cortex cells, green fluorescence derived from *AtIREG2-GFP* was localized internal of red

fluorescence derived from the lipophilic dye FM4-64, which labels the plasma membrane after short term incubation (Takano et al., 2005). These observations indicated that AtIREG2 is targeted to vacuolar membranes and suggested a role of AtIREG2 in substrate transport across the tonoplast.

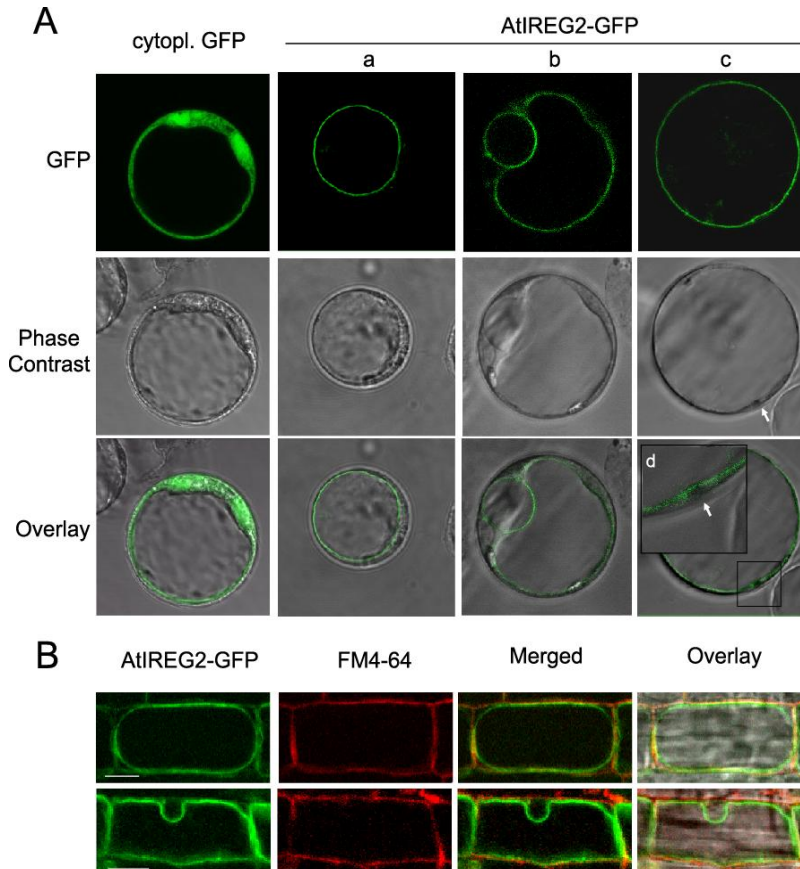


**Figure 39: Tonoplast localization of GFP-fused AtIREG2.**

*A, upper panel*, GFP-derived fluorescence from protoplasts transformed with pCF203-GFP alone (*left*) or pCF203-AtIREG2-GFP (*panels a–c*). *Middle panel*, phase contrast views. *Lower panel*, overlay of GFP-derived fluorescence and phase contrast; *panel d*, magnified insert from *panel c*. Protoplasts derived from a dark-adapted *Arabidopsis* cell suspension culture and were assayed by confocal laser scanning microscopy. *B*, root cell of a *atireg2-1* plant retransformed with an *AtIREG2*-promoter-*AtIREG2-GFP* fusion construct (*line 12*) grown on half-strength MS medium for 2 weeks before image analysis using an ApoTome imaging system in an inverted fluorescence microscope. *Bar*, 10  $\mu$ m.

### 4.3.6 Influence of *AtIREG2* expression level on nickel transport and distribution *in planta*

#### 4.3.6.1 Nickel accumulation in dependency on *AtIREG2* expression level

To examine Ni concentrations in dependence on *AtIREG2* expression, wildtype and transgenic lines were grown hydroponically for 6 weeks before supplementing the nutrient solution with 10  $\mu\text{M}$  Ni for 10 days. A subsequent analysis of transition metals in shoots showed no clear differences between lines, only a low but significant decrease of Cu concentration in *AtIREG2* T-DNA insertion lines. Decrease in Zn concentration was only found in one of the two *ireg2* lines. In roots of both *ireg2* insertion lines, Ni concentrations were only half of those of wildtype plants (Fig. 40). All other metal concentrations in *ireg2* roots were similar to wildtype plants. In contrast, overexpression of *AtIREG2* led to a significantly higher accumulation in roots of Ni but also of Mn, Cu and Zn (Fig. 40).

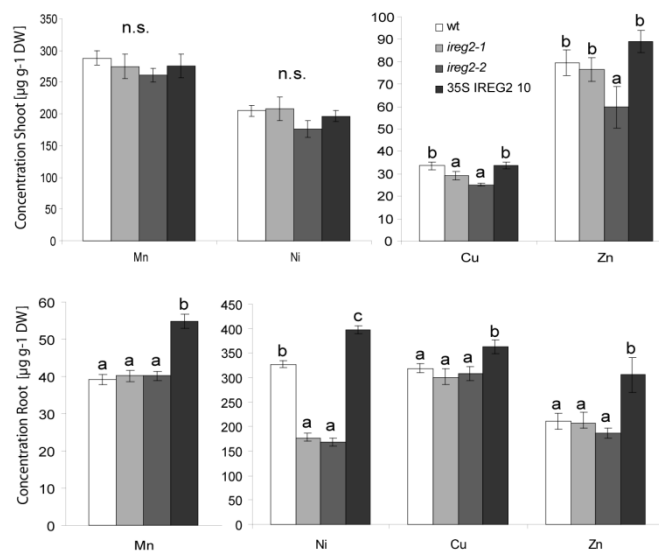


**Figure 40: Loss of *AtIREG2* leads to reduced nickel accumulation in roots.**

Accumulation of nickel, copper, zinc, and manganese in roots of wildtype, *ireg2-1* and *ireg2-2* plants and the *AtIREG2*-overexpressing line 10, which were cultured for 10 days on nutrient solution supplied with 10  $\mu\text{M}$  Ni. Significant differences at  $p < 0.05$  are indicated by different letters (n.s.: not significant),  $n = 4$ , 3 plants per replicate.

### 4.3.6.2 Metal concentrations in Arabidopsis xylem exudates in dependency of *AtIREG2* expression

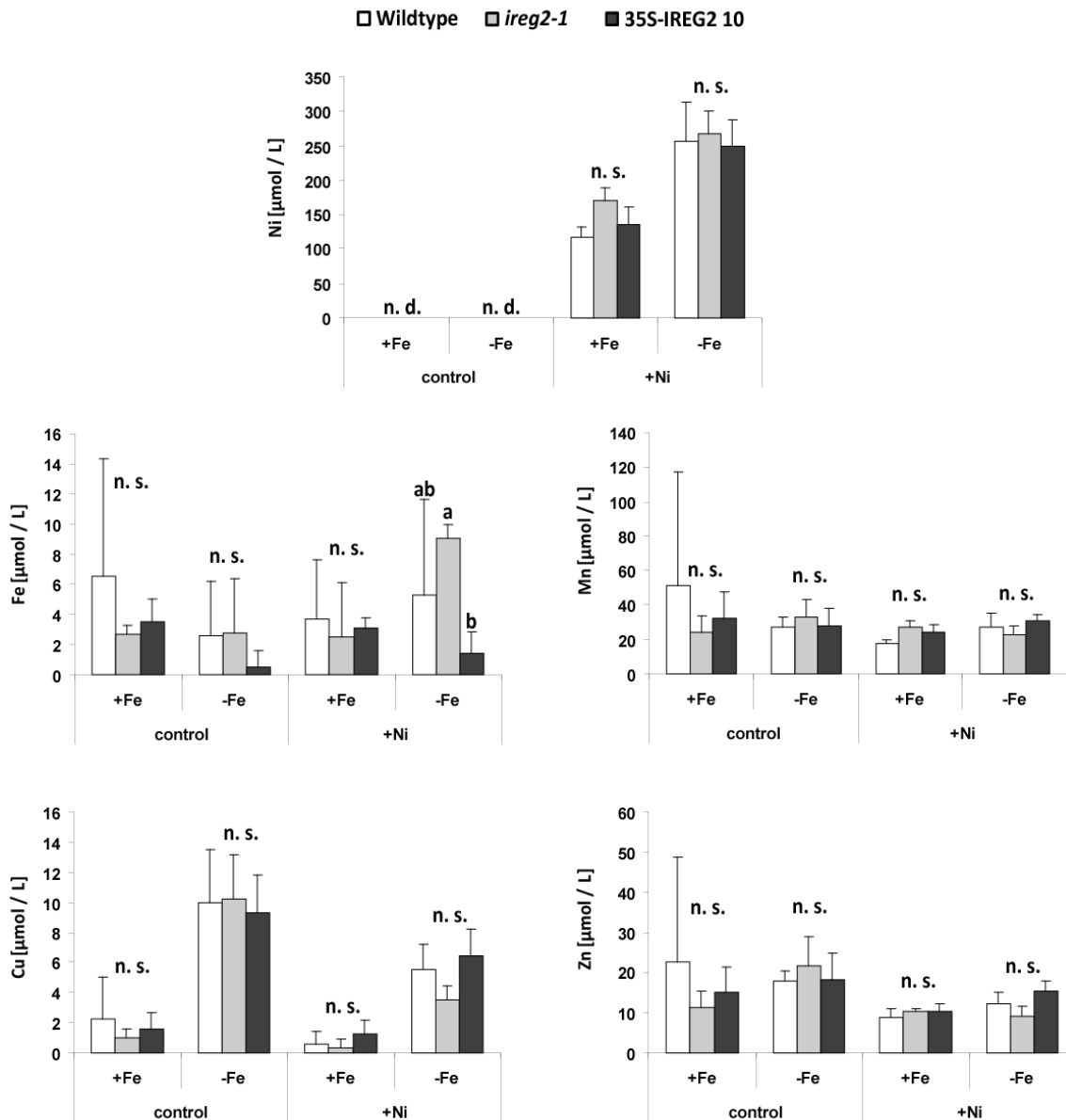


**Figure 41: Changes in *AtIREG2* expression do not lead to altered metal concentrations in Arabidopsis xylem exudate.**

Concentrations of Ni, Fe, Mn, Zn and Cu in xylem sap of hydroponically grown wildtype, *ireg2-1* and *AtIREG2* overexpressors (line 10), that were precultured for 6 weeks in presence of 50 μM Fe(III)-EDTA and then continued to grow on adequate Fe (+Fe) or were starved for Fe for 6 days. Plants were either set on nutrient solution without Ni (control) or with 10 μM Ni (+Ni) 1 d before xylem exudates collection. n.d.: not detectable. Significant differences at  $p < 0.05$  are indicated by different letters (n.s.: not significant),  $n = 4$ , 3 plants per replicate.

To investigate a possible function of AtIREG2 in xylem loading, wildtype, an *AtIREG2* T-DNA insertion line and an *AtIREG2* overexpressing line were grown hydroponically. Because of the upregulation of *AtIREG2* in response to Fe deficiency xylem exudates of plants grown under Fe-sufficient or Fe-deficient conditions were collected (Fig. 41). Plants were transferred to nutrient solution without Ni or with 10  $\mu$ M Ni one day before collection of xylem exudates. Ni could not be detected in the xylem exudates when plants were cultured without additional Ni supply to the medium. No differences among these lines were detected with regard of their concentrations of Ni, Fe, Mn, Cu or Zn in the xylem sap. Differences in the Fe concentrations in the Ni treatments probably derived from the low Fe sensitivity of the ICP-MS method used for the measurements of metals in the xylem exudates.

#### 4.3.6.3 Vacuole isolation from Arabidopsis leaves

The tonoplast localization of AtIREG2 (Fig. 39) and the increased Ni sensitivity of *AtIREG2* T-DNA insertion lines, as well as the increased Ni tolerance of *AtIREG2* overexpressors pointed to a function of AtIREG2 in metal detoxification by transporting Ni to the vacuole. To verify this hypothesis, a protocol was established to isolate vacuoles from Arabidopsis plant material, with the aim to measure Ni concentration in isolated vacuoles of wildtype and transgenic lines. The used method (chapter 3.8) resulted from an optimization of a protocol kindly provided by Oliver Trentmann (University of Kaiserslautern). Especially the conditions for protoplast isolation (digestion of leaves and protoplast purification) and the composition of the lysis buffer used to break the protoplasts and to release vacuoles from the cells required optimization, because these proved to be the limiting steps in vacuole isolation. As the results presented in this thesis pointed to an expression and function of AtIREG2 primarily in Arabidopsis roots, several efforts were made to isolate vacuoles not only from leaves, but also from roots. Generation of protoplasts from roots turned out to be difficult, although different buffers, different enzyme combinations for digestion of the cell walls and different digestion conditions were used. All these efforts did not yield an amount of protoplasts sufficient for vacuole isolation, as also the purification of the generated protoplasts was difficult. It was therefore decided to use vacuoles from leaves

for the examination of Ni concentrations in vacuoles, because a difference between wildtype and *AtIREG2* overexpressing lines could be expected. Another problem was the large variations in vacuolar yield in dependence of the plant lines and the growth conditions (Fig. 42).

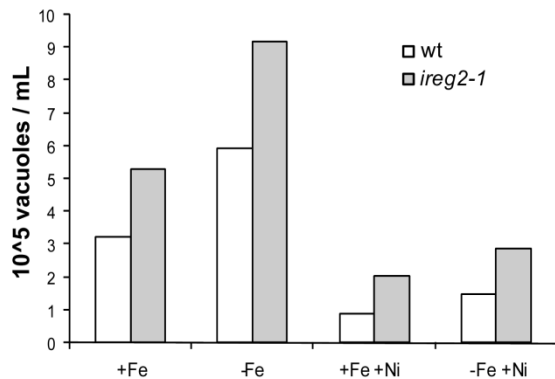


**Figure 42: Vacuolar yield varies strongly in dependence on plant lines and growth conditions.**

Number of vacuoles isolated from wildtype (wt) and an *AtIREG2* T-DNA insertion line (*ireg2-1*) from leaves of Arabidopsis plants grown hydroponically under Fe-sufficient conditions (50  $\mu$ M Fe-EDTA, +Fe) or Fe-deficient conditions for 5 days (-Fe). 10  $\mu$ M Ni was added to the nutrient solution 5 days before vacuole isolation (+Ni).

Surprisingly, the number of vacuoles was always much lower when plants were grown on Ni-containing medium (Fig. 42). Unfortunately, this treatment was considered to be the most interesting for a comparison of Ni contents in vacuoles. As the number, purification and lysis of protoplasts was not affected, the limiting step was obviously the purification of the vacuoles via a density gradient, leading to the conclusion that density of the vacuoles was different when plants were grown under elevated Ni supply. It also turned out that the number of isolated vacuoles was different between lines: a higher number of vacuoles could be isolated from *ireg2-1* leaves than from the wildtype (Fig. 42). These differences made it difficult to generate samples with comparable number of vacuoles. When vacuole samples were obtained from Ni-loaded wildtype, *ireg2-1* and 35S *AtIREG2* plants, Ni measurements were kindly performed by Günther Weber (ISAS Dortmund), who used a highly sensitive *adsorptive stripping voltammetry* method to detect Ni in the samples. In this approach the ligand DMG (dimethylglyoxime) was added to the Ni-containing samples to form a stable Ni-DMG-complex. This complex was then detected voltammetrically. In this approach, detection limits for Ni are low, because Ni in form of Ni-DMG accumulates at the electrode. A sample without plant material was prepared with the same protocol and served as blank. Ni concentrations in the blank were already so high, that an assessment of plant samples

made no more sense (data not shown). Thus, the high Ni content in the buffer solution was the major obstacle for this approach rather than the detection limit of Ni. Therefore, AtIREG2-mediated changes in vacuolar Ni concentrations could not be directly determined.

## 4.4 Assessment of a functional relationship between AtIREG1 and AtIREG2

### 4.4.1 Comparative analysis of the phenotype of transgenic lines with altered expression of *AtIREG1* and *AtIREG2*

In the previous chapters it was shown, that *AtIREG1* mutants show altered growth on Ni- and Co-supplemented medium, whereas *AtIREG2* mutants only differed from the wildtype on Ni but not on Co. So far, either mutants of *AtIREG1* or of *AtIREG2* were grown and assessed in separate experiments. To exclude that differences in the experimental setup have influenced the results, *ireg1-1* and *ireg2-1* plants were grown on Co-containing plates for a direct comparison of growth (Fig.43). The *AtIREG2* T-DNA insertion line showed no differences to the wildtype with regard to leaf colour, leaf number, root length or the formation of root hairs, but all these parameters were affected in the *AtIREG1* T-DNA insertion lines, confirming the conclusion that Co is a substrate for AtIREG1 not but not for AtIREG2. The same experiment was repeated with Ni, and in accordance to the previous results *AtIREG1* and *AtIREG2* T-DNA insertion lines showed increased Ni tolerance (data not shown, but similar results are presented in Fig. 45 and 48).

To confirm the increased Ni tolerance of *AtIREG1* and *AtIREG2* overexpressing lines in a comparative experiment, seeds of these lines were placed in concentric circles on agar plates (Fig. 44). A diffusion gradient of Ni was generated by placing a NiCl<sub>2</sub>-containing filter disc to the middle of the plate.

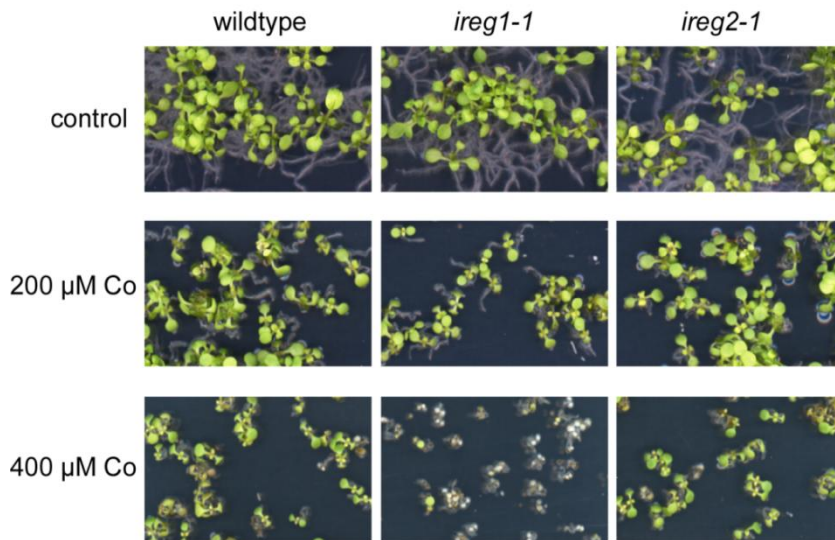


**Figure 43: Loss of *AtIREG1* but not of *AtIREG2* increases Co sensitivity in Arabidopsis.**

Growth phenotype of wildtype, an *AtIREG1* T-DNA insertion line (*ireg1-1*) and an *AtIREG2* T-DNA insertion line (*ireg2-1*) germinated on half strength MS agar plates supplemented with different concentrations of Co. Pictures of representative plates from 3 replicates are shown.

Wildtype seeds only germinated and developed cotyledons when placed in the outermost circles, whereas *AtIREG1* and *AtIREG2* overexpressing lines germinated and even developed up to four leaves at a comparable position. The *AtIREG1* overexpressing line showed a higher level of tolerance than the 35S *AtIREG2* line, with a higher germination rate and better root growth even in the innermost circle (Fig. 44).

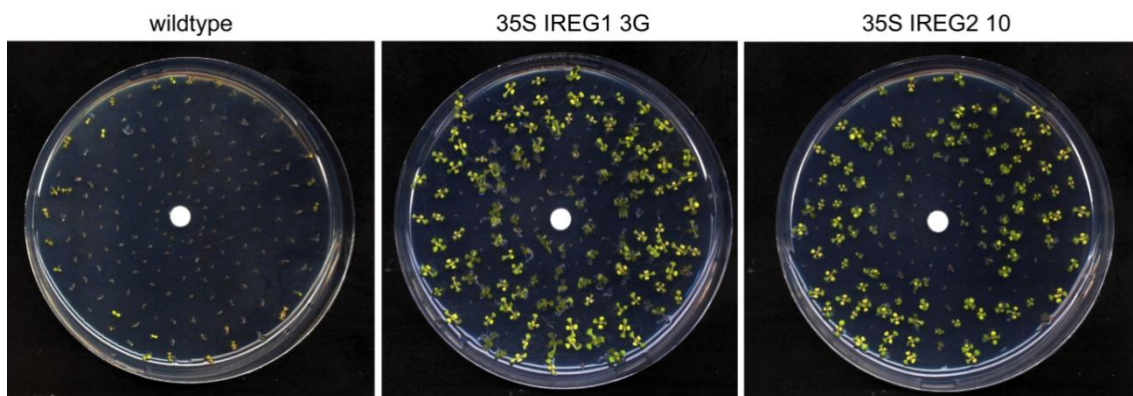


**Figure 44: Overexpression of *AtIREG1* and *AtIREG2* increases Ni tolerance in Arabidopsis.**

Phenotype of wildtype, an *AtIREG1* overexpressing line (35S IREG1 3G) and an *AtIREG2* overexpressing line (35S IREG2 10) germinated on plates with a Ni gradient. Seeds were placed in concentric circles on half strength MS agar plates. Sterile filter discs were soaked with 10  $\mu$ L of 100  $\mu$ M  $\text{NiCl}_2$  solution and were placed in the middle of the plates, to generate a diffusion gradient of Ni.

#### 4.4.2 Characterization of the double T-DNA insertion line *ireg1ireg2*

As the loss of *AtIREG1* as well as *AtIREG2* led to an increased sensitivity to Ni, but both transporters differed in membrane localization and in the response to the Fe nutritional status of the plants, the aim of the next experiments was to investigate whether both transporters function in an additive manner. The single T-DNA insertion lines *ireg1-1* and *ireg2-1* were crossed, and plants homozygous in both alleles were selected. Absence of *AtIREG1* and *AtIREG2* expression was confirmed by RNA gel blot analysis (data not shown). Germination and plant growth of the single and double insertion lines was compared on agar plates supplemented with increasing concentrations of Ni (Fig. 45).

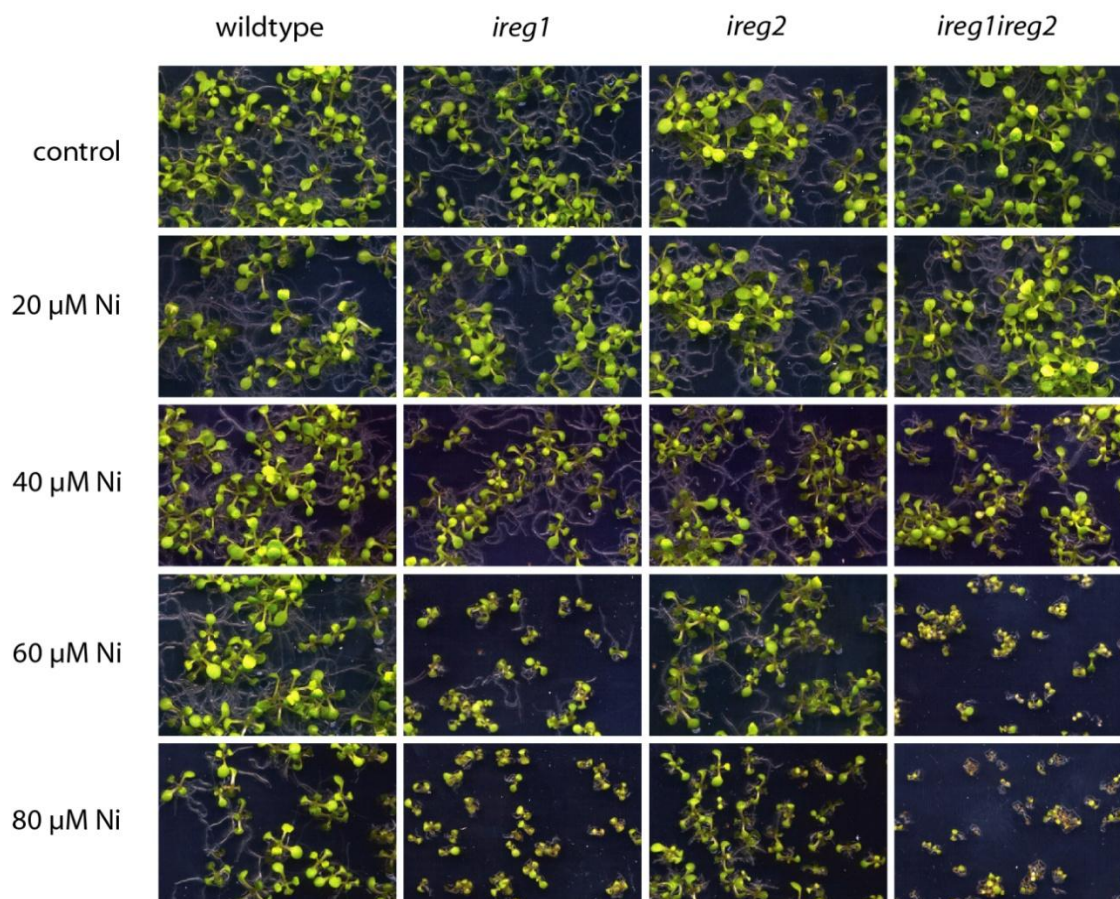


**Figure 45: The double T-DNA insertion line *ireg1ireg2* is highly sensitive to nickel.**

Growth phenotype of wildtype, single T-DNA insertion lines (*ireg1* and *ireg2*) and the double T-DNA insertion line *ireg1ireg2* germinated on half strength MS agar plates supplemented with different concentrations of Ni. Pictures of representative plates from 3 replicates are shown.

Growth of all lines was similar up to 40  $\mu\text{M}$  Ni. In accordance to previous results, *ireg1-1* showed a severe reduction of shoot development and leaf size when germinated on plates supplemented with 60  $\mu\text{M}$  Ni, whereas *ireg2-1* was mainly affected in root length and root development. The double T-DNA insertion line *ireglireg2* showed an additive phenotype, with a repression in growth that was more severe than in both single T-DNA insertion lines. At 80  $\mu\text{M}$  Ni *ireglireg2* seeds germinated poorly and most of the seedlings developed only small cotyledons. In contrast, *ireg1-1* plants showed a reduction in both root and shoot development and severe chlorosis, whereas in *ireg2-1* root elongation was completely arrested. At 60 and 80  $\mu\text{M}$  Ni supply root and shoot development of *ireglireg2* was more reduced than in any of the two single T-DNA insertion lines. For generation of line *ireglireg2* the single T-DNA insertion line *ireg1-2* was used as maternal line for crossing, but lines obtained from pollination of flowers of *ireg2-1* with *ireg1-2* pollen showed the same growth phenotype (data not shown).

#### 4.4.3 Ni-induced ROS (reactive oxygen species) production in dependency of the *AtIREG1* and *AtIREG2* expression level

Since Ni can induce the formation of reactive oxygen species (ROS) in plants (chapter 2.2.2), the question was addressed whether the enhanced Ni sensitivity of *AtIREG1* and *AtIREG2* T-DNA insertion lines could be related to a higher ROS production under Ni stress. To visualize the ROS formation in Arabidopsis roots, plants were stained with H<sub>2</sub>DCFDA (2', 7' - dichlorodihydrofluorecein diacetate). H<sub>2</sub>DCFDA is a fluorogenic reagent to detect reactive oxygen intermediates (hydrogen peroxide, peroxy radicals and peroxy nitrite anions) in cells. Upon oxidation, H<sub>2</sub>DCFDA becomes the highly green fluorescent 2',7'-dichlorofluorescein. Arabidopsis seedlings were grown on plates with or without addition of Ni and pictures were taken directly after 15 minutes staining with H<sub>2</sub>DCFDA. Ni supply induced the formation of ROS in wildtype plants, visible as a green fluorescence in mature roots and especially in lateral root tips. This could not be detected in plants grown on control plates without Ni (data not shown). Ni-induced ROS formation was then compared among wildtype and *AtIREG1* and *AtIREG2* T-DNA

insertion lines (Fig. 46). *Ireg1-1* clearly showed a higher fluorescence which was distributed evenly all over the root system and was only absent in the oldest most apical root parts, whereas the Ni-induced signal in *ireg2-1* was even higher, but here a pattern was obvious with especially high fluorescence in lateral (but not in primary) root tips

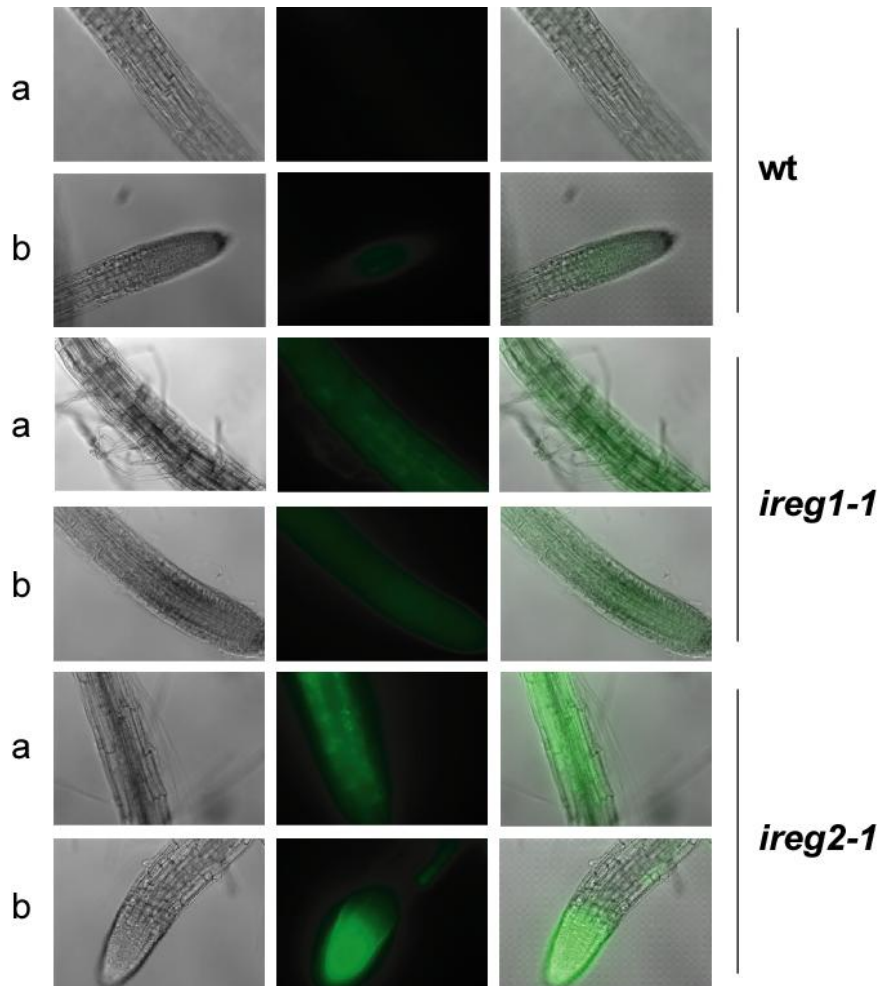


(Fig. 46).

**Figure 46: Loss of *AtIREG1* or *AtIREG2* increases Ni-induced ROS formation in Arabidopsis roots.** Detection of ROS visualized by fluorescence derived from oxidation of H<sub>2</sub>DCFDA (2', 7' - dichlorodihydrofluorecein diacetate) in roots of 10 d old wildtype (wt), an *AtIREG1* (*ireg1-1*) and an *AtIREG2* (*ireg2-1*) T-DNA insertion line, cultured on agar plates with 40  $\mu$ M Ni. *Left column*, phase contrast views. *Middle column*, H<sub>2</sub>DCFDA-derived fluorescence. *Right column*, overlay of H<sub>2</sub>DCFDA-derived fluorescence and phase contrast; *Panels a*, picture of the mature root in the root hair zone. *Panels b*, lateral root tips. Images were analysed using an ApoTome imaging system in an inverted fluorescence microscope.

As the double T-DNA insertion *ireg1ireg2* is more sensitive to Ni than the single T-DNA insertion lines *ireg1-1* and *ireg2-1* (Fig. 45), also this line was used for the detection of Ni-induced ROS formation. As expected, the additive action of AtIREG1 and AtIREG2 led to higher ROS production in the double T-DNA insertion line (Fig. 47), with a particular high fluorescence in lateral root tips and in mature roots.

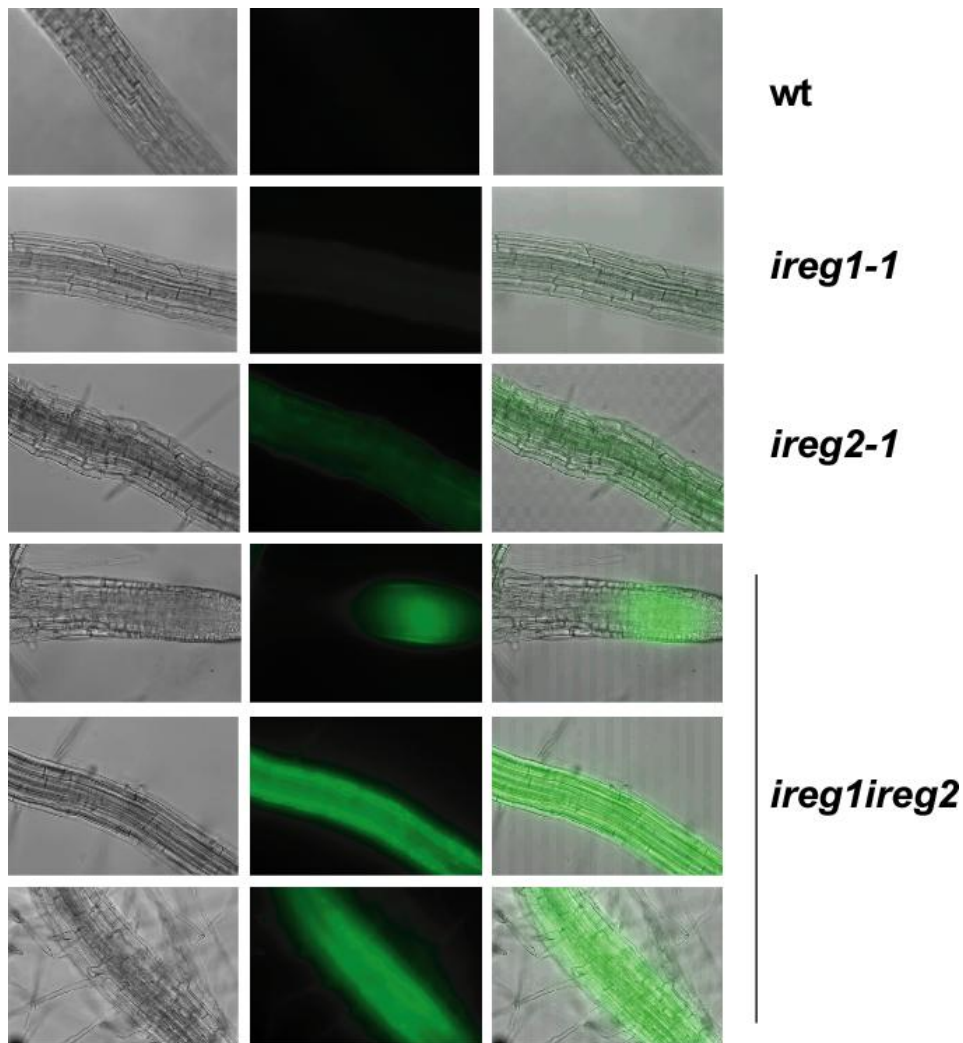


**Figure 47: Ni-induced ROS formation is higher in *ireg1ireg2* than in single T-DNA insertion lines.** Detection of ROS visualized by fluorescence derived from oxidation of H<sub>2</sub>DCFDA (2', 7' - dichlorodihydrofluorecein diacetate) in roots of 10 d old wildtype (wt), *ireg1-1*, *ireg2-1* and *ireg1ireg2* plants, cultured on agar plates with 40  $\mu$ M Ni. *Left column*, phase contrast views. *Middle column*, H<sub>2</sub>DCFDA-derived fluorescence. *Right column*, overlay of H<sub>2</sub>DCFDA-derived fluorescence and phase contrast. Images were taken using an ApoTome imaging system in an inverted fluorescence microscope.

## 4.5 AtIREG3

Two independent T-DNA insertion lines SALK\_034189 (*ireg3-1*) and SALK\_016772 (*ireg3-2*) were ordered from the Salk Institute, homozygous plants were selected, tested via PCR analyses and seeds were amplified. As mutants in *AtIREG1* or *AtIREG2* showed metal transport-related phenotypes, the *AtIREG3* T-DNA insertion lines were tested in a large screen on plates supplemented with different metals at different concentrations (Fig. 48 and 49). As a control, *AtIREG1* and *AtIREG2* T-DNA insertion lines were included in the test. In a first screen Ni and Co sensitivity was assessed. While the phenotypes for the *AtIREG1* and *AtIREG2* T-DNA insertion lines were repeated, both *AtIREG3* T-DNA insertion lines showed no growth difference to the wildtype (Fig. 47).

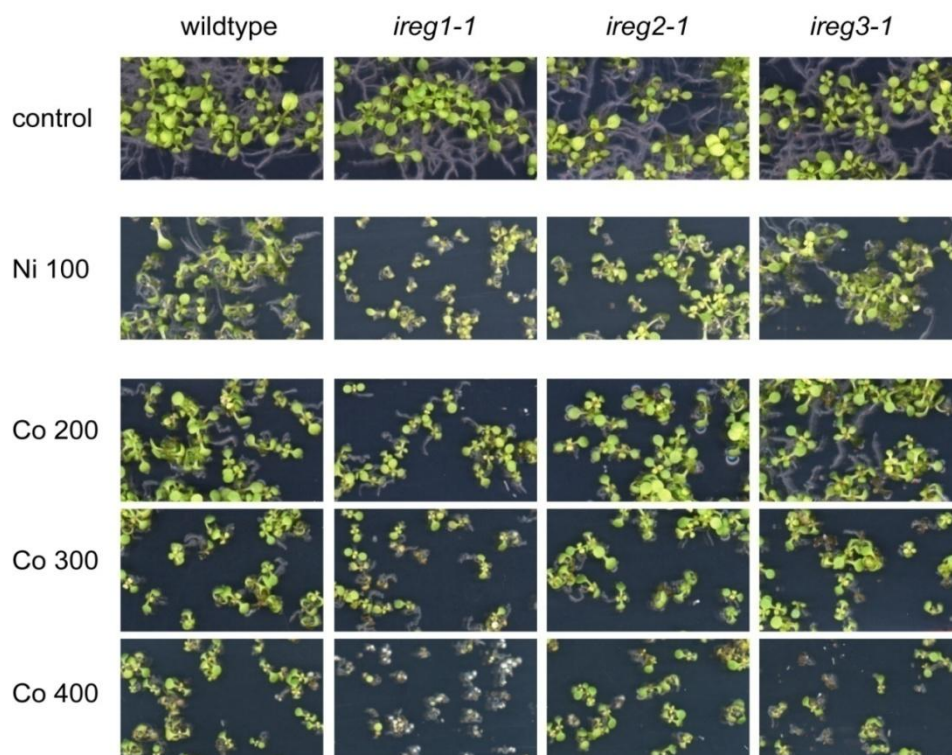


**Figure 48: Loss of *AtIREG3* does not increase Ni or Co tolerance.**

Growth phenotype of wildtype and the T-DNA insertion lines *ireg1-1*, *ireg2-1* and *ireg3-1* germinated on half strength MS agar plates supplemented with different concentrations of Ni or Co. Metal concentrations are given in  $\mu\text{M}$ . Pictures of representative plates from 3 replicates are shown.

To verify the result, the experiment was repeated with a larger range of Ni and Co concentrations and with both *AtIREG3* T-DNA insertion lines, but no differences to the growth of wildtype plants were observed (data not shown). Then, phenotypical analysis was extended to other metals, including Mn, Cd and Zn (Fig. 49), but *ireg3-1* showed no differences to wildtype plants at any of the tested metal concentrations.

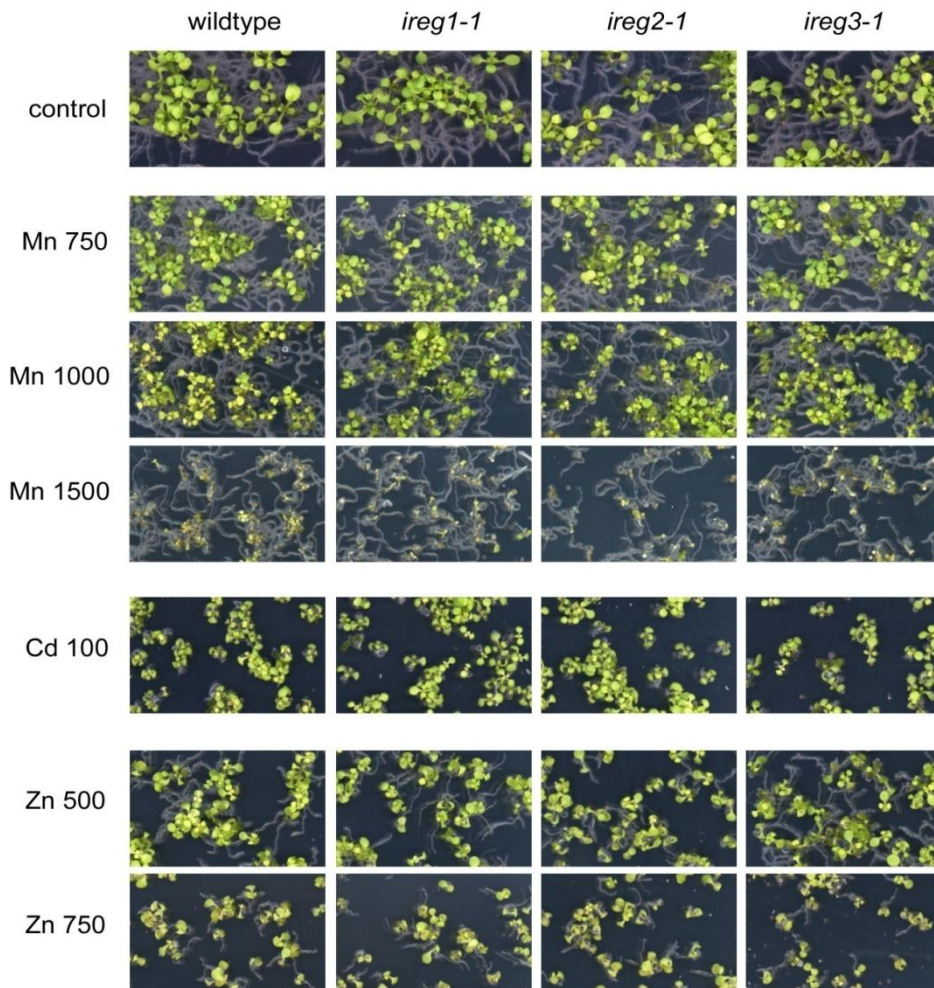


**Figure 49: Loss of *AtIREG3* does not alter plant growth on manganese, cadmium or zinc.**

Growth phenotype of wildtype and the T-DNA insertion lines *ireg1-1*, *ireg2-1* and *ireg3-1* germinated on half-strength MS agar plates supplemented with different concentrations of Mn, Cd and Zn. Metal concentrations are given in  $\mu\text{M}$ . Pictures of representative plates from 3 replicates are shown.

These results did not indicate a metal transport function of *AtIREG3* similar to those of *AtIREG1* or *AtIREG2*. Germination and growth tests were also performed on plates with Fe-deficient medium or at high Fe supply. Due to the absence of a metal-dependent growth phenotype and any other hint for a transport function by *AtIREG3*, no further attempts were made to examine the function of *AtIREG3*.

## 5 Discussion

Starting point for the present thesis was the identification of IREG1 as a Fe exporter in different tissues of vertebrates (Abboud and Haile, 2000; Donovan et al., 2000; McKie et al., 2000), especially in duodenal enterocytes where it mediates the export of Fe into the vascular system (chapter 2.5). IREG1 homologues were also found in other organisms including three homologues in *Arabidopsis thaliana* (McKie et al., 2000). Due to the similarity of the three AtIREGs to the vertebrate Fe exporter IREG1, there was a high likelihood that the Arabidopsis IREG family members also represent Fe efflux proteins. As an initial gene expression analysis for *AtIREGs* indicated an upregulation of *AtIREG2* in Arabidopsis plants grown under Fe-deficient conditions, which supported a possible Fe transport function of the corresponding protein, AtIREG2 was chosen as the first of the three AtIREGs to be characterized.

### 5.1 *AtIREG2* encodes a tonoplast transport protein involved in nickel detoxification in *Arabidopsis thaliana* roots

#### AtIREG2 has a function in Ni transport

The assumed Fe transport function of AtIREG2 could not be affirmed. Heterologous expression in yeast (chapter 4.3.1) did not provide any hint for a function of AtIREG2 in Fe transport, even though different growth complementation or Fe transport assay were tested (chapter 4.3.1). In general, plant Fe transporters often discriminate poorly between Fe and other transition metals. For example, AtIRT1 does not only transport Fe but also a range of other metals, such as Mn, Zn, Co or Cd (Eide et al., 1996; Korshunova et al., 1999; Connolly et al., 2002; Vert et al., 2002; chapter 2.4). The finding that single amino acid changes can alter the substrate specificity of AtIRT1 (Rogers et al., 2000) led to the speculation that the AtIREGs might exhibit different substrate specificity in spite of their similarity to the vertebrate Fe exporters. It was therefore decided to screen for a heavy metal transport function of AtIREG2, employing yeast mutants with increased heavy metal sensitivities at increasing concentrations of

different transition metals. Expression of *AtIREG2* in the Ni sensitive *cot1* deletion strain conferred yeast growth on elevated Ni concentrations (Fig. 26). To specify the range of metals being transported by AtIREG2, the accumulation of radiolabeled  $^{109}\text{Cd}$ ,  $^{54}\text{Mn}$ ,  $^{65}\text{Zn}$ ,  $^{63}\text{Ni}$  or  $^{59}\text{Fe}$  supplied at different concentrations to *AtIREG2*-expressing yeast cells was determined and it was found that only the accumulation of radiolabeled Ni was decreased (Appendix 1). A function in Ni transport was further supported by the increased Ni tolerance of *AtIREG2*-overexpressing *Arabidopsis* lines (Fig. 29). Overexpression of *AtIREG2* also led to an increase in Ni accumulation in roots, whereas *AtIREG2* T-DNA insertion lines accumulated less Ni (Fig. 40). Growth of *AtIREG2* T-DNA insertion lines was then tested on different metals, including Fe, Cu, Mn, Cd, Zn, Mn, Co and Ni. Lacking expression of *AtIREG2* caused an increased sensitivity to external Ni, but did not alter plant growth on any of the other metals (Fig. 45, 48 and 49).

Taken together, all results of the heterologous expression of *AtIREG2* in yeast and the growth phenotypes of *Arabidopsis* lines with altered *AtIREG2* expression did not provide any indication for a role of AtIREG2 in Fe transport, whereas Ni was confirmed as a transported substrate for AtIREG2 in yeast and in plants. This was surprising, because so far Fe has been described as the only substrate for vertebrate IREGs (Abboud and Haile, 2000; Donovan et al., 2000; McKie et al., 2000). However, from the given results it can be concluded, that Fe transport is no (or at least not the primary) function of AtIREG2. Although overexpression of *AtIREG2* in *Arabidopsis* significantly increased Mn, Cu and Zn accumulation in roots (Fig. 40), growth tests of *AtIREG2*-overexpressing *Arabidopsis* lines and wild-type plants on agar medium supplied with elevated concentrations of Mn, Cd, Fe and Zn revealed no growth differences (data not shown). These observations indicate that Ni is a preferential substrate of AtIREG2, even though other transition metals might be transported, in particular when *AtIREG2* is overexpressed.

### **AtIREG2 is a pH-dependent tonoplast transporter in Arabidopsis roots**

*AtIREG2* is mainly expressed in Arabidopsis roots and only at a low level in shoots (Fig. 27). When an *AtIREG2-GFP* fusion construct was transiently expressed in Arabidopsis protoplasts, the localization of the AtIREG2 protein at the tonoplast membrane was observed. In roots of intact plants transformed with an *AtIREG2*-promoter-*AtIREG2-GFP* construct, the AtIREG2-GFP fusion protein clearly localized to the vacuolar membrane, verifying the tonoplast localization of *AtIREG2 in planta* (Fig. 39).

In yeast, AtIREG2-mediated Ni tolerance was only observed at pH 5, but could not be observed at pH 6 or higher (Fig. 26; Appendix 3). In general, the dependence of metal tolerance in yeast on acidic pH is most likely reflected by pH-dependent metal detoxification mechanisms as represented by the CDF family members COT1 and ZRC1 (Conklin et al., 1992; Kamizono et al., 1989). The pH-dependent contribution of AtIREG2 to Ni tolerance most likely indicates that *AtIREG2 in planta* depends directly on the electrochemical gradient across the tonoplast and might function as a metal proton antiporter as is the case for substrate/proton antiporters of the CAX family (Cheng and Hirschi, 2003).

### **AtIREG2 plays a role in iron deficiency-induced nickel detoxification**

The results presented in this thesis suggest that AtIREG2 mediates Ni transport out of the cytoplasm and into the vacuole, a less metal-sensitive compartment. This is supported by the tonoplast localization of AtIREG2 (Fig. 39) and the enhanced Ni tolerance and Ni accumulation in roots of Fe-deficient wild-type plants relative to the insertion lines (Fig. 32, 33 and 40). For a further proof, a protocol for the isolation of vacuoles from Arabidopsis leaves was developed. The aim was to measure Ni directly in the vacuolar fluid and to compare Ni (and other metal) content in vacuoles between lines with differing AtIREG2 expression level. This dataset would have provided direct evidence for the function of AtIREG2 in transport of Ni from the cytosol to the vacuole. But measurements of Ni failed in these preparations, due to the high background Ni concentrations derived from the chemicals used for the preparation of buffers and solutions in this procedure (Fig. 42). As this approach was not successful, a change in

the approach or functional expression in oocytes together with electrophysiological measurements might provide further information on the substrate specificity and molecular transport mechanism.

Considering its function in Ni detoxification, *AtIREG2* showed an unexpected transcriptional regulation. An increasing supply of Ni did not induce gene expression in roots (Fig. 28), whereas Fe deficiency did (Fig. 27). Most interestingly, Fe deficiency-induced upregulation of *AtIREG2* was controlled by the transcription factor FIT. Recent studies identified FIT (formerly also called FRU or FIT1) as a major regulator coordinating the expression of genes involved in Fe deficiency-induced Fe acquisition in *Arabidopsis*, such as *AtIRT1*, *AtFRO2*, and others (Colangelo et al., 2004; Jakoby et al., 2004; chapter 2.3). A comparative transcriptome analysis in *Arabidopsis* wildtype and *atfit1* T-DNA insertion lines identified *AtIREG2* as another downstream target gene of FIT (Colangelo et al., 2004). These observations indicated that the function of *AtIREG2* is related to the Fe deficiency stress response rather than to substrate-induced metal transport. To address the physiological requirement for a Fe deficiency-induced vacuolar Ni loader, Ni accumulation in *Arabidopsis* roots under Fe-deficient growth conditions was examined. Indeed, even short term  $^{63}\text{Ni}$  uptake rates in roots of wildtype plants increased with Fe starvation (Appendix 4), demonstrating that Ni is enriched in Fe-deficient plants, similar to several other transition metals (von Wirén et al., 1994; Crooke et al., 1954; Kukier et al., 2001; Vert et al., 2002). In strong agreement with the broad substrate specificity of *AtIRT1* (Rogers et al., 2000; Eide et al., 1996), *AtIRT1* was identified as a major pathway for the excess uptake of Zn, Co and Mn under Fe-deficient growth conditions (Vert et al., 2002; Korshunova et al., 1999; Connolly et al., 2002). A physiological requirement for metal detoxification under Fe deficiency has been further indicated by the upregulation of *NICOTIANAMINE SYNTHASE 1 (NAS1)* in *atfit1* mutant lines (Colangelo and Guerinot, 2004). Nicotianamine synthase is supposed to have a function in Ni detoxification by an enhancement of Ni translocation to the shoots in form of a nicotianamine-Ni chelate (Vacchina et al., 2003; Pianelli et al., 2005; Kim et al., 2005). Moreover, other genes involved in heavy metal transport or detoxification have been found to be under control of *AtFIT*, such as *AtHMA3* (a Cd transporting ATPase), *AtZIP9* (a Fe(II) and Zn transporter) or *AtCOPT2* (involved in Cu transport).

*AtIREG2* is preferentially expressed in roots (Fig. 27) where cellular Fe acquisition mechanisms are expressed at the highest levels. Even if a detailed analysis of the tissue-specific expression of *AtIREG2* is still under way, the presented results indicate that *AtIREG2* can prevent toxicity of Ni in the same tissue that also expresses *AtIRT1* and that the physiological function of *AtIREG2* is the deposition of excess Ni into the vacuole to counterbalance the low substrate specificity of *AtIRT1* and other iron transport systems at the root plasma membrane (Fig. 50). Hence, *AtIREG2* can be regarded as a so far unrecognized component in the Fe deficiency stress response of plants.

## **5.2 *AtIREG1* encodes a plasma membrane protein involved in nickel and cobalt detoxification in *Arabidopsis thaliana***

### **AtIREG1 has a function in nickel and cobalt transport**

Comparable to the results obtained for *AtIREG2*, the assumed Fe transport function of further *Arabidopsis* homologues of the IREG superfamily could also not be affirmed for *AtIREG1*, neither by heterologous expression of *AtIREG1* in yeast, nor by growth phenotypes of *AtIREG1* mutant lines under different Fe regimes (data not shown). Interestingly, a determination of the accumulation of radiolabeled  $^{109}\text{Cd}$ ,  $^{54}\text{Mn}$ ,  $^{65}\text{Zn}$ ,  $^{63}\text{Ni}$  or  $^{59}\text{Fe}$  in *AtIREG1*-expressing yeast cells revealed a decrease of Ni accumulation, similar to that observed in *AtIREG2*-expressing yeast cells (Appendix 1). For a more detailed investigation of the heavy metal transport function of *AtIREG1*, the growth of *Arabidopsis* T-DNA insertion lines on different metal concentrations (including Ni, Co, Zn, Cu, Mn and Cd) was monitored. Growth phenotypes differing from wildtype plants were observed only on Ni and Co (Fig. 11-14). A function of *AtIREG1* in Ni and Co transport was further supported by an increased Ni and Co tolerance of *AtIREG1*-overexpressing *Arabidopsis* lines (Fig. 6-9). Accumulation experiments showed that loss of *AtIREG1* caused decreased Ni concentrations in shoots, whereas overexpression of *AtIREG1* lowered Ni concentration in roots (Fig. 18), but measurements of metals in

the xylem sap of *AtIREG1* mutant lines did not provide hints for a function of AtIREG1 in metal loading to the xylem (Fig. 19).

Like in the case of AtIREG2, a Fe transport function of AtIREG1 can not be excluded, but none of the performed experiments supported an involvement of AtIREG1 in Fe transport. Instead, the described observations indicate that Ni and Co are preferential substrates for AtIREG1.

### **AtIREG1 is a plasma membrane transporter in Arabidopsis roots and shoots**

*AtIREG1* expression in yeast did not reveal a clear pH-dependence of Ni and Co transport (Appendix 3). In contrast to *AtIREG2* that conferred yeast growth on elevated Ni concentrations, *AtIREG1* expression in yeast even led to a higher sensitivity to Ni. This result was surprising, as expression of both, *AtIREG1* and *AtIREG2*, in yeast led to a decrease in Ni accumulation (Appendix 1). Furthermore, overexpression of any of the two genes conferred higher Ni tolerance in Arabidopsis plants. Thus, the growth impairment of *AtIREG1* expressing yeast on Ni might be due to a secondary effect, as a similar effect is not seen when the same cells were grown on control or Co containing medium (Appendix 3).

In Arabidopsis, expression of AtIREG1 was detected in both, roots and shoots (Fig. 4 and Appendix 6), with a slightly higher expression in roots. An AtIREG1-GFP fusion protein localized to the plasma membrane, when transiently expressed in Arabidopsis protoplasts (Fig. 17). Several attempts failed to localize *AtIREG1* gene or protein expression *in planta* (chapter 4.2.4). To verify a cellular Ni export function of AtIREG1 by a physiological approach, urease was used as a means to determine AtIREG1-mediated changes in cytoplasmic Ni availability. Indeed, transport of Ni through AtIREG1 decreased urea hydrolysis probably by a lower Ni availability (Fig. 21-24). Urease activity was drastically decreased in roots of *AtIREG1*-overexpressing lines and increased in *AtIREG1* T-DNA insertion lines, when plants were grown on urea as the sole nitrogen source (Fig. 25). High external Ni supply could compensate the AtIREG1-mediated loss of Ni availability for the urease in CaMV35S::*AtIREG1* lines (Fig. 23), showing that indeed the higher Ni export activity of AtIREG1 was the cause for the

detected phenotypes and changes in urease activity in *AtIREG1* overexpressing lines. Interestingly, in all *Arabidopsis* lines and in all treatments, urease activity was lower in leaves than in roots, showing that in *Arabidopsis* the root is the main site for urea breakdown. This is supported by the finding, that in plants grown on  $\text{NH}_4\text{NO}_3$ , urease activity in shoots was even below the detection limit (Fig.25), whereas there was some basic urease activity in roots. This is concordant with results obtained in previous experiments (Anne Bohner, personal correspondence). In contrast to the findings in *Arabidopsis*, it has been shown that urease activity is ubiquitously present in other dicotyledonous plants, for example in potato (Witte et al, 2004), which is confirmed by results of urease activity measurements in different potato tissues (Witte et al., 2002b). In rice, urea even seems to be transported to the shoot and to be primarily hydrolyzed in leaf tissue, leading to much higher urease activities in leaves than in roots, and accumulation of urea in leaves of plants grown with urea as a sole nitrogen source under conditions of Ni deficiency (Gerendás et al., 1998).

In summary, in spite of lacking data on *AtIREG1* protein localization in intact plants, there were three independent findings that support a plasma membrane localization of *AtIREG1 in planta*: first, *AtIREG1*-GFP localizes to the plasma membrane in protoplasts; second, Ni transport through *AtIREG1* decreased Ni availability for urea hydrolysis, most likely by export of Ni out of the cytoplasm; third, *atireg1* lines showed higher sensitivity to Ni and Co, whereas *AtIREG1*-overexpressing lines were more tolerant to Ni and Co, and accumulated less Ni and Co in roots.

### **The function of *AtIREG1* in nickel and cobalt detoxification is not Fe-dependent**

In contrast to *AtIREG2*, northern blot and RT-PCR experiments (Fig. 2 and 5) showed that *AtIREG1* expression is not induced by Fe-deficiency. These results suggest that *AtIREG1* expression is not regulated by the transcription factor FIT, which induces the upregulation of genes like *AtIRT1*, *AtFRO2* and *AtIREG2* under Fe-deficient conditions (chapter 2.3). The assumption that *AtIREG1* is not regulated by FIT is supported by a comparative transcriptome analysis in *Arabidopsis* wildtype and *atfit1* T-DNA insertion lines that identified *AtIREG2*, but not *AtIREG1*, as a downstream target gene of FIT

(Colangelo et al., 2004). Furthermore, the Ni sensitivity of *AtIREG1* T-DNA insertion lines was not enhanced under Fe-deficient conditions (Fig. 15 and 16). The differences in primary root length of wildtype plants compared to *AtIREG1* T-DNA insertion lines were even lower on Fe-deficient medium (Fig. 15), showing that the impact of *AtIREG1*-mediated Ni sensitivity does not increase (or does probably even decrease) with Fe deficiency. These observations indicated that the function of *AtIREG1* does not seem to be related to the Fe-deficiency stress response. An induction of *AtIREG1* by Ni or Co should be investigated in future studies to better characterize a possible substrate-induced metal transport function of *AtIREG1*. *AtIRT1* as the major pathway for excess uptake of Zn, Co and Mn (Vert et al., 2002; Korshunova et al., 1999; Connolly et al., 2002) accounts for the physiological requirement of metal detoxification under Fe-deficient conditions. *AtIREG1* does not seem to be involved in a Fe-dependent detoxification mechanism, but functions in Fe-independent detoxification of Ni and Co. Uptake of other metals besides Fe was also found in Arabidopsis plants grown under Fe-sufficient conditions (Korshunova et al., 1999; Vert et al., 2002). This might be especially the case when plants grow on soil with high metal content (McBride, 1994). Hence, *AtIREG1* is more likely to represent a substrate-induced detoxification system. If no upregulation by Ni and Co will be shown in future experiments, *AtIREG1* might be even considered as a constitutive detoxification system. The expression of *AtIREG1* in roots and shoots and the finding that no changes in *AtIREG1* expression were detected in any treatment of several microarray experiments (chapter 4.1) support the function of *AtIREG1* as a housekeeping gene. Further support of a constitutive expression of *AtIREG1* was presented in a study employing a gene expression map of Arabidopsis roots, where no significant differences in *AtIREG1* expression were found between root cell types (Birnbaum et al., 2003).

### 5.3 AtIREG1 and AtIREG2 share similar functions but different localization, substrate specificity and regulation

#### **AtIREG1 and AtIREG2 both function in Ni transport and act in an additive manner**

As different assays revealed that Ni is a common substrate for AtIREG1 and AtIREG2, a double T-DNA insertion line *ireglireg2* was generated and employed to test whether AtIREG1 and AtIREG2 function in an additive manner. Indeed, the Ni sensitivity of *ireglireg2* was higher than that of either single T-DNA insertion line. Thus, an additive function of both transporters in Ni transport could be confirmed. Ni has been shown to lead to the production of reactive oxygen species (ROS), mainly through the interaction with protein ligands, such as the imidazole ring of histidine (Datta et al, 1991; Athar et al, 1987; Huang et al., 1993; chapter 2.2.2). In another study on the relation between glutathione accumulation and plant tolerance to Ni, it was shown that Ni toxicity goes along with the Ni-induced accumulation of ROS in root tips of Arabidopsis (Freeman et al., 2004). The Ni-sensitivity of *AtIREG1* and *AtIREG2* T-DNA insertion lines was accompanied by an increase in Ni-induced formation of ROS (Fig. 46). Moreover in roots of Ni-stressed *ireglireg2* plants the production of ROS was higher than in either single T-DNA insertion lines (Fig. 47), confirming the additive action of AtIREG1 and AtIREG2 in Ni detoxification.

#### **AtIREG1 and AtIREG2 differ in their tissue-specific expression, cellular localization and substrate specificity**

In spite of their overlap in substrate specificity and their additive function in Ni transport, AtIREG1 and AtIREG2 exhibit several differences. *AtIREG2* is mainly expressed in roots (Fig. 27), whereas *AtIREG1* expression was only slightly higher in roots but was also detected in shoots (Fig. 3-5). This result was confirmed by publicly available microarray data, reporting that *AtIREG1* was expressed at a similar level in all tested plant organs (<http://jsp.weigelworld.org/expviz/expviz.jsp>; <https://www.geneinvestigator.ethz.ch>; chapter 4.1). AtIREG1 and AtIREG2 act in an

additive manner in the export of Ni from the cytoplasm, but to different cellular compartments: AtIREG2 is localized at the tonoplast and detoxifies Ni by transporting it to the vacuole, whereas AtIREG1 mediates Ni-transport over the plasma membrane, most likely to release Ni directly to the apoplastic fluid. In plants, the cellular tolerance to or detoxification of heavy metals likely involves the efflux of metals out of the cell as well as the sequestration to a less sensitive compartment like the vacuole, as through both ways the levels of toxic metals in the cytosol can be reduced. By now there is no direct evidence for a role of plasma membrane efflux transporters in heavy metal tolerance, but as not all components of the metal homeostasis have been identified and several members of the above mentioned gene families are not yet characterized, there might be possible candidates for the mediation of cellular metal tolerance by export of metals. Early studies showed that the vacuole is the site for the accumulation of a number of heavy metals, including Zn and Cd (reviewed in Ernst et al., 1992). Enhanced vacuolar sequestration has, for example, been implicated in Cd and Zn tolerance (Chardonens et al., 1998; Verkleij et al., 1998). The most direct evidence was obtained from a Zn tolerant ecotype of *Silene vulgaris* that showed highly increased transport of Zn to the vacuole. It was shown that the *Arabidopsis* metal tolerance proteins AtMTP1 and AtMTP3 act in the sequestration of Zn to vacuoles, thereby functioning in the detoxification of Zn (Kobau et al., 2004; Desbrosses-Fonrouge et al., 2005; Arrivault et al., 2006). The role of these transporters and their differences and similarities to the function of AtIREG1 and AtIREG2 will be further discussed in chapter 5.5.

Additional to Ni, that is substrate of both AtIREG1 and AtIREG2, Co was identified as a substrate for only AtIREG1. Co was excluded as a substrate for AtIREG2, as a loss of *AtIREG2* did not influence plant growth on Co (Fig. 34 and 35) or germination on Co containing medium (Fig. 43), whereas overexpression of *AtIREG2* did not increase Co tolerance (Fig. 29) or influence germination on plates supplemented with Co (Appendix 5).

### **AtIREG1 and AtIREG2 are differentially regulated**

AtIREG2 mediates the detoxification of Ni under Fe-deficiency and thus functions downstream of cellular Fe acquisition. This goes along with an induction of *AtIREG2* by Fe deficiency and an increased Ni sensitivity of *AtIREG2* T-DNA insertion lines under Fe-deficient conditions (Fig. 38). In contrast, the function of AtIREG1 did not seem to be Fe dependent, the impact of the loss of *AtIREG1* on Ni sensitivity did even decrease under conditions of Fe deficiency (Fig. 16). A phenotypical analysis revealed that the root/shoot-ratio is strongly decreased in *atireg2* plants that were grown under Fe-deficient conditions (Fig. 38), mainly because the production of root biomass was impaired. Under Fe-sufficient growth conditions, root/shoot-ratios were similar in wildtype and *atireg2* plants. Loss of *AtIREG1* did not lead to a change in the root/shoot-ratio, not even under Fe-deficient conditions.

The transcription factor FIT (formerly also called FRU or FIT1) functions as a major regulator in the coordination of the expression of genes involved in Fe acquisition. *AtIREG2*, but not *AtIREG1*, was identified as a downstream target gene of FIT (Colangelo et al., 2004). This was confirmed in an investigation of *AtIREG1* and *AtIREG2* expression in transgenic Arabidopsis lines with altered *FIT* expression (Appendix 6, kindly provided by Petra Bauer, Saarland University). In plants lacking the expression of *FIT*, *AtIREG2* was no longer induced under Fe-deficient conditions, whereas overexpression of *FIT* led to a Fe-deficiency induced expression of *AtIREG2* even in leaves. *AtIREG1* was expressed at the same level in roots and shoots of all lines, independent of the *FIT* expression level (Appendix 6). The regulation of *AtIREG2* by *FIT* is in agreement with the Fe deficiency-induced expression of *AtIREG2* in roots, in the same tissue that also expresses the *FIT*-regulated Fe-acquisition genes, e.g. *AtIRT1*, at the highest level. Localization of *AtIREG1* expression could be detected in root and shoot tissue and is thus not analogous to that of *AtIRT1*.

Hints for differences in *AtIREG1* and *AtIREG2* regulation were also provided by a study on the orchid transcription factor *DwMYB2*. Expression of *DwMYB2* in Arabidopsis led to hypersensitivity to Fe deficiency, with higher content of Fe in roots and a decreased content in shoots (Chen et al., 2006). Genes for Fe uptake like *AtIRT1* and the ferric reductase *AtFRO2* were upregulated in *DwMYB2* overexpressing Arabidopsis plants,

whereas *AtFRD3*, *NRAMP1* and *AtIREG1* (but not *AtIREG2*) were downregulated. The author explained the downregulation of these three genes by an involvement of the corresponding proteins in Fe homeostasis or translocation. *AtFRD3* is indeed involved in Fe translocation, most likely by loading of citrate to the xylem (Rogers and Guerinot, 2002; Green and Rogers, 2004), where Fe is then moved in form of a ferric-citrate complex (Durrett et al., 2007). *AtNRAMP1* has a Fe transport function, since *AtNRAMP1* overexpression led to resistance to toxic Fe concentrations, whereas loss of *AtNRAMP1* caused Fe hypersensitivity (Curie et al., 2000). Despite the fact that a heterologous gene was expressed, it might be interesting to further analyse why *AtIREG1* was coregulated with *AtFRD3* and *AtNRAMP1* by DwMYB2.

In yeast, similar to the regulation of *AtIREG2* and the Arabidopsis Fe uptake system by FIT, the Zn/Co transporter gene *COT1* was also coregulated with other Fe-deficiency induced genes and appeared to be under control of the Fe-regulated transcription factor AFT1 (Foury and Talibi, 2001). In addition, *COT1* was also up-regulated after external supply of Co (Stadler und Schweyen, 2002). Thus, induction of gene expression by Co appeared as a major difference in the regulation between *COT1* in yeast and *AtIREG2* in Arabidopsis roots (Fig. 28). In Arabidopsis substrate-induced and Fe deficiency-induced metal detoxification might be partially uncoupled: *AtIREG2* detoxifies Ni that is taken up under Fe-deficient conditions, whereas Ni and Co detoxification by *AtIREG1* is not Fe-dependent, but could possibly be induced by Ni and / or Co.

## 5.4 Preliminary characterization of *AtIREG3*

Whereas *AtIREG1* and *AtIREG2* share 84.6% similarity at the protein level (Table 1), *AtIREG3* falls into another cluster in the phylogenetic tree of IREG homologs (Introductory Fig. 2) and has a similarity of only 20% to both other *AtIREGs*. An amino acid alignment showed a divergence of *AtIREG3* especially in the N-terminal region of the protein, which is longer than that of *AtIREG1* or *AtIREG2* (Fig. 1). The number and distribution of transmembrane domains over the entire amino acid sequence, which is similar in all three *AtIREGs*, allowed to predict a transport function also for *AtIREG3*. A first investigation did not show any germination or growth

differences of *AtIREG3* T-DNA insertion lines on Ni, Co, Mn, Cd or Zn (Fig. 48 and 49). These results gave no hint for a metal transport function of *AtIREG3*. Different computer predictions revealed a very high probability that *AtIREG3* localizes to plastid, in particular to the inner plastidic envelope (chapter 4.1; Koo and Ohlrogge, 2002). Thus, a metal transport function of *AtIREG3* might not be detected using plate growth experiments, but further experiments should be conducted to verify the localization of *AtIREG3* and to investigate a possible function in metal homeostasis and compartmentalization by transport of metals over the plastidic envelope.

## 5.5 The *AtIREG*s constitute a previously uncharacterized metal transporter gene family in *Arabidopsis*

With respect to the large amount of expanded metal transporter families in *Arabidopsis* and the broad range of functions they fulfil (chapter 2.2.3), not many transition metal transporters have been characterized in detail by now. Metals are taken up from the soil and have to cross several cell membranes before they are transferred to the xylem and delivered to growing tissues. The best characterized transporter for heavy metal uptake in *Arabidopsis* is the previously mentioned *AtIRT1*, which is localized at the plasma membrane of rhizodermal cells and transports  $\text{Fe}^{2+}$  into the root (chapter 2.3). *AtYSL2* probably is a transporter that acts further downstream to transport Fe through the *Arabidopsis* root tissue towards the xylem. YSL proteins are thought to mediate the transport of metals that are complexed with plant-derived phytosiderophores or NA, a precursor for phytosiderophore synthesis in grasses (Curie et al., 2001). YSL2 is localized in the pericycle and endodermis (Schaaf et al., 2005), and is upregulated under conditions of Fe sufficiency or Fe resupply (DiDonato et al., 2004; Schaaf et al., 2005). This expression pattern suggests a function of *AtYSL2* in the lateral transport of metals in *Arabidopsis* roots. Two  $\text{P}_{1\text{B}}$ -ATPases, *AtHMA2* and *AtHMA4*, have been reported to function redundantly in the translocation of Zn from the root to the shoot (Hussain et al., 2004; Verret et al., 2004). Expression of *AtHMA2* and *AtHMA4* in the root vasculature and lower Zn levels in the shoots of *hma2hma4* plants point to a role of these two

proteins in xylem loading of Zn (Hussain et al., 2004). These transporters are plasma membrane localized and function in the radial movement of metals in *Arabidopsis* roots. Probably even less is known about intracellular transporters in *Arabidopsis* that contribute to metal compartmentalization and homeostasis at the cellular level (Fig. 50).

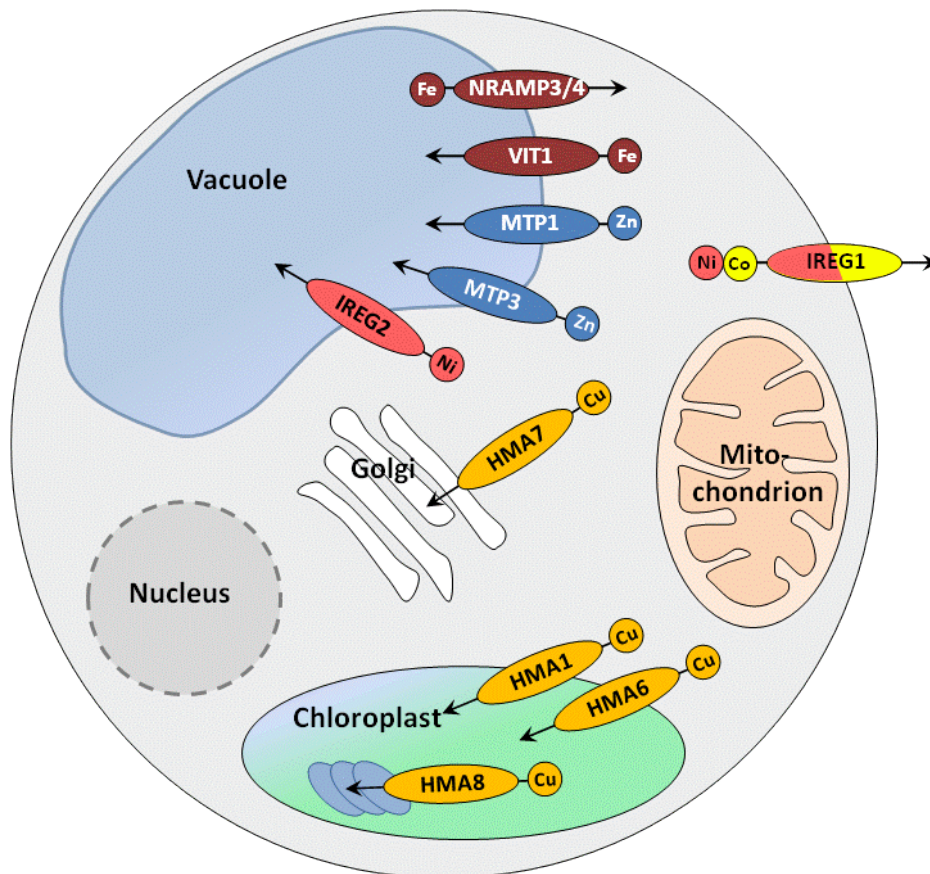


**Figure 50: Intracellular metal transport in a generic *Arabidopsis* cell.**

The localization of intracellular metal transporters and their substrates in a generalized *Arabidopsis thaliana* cell are shown. Arrows indicate the direction of transport. NRAMP3 and NRAMP4 function redundantly in the mobilization of Fe from the vacuole. VIT1 mediates Fe sequestration into the vacuole in *Arabidopsis* seeds. Four  $P_{1B}$ -ATPases are involved in Cu homeostasis. HMA1 and 6 transport Cu to the stroma of chloroplast, HMA8 functions in the transport of Cu to the thylakoid lumen, and HMA7 delivers Cu to the Golgi. MTP1 and MTP3 both transport Zn to the vacuole, but are differentially regulated. MTP3 is important under conditions of Fe-deficiency, whereas MTP1 is thought to be constitutively expressed. IREG2 is localized at the tonoplast and detoxifies Ni by transporting it to the vacuole under conditions of Fe-deficiency, whereas IREG1 mediates Fe-independent Ni- and Co-transport across the plasma membrane into the apoplast.

Four members of the  $P_{1B}$ -ATPases are implicated in Cu homeostasis in *Arabidopsis* cells and have been localized: AtHMA1 and AtHMA6 (also referred to as PAA1) are localized at the plastid envelope, where they deliver Cu to the stroma (Seigneurin-Berny et al., 2005; Shikanai et al., 2003; Abdel-Ghany et al., 2005), while AtHMA8 (also

referred to as PAA2) functions at the thylakoid membrane to deliver Cu to the thylakoid lumen (Shikanai et al., 2003; Abdel-Ghany et al., 2005). AtHMA7 (RAN1) resides at the Golgi and delivers Cu<sup>+</sup> across post-Golgi membranes (Hirayama et al., 1999; Woeste and Kieber, 2000). The only known transporters that participate in cellular Fe homeostasis are AtNRAMP3, AtNRAMP4 and AtVIT1. AtNRAMP3 and 4 function redundantly in the mobilization of Fe from the vacuole. However, these Fe transporters are only expressed during germination, which appears as a particular Fe-sensitive developmental phase requiring the utilization of Fe stores (Lanquar et al., 2005; Thomine et al., 2003). AtVIT1 was identified by Kim et al. (2006) as an Arabidopsis homologue of yeast CCC1, a transporter that mediates vacuolar Fe storage in yeast by transporting Fe from the cytosol to the vacuole (Li et al., 2001). AtVIT1 rescued the Fe-sensitive phenotype of the yeast mutant lacking CCC1 and was highly expressed in developing seeds. X-ray fluorescence microtomography demonstrated that loss of *VIT1* led to a strong decrease of Fe in germinating seed, especially in provascular cells of the hypocotyls, radical and cotyledon embryonic seed tissue (Kim et al., 2006). AtNRAMP1 might also have a function in cellular Fe transport, since *AtNRAMP1* overexpressing plants were resistant to toxic Fe concentrations, whereas loss of *AtNRAMP1* caused Fe hypersensitivity (Curie et al., 2000). Computer predictions based on the proteomic analysis of the plastid envelope gave a very high probability for the AtNRAMP1 protein to be located in plastids (Koo and Ohlrogge, 2002; Ferro et al., 2002). AtNRAMP1 might thus play a role in Fe loading into plastids, where Fe is stored as phytoferritin, and hence play a role in Fe homeostasis in plants.

### **The physiological role and future potential of AtIREG1 and AtIREG2 in the context of metal detoxification strategies in plants**

The vacuole is a known site for the accumulation of a number of heavy metals, and has been implicated in Cd and Zn tolerance (chapter 2.2.3). A role of vacuolar loading of metals has already been reported for transition metal transporters of the CDF family, namely AtMTP1 and AtMTP3 (Kobae et al., 2004; Desbrosses-Fonrouge et al., 2005). The *AtMTP1* gene is, in contrast to *AtIREG2* (and similar to *AtIREG1*), expressed to the same level in roots and shoots. Another member of the CDF family in Arabidopsis,

AtMTP3, seems to fulfil a function similar to that of AtIREG2. AtMTP3 contributes to cellular Zn tolerance and controls Zn partitioning, particularly under conditions of high Zn uptake, for example under conditions of Zn overload or Fe deficiency (Arrivault et al., 2006) and is expressed mainly in roots. Thus, Zn and Ni detoxification in *Arabidopsis* show similarities: both metals require a set of two transporters, one of which is upregulated under conditions of Fe deficiency and functions mainly in roots, whereas the other is regulated in a Fe-independent manner and is expressed in root and in shoot.

Generally, among the functionally characterized heavy metal transporters, metal selectivity is lower in the transporters mediating metal influx into the cytoplasm from an extra-cytoplasmic compartment (Krämer et al., 2007). The broad substrate specificity of heavy metal importers may ensure their universal potential to fulfil different transport functions in different plant organs. The price for this universal potential is a lack of full control over the composition of metals entering the cell (chapter 2.4). Examples for the low specificity of metal uptake are Fe uptake systems in plants. Fe acquisition by non-graminaceous plant roots, as in yeast cells and the vertebrate intestine, is based on the reduction of ferric iron via a membrane-bound reductase and on the subsequent uptake of ferrous iron across the plasma membrane via a transporter for  $\text{Fe}^{2+}$ , whereas the grasses activate a chelation-based strategy. In most organisms analyzed so far the relevant Fe transporters discriminate poorly among transition metals (Li and Kaplan, 1998; Vert et al., 2002; Gunshin et al., 1997; von Wirén et al., 1996; Schaaf et al., 2004; described in detail in chapter 2.4). One exception is the yeast FTR1 transporter, which appears to be more specific because of the coupling with the Fe(III) oxidase FET3 (Stearman et al., 1996). An excess accumulation of other transition metals due to unspecific metal uptake, however, provokes a secondary stress that increases with the extent of Fe deficiency (Crooke et al., 1954; Li and Kaplan, 1998). An analysis of the substrate selectivity of mutated AtIRT1 proteins supports the view that it might be difficult to evolve highly specific Fe transporter proteins (Rogers et al., 2000). Therefore, plants have to cope with undesired uptake of heavy metals and with metal imbalances in the cytoplasm, especially under conditions of toxic metal concentrations in the soil or under Fe deficiency. This might be the cause why during evolution plants have developed a set of specific transporters for the export of heavy metals, like the

described AtMTP1 and AtMTP3, which are highly specific for the export of Zn from the cytoplasm to the vacuole (Krämer, 2005; Kobae et al., 2004; Arrivault et al., 2006), and the newly identified AtIREG1 and AtIREG2, which seem to be specific for transport of Ni (or Ni and Co, respectively). In this way plants are able to counterbalance the low specificity of metal uptake.

In the last centuries, human industrial, mining and military activities as well as farming and waste practices have contaminated large areas with high concentrations of heavy metals (reviewed in Peuke and Rennenberg, 2005). Some plants have the ability to accumulate metals and could be used to remove pollutant metals from the environment. It might be of interest to further examine the biotechnological potential of the AtIREGs in phytoremediation or in the development of metal-tolerant plants. As Ni phytomining has become a highly profitable agricultural industry (Li et al., 2003; Chaney et al., 2005; Chaney et al., 2007), the Ni transporters AtIREG1 and AtIREG2 might be of interest for the development of commercial phytoextraction technologies. Support for a potential of the AtIREGs in phytoremediation is provided by a comparison of gene copy numbers between *Arabidopsis thaliana* and the metal hyperaccumulator *A. halleri*, which showed that *AtIREG1* is fivefold higher expressed in the roots of the hyperaccumulating species than in *A. thaliana* (Talke et al., 2006; the gene is in the publication wrongly labelled “IREG2”). As a vacuolar Ni loader, expression of *AtIREG2* in leaves might provide a means to increase Ni accumulation in plants. New applications of transporters in phytoremediation are opened by mutant screening techniques that are aimed at designing transporters that specifically accumulate certain cations while excluding others. For AtIRT1, for example, it was shown that single amino acid substitutions can lead to changes in the substrate specificity for Fe, Zn, Mn and Cd transport (Rogers et al., 2000). Single amino acid changes led for example to a loss of the Zn transport activity or abolished the Fe and Mn transport function of AtIRT1. Just recently, a study showed that single amino acid changes in the yeast vacuolar metal transporters ZRC1 and COT1 alters their substrate specificity (Lin et al., 2008). *Saccharomyces cerevisiae* mutants were selected, which permitted Fe sensitive *ccc1* cells to grow under high Fe conditions. A mutation was identified, that changed the substrate specificity of ZRC1 from Zn to Fe, whereas another mutation in the Zn and Co transporter COT1 led to a Fe transport function and decreased Co transport

ability (Lin et al., 2008). Similar approaches might also be conceivable for IREG transporters.

In conclusion, with the presented results the first cellular Ni and Co homeostasis mechanisms have been identified. Until the start of the work for this thesis there was no direct evidence for a role of plasma membrane efflux transporters in heavy metal tolerance, but with AtIREG1 the first plasma membrane exporter involved in cellular metal tolerance has been characterized. While the results presented in this thesis lead to a deeper understanding of the function of AtIREG1 and AtIREG2, and thus of the cellular metal homeostasis network in plants, it might be of further interest to address the question whether AtIREG1 is substrate-induced or constitutively expressed. Analysis of a possible plastid localization and plastidic metal homeostasis function of AtIREG3 will give further insights to its function and might provide the most important piece of information to design experimental protocols for a phenotypic analysis of the corresponding T-DNA insertion lines. Finally, functional expression in oocytes together with electrophysiological measurements would allow addressing questions on the substrate specificity of IREG transporters in more detail and thus would further contribute to a deeper characterization of their function in plants and of their biotechnological potential in phytoremediation or the development of metal-tolerant plants.

## 6 References

- Abboud S, Haile DJ** (2000): A novel mammalian iron-regulated protein involved in intracellular iron metabolism. *J Biol Chem* 275: 19906-19912
- Abdel-Ghany SE, Muller-Moule P, Niyogi KK, Pilon M, Shikanai T** (2005): Two P-type ATPases are required for copper delivery in *Arabidopsis thaliana* chloroplasts. *Plant Cell* 17: 1233-1251
- Alonso JM, Stepanova AN, Leisse TJ, Kim CJ, Chen HM, Shinn P, Stevenson DK, Zimmerman J, Barajas P, Cheuk R, Gadrinab C, Heller C, Jeske A, Koesema E, Meyers CC, Parker H, Prednis L, Ansari Y, Choy N, Deen H, Geralt M, Hazari N, Hom E, Karnes M, Mulholland C, Ndubaku R, Schmidt I, Guzman P, Aguilar-Henonin L, Schmid M, Weigel D, Carter DE, Marchand T, Risseeuw E, Brogden D, Zeko A, Crosby WL, Berry CC, Ecker JR** (2003): Genome-wide insertional mutagenesis of *Arabidopsis thaliana*. *Science* 301, 653–657
- Andres-Colas N, Sancenon V, Rodriguez-Navarro S, Mayo S, Thiele DJ, Ecker JR, Puig S, Penarrubia L** (2006): The *Arabidopsis* heavy metal P-type ATPase HMA5 interacts with metallochaperones and functions in copper detoxification of roots. *Plant J* 45: 225-236
- Arnon DI, Stout PR** (1939): The essentiality of certain elements in minute quantity for plants with special reference to copper. *Plant Physiol* 14(2): 371-5
- Arrivault S, Senger T, Krämer U** (2006): The *Arabidopsis* metal tolerance protein AtMTP3 maintains metal homeostasis by mediating Zn exclusion from the shoot under Fe deficiency and Zn oversupply. *Plant J* 46(5): 861-79
- Athar M, Hasan SK, Srivastava RC** (1987): Evidence for the involvement of hydroxyl radicals in nickel mediated enhancement of lipid peroxidation: Implications for nickel carcinogenesis. *Biochem Biophys Res Commun* 147: 1276-1281
- Axelsen KB, Palmgren MG** (2001): Inventory of the superfamily of P-type ion pumps in *Arabidopsis*. *Plant Physiol* 126: 696-706
- Baccouch S, Chaoui A, El Ferjani E** (1998): Nickel-induced oxidative damage and antioxidant responses in *Zea mays* shoots. *Plant Physiol Biochem* 36: 689-694
- Bauer P, Ling HQ, Guerinot ML** (2007): FIT, the FER-LIKE IRON DEFICIENCY INDUCED TRANSCRIPTION FACTOR in *Arabidopsis*. *Plant Physiol Biochem*. 45(5):260-1
- Berezcky Z, Wang HY, Schubert V, Ganai M, Bauer P** (2003): Differential regulation of nramp and irt metal transporter genes in wild type and iron uptake mutants of tomato. *J Biol Chem* 278: 24697-24704
- Birnbaum K, Shasha DE, Wang JY, Jung JW, Lambert GM, Galbraith DW, Benfey PN** (2003): A gene expression map of the *Arabidopsis* root. *Science* 302(5652):1956-60
- Briat JF, Lebrun M** (1999): Plant responses to metal toxicity. *C R Acad Sci III* 322: 43-54
- Briat JF, Curie C, Gaymard F** (2007): Iron utilization and metabolism in plants. *Curr Opin Plant Biol* 10(3): 276-82
- Brown PH, Welch RM, Cary EE** (1987): Nickel: A Micronutrient Essential for Higher Plants. *Plant Physiology* 85 (3): 801 – 803
- Brumbarova T, Bauer P** (2005): Iron-mediated control of the basic helix-loop-helix protein FER, a regulator of iron uptake in tomato. *Plant Physiol* 137(3): 1018-26

- Cadenas E** (1989): Biochemistry of oxygen toxicity. *Annu Rev Biochem* 58: 79-110
- Chaney RL, Angle JS, McIntosh MS, Reeves RD, Li YM, Brewer EP, Chen KY, Roseberg RJ, Perner H, Synkowski EC, Broadhurst CL, Wang S, Baker AJ** (2005): Using hyperaccumulator plants to phytoextract soil Ni and Cd. *Z Naturforsch [C]* 60(3-4):190-8
- Chaney RL, Angle JS, Broadhurst CL, Peters CA, Tappero RV, Sparks DL** (2007): Improved understanding of hyperaccumulation yields commercial phytoextraction and phytomining technologies. *J Environ Qual* 36(5):1429-43
- Chen YH, Wu XM, Ling HQ, Yang WC** (2006): Transgenic expression of *DwMYB2* impairs iron transport from root to shoot in *Arabidopsis thaliana*. *Cell Research* 16: 830-840
- Cheng NH, Hirschi KD** (2003): Cloning and characterization of CXIP1, a novel PICOT domain-containing Arabidopsis protein that associates with CAX1. *J. Biol. Chem.* 278, 6503–6509
- Chrestensen CA, Starke DW, Mieyal JJ** (2000): Acute cadmium exposure inactivates thioltransferase (glutaredoxin), inhibits intracellular reduction of protein-glutathionyl-mixed disulfides, and initiates apoptosis. *J Biol Chem* 275: 26556-65
- Clemens S** (2001): Molecular mechanisms of plant metal tolerance and homeostasis. *Planta* 212(4):475-86
- Clemens S, Palmgren MG, Krämer U** (2002): A long way ahead: understanding and engineering plant metal accumulation. *Trends Plant Sci* 7: 309–315
- Clemens S** (2006): Toxic metal accumulation, responses to exposure and mechanisms of tolerance in plants. *Biochimie* 88: 1707–1719
- Cobbett CS, Hussain D, Haydon MJ** (2003): Structural and functional relationships between type 1B heavy metal-transporting P-type ATPases in Arabidopsis. *New Phytol* 159: 315-321
- Cohen CK, Fox TC, Garvin DF, Kochian LV** (1998): The role of iron-deficiency stress responses in stimulating heavy-metal transport in plants. *Plant Physiol* 116: 1063-1072
- Colangelo EP, Guerinot ML** (2004): The essential basic helix-loop-helix protein FIT1 is required for the iron deficiency response. *Plant Cell* 16: 3400–3412
- Colangelo EP, Guerinot ML** (2006): Put the metal to the petal: metal uptake and transport throughout plants. *Curr Opin Plant Biol* 9(3): 322-30
- Conklin DS, McMaster JA, Culbertson MR, Kung C** (1992): *COT1*, a gene involved in cobalt accumulation in *Saccharomyces cerevisiae*. *Mol. Cell Biol.* 12, 3678–3688
- Connolly EL, Fett JP, Guerinot ML** (2002): Expression of the *IRT1* metal transporter is controlled by metals at the levels of transcript and protein accumulation. *Plant Cell* 14: 1347-1357
- Connolly EL, Campbell NH, Grotz N, Prichard CL, Guerinot ML** (2003): Overexpression of the *FRO2* iron reductase confers tolerance to growth on low iron and uncovers posttranscriptional control. *Plant Physiol* 133: 1102–1110
- Crooke WM, Hunter JG, Vergnano O** (1954): The relationship between nickel toxicity and iron supply. *Ann. Applied Biol.* 41, 311–324
- Curie C, Alonso JM, Le Jean M, Ecker JR, Briat JF** (2000): Involvement of NRAMP1 from *Arabidopsis thaliana* in iron transport. *Biochem J* 347: 749-755

- Curie C, Panaviene Z, Loulergue C, Dellaporta SL, Briat JF, Walker EL** (2001): *Maize yellow stripe1* encodes a membrane protein directly involved in Fe(III) uptake. *Nature* 409: 346-349
- Dat J, Vandenabeele S, Vranova E, Van Montagu M, Inze D, Van Breusegem F** (2000): Review, Dual action of the active oxygen species during plant stress responses. *Cell Mol Life Sci* 57: 779-795
- Datta AK, Misra M, North SL, Kasprzak KS** (1992): Enhancement by nickel(II) and L-histidine of 2'-deoxyguanosineoxidation with hydrogen peroxide. *Carcinogenesis* 13(2): 283-287
- De Domenico I, McVey Ward D, Nemeth E, Vaughn MB, Musci G, Ganz T, Kaplan J** (2005): The molecular basis of ferroportin-linked hemochromatosis. *Proc Natl Acad Sci* 102: 8955-8960
- De Domenico I, Ward DM, Nemeth E, Musci G, Kaplan J** (2006): Iron overload due to mutations in ferroportin. *Haematologica*. 91(1):92-5. Review.
- De Domenico I, Ward DM, Musci G, Kaplan J** (2007): Evidence for the multimeric structure of ferroportin. *Blood* 109(5):2205-9.
- Delhaize E, Kataoka T, Hebb DM, White RG, Ryan PR** (2003): Genes encoding proteins of the cation diffusion facilitator family that confer manganese tolerance. *Plant Cell* 15: 1131-1142
- Delwiche CC, Johnson CM, Reisenauer HM** (1961): Influence of cobalt on nitrogen fixation by medicago. *Plant Physiol* 36(1): 73-78
- Desbrosses-Fonrouge AG, Voigt K, Schroder A, Arrivault S, Thomine S, Krämer U** (2005): *Arabidopsis thaliana* MTP1 is a Zn transporter in the vacuolar membrane which mediates Zn detoxification and drives leaf Zn accumulation. *FEBS Lett* 579: 4165-4174
- DiDonato RJ Jr, Roberts LA, Sanderson T, Easley RB, Walker EL** (2004): *Arabidopsis* YELLOW STRIPE-LIKE2 (YSL2): a metal-regulated gene encoding a plasma membrane transporter of nicotianamine-metal complexes. *Plant J* 39:403-414.
- Dixon NE, Gazzola C, Blakeley RL, Zerner B** (1975): Jack bean urease (EC 3.1.5.1). A metalloenzyme. A simple biological role for nickel. *J Am Chem Soc* 97: 4131-4133
- Donovan A, Brownlie A, Zhou Y, Shepard J, Pratt SJ, Moynihan J, Paw BH, Drejer A, Barut B, Zapata A, Law TC, Brugnara C, Lux SE, Pinkus GS, Pinkus JL, Kingsley PD, Palis J, Fleming MD, Andrews NC, Zon LI** (2000): Positional cloning of zebrafish ferroportin1 identifies a conserved vertebrate iron exporter. *Nature* 403: 776-781
- Drager DB, Desbrosses-Fonrouge AG, Krach C, Chardonnens AN, Meyer RC, Saumitou-Laprade P, Krämer U** (2004): Two genes encoding *Arabidopsis halleri* MTP1 metal transport proteins cosegregate with zinc tolerance and account for high MTP1 transcript levels. *Plant J* 39: 425-439
- Drakesmith H, Schimanski LM, Ormerod E** (2005): Resistance to hepcidin is conferred by hemochromatosis-associated mutations of ferroportin. *Blood* 106: 1092-1097
- Duffus JH** (2002): "Heavy metals" a meaningless term? (IUPAC Technical Report). *Pure Appl Chem* 74/5: 793-807
- Durrett TP, Gassmann W, Rogers EE** (2007): The FRD3-mediated efflux of citrate into the root vasculature is necessary for efficient iron translocation. *Plant Physiol* 144(1): 197-205
- Eide DJ, Broderius M, Fett J, Guerinot ML** (1996): A novel iron regulated metal transporter from plants identified by functional expression in yeast. *Proc Nat Acad Sci* 93: 5624-5628
- Eide DJ** (1998): The molecular biology of metal ion transport in *Saccharomyces cerevisiae*. *Ann Rev Nutr* 18: 441-469

- El-Jaoual T, Cox DA** (1998): Manganese toxicity in plants: A review. *J Plant Nutr* 21: 353-386
- Eng BH, Guerinot ML, Eide D, Saier MH Jr.** (1998): Sequence Analyses and Phylogenetic Characterization of the ZIP Family of Metal Ion Transport Proteins. *J Membrane Biol* 166, 1–7
- Eren E, Argüello JM** (2004): Arabidopsis HMA2, a divalent heavy metal transporting P(1B)-type ATPase, is involved in cytoplasmic Zn<sup>2+</sup> homeostasis. *Plant Physiol* 136: 3712-3723
- Ernst WHO, Verkleij JAC, Schat H** (1992): Metal tolerance in plants. *Acta Botanica Neerlandica* 41: 229-248
- Farnaud S, Rapisarda C, Bui T, Drake A, Cammack R, Evans RW** (2008): Identification of an iron-hepcidin complex. *Biochem J*, Epub ahead of print (doi:10.1042/BJ20080406 )
- Fenton HJH** (1984): The oxidation of tartaric acid in presence of iron. *J Chem Soc, Proc* 10: 157-158
- Ferro M, Salvi D, RiviereRolland H** (2002): Integral membrane proteins of the chloroplast envelope: Identification and subcellular localization of new transporters. *Proc Natl Acad Sci USA* 99: 11487-92
- Finney LA, O'Halloran TV** (2003): Transition metal speciation in the cell: insights from the chemistry of metal ion receptors. *Science* 300(5621): 931-6
- Fleming MD, Trenor CC, Su MA, Foerzler D, Beier DR, Dietrich WF, Andrews NC** (1997): Microcytic anaemia mice have a mutation in *Nramp2*, a candidate transporter gene. *Nat Genet* 16: 383-386
- Foury F, Talibi D** (2001): Mitochondrial control of iron homeostasis. A genome wide analysis of gene expression in a yeast frataxin-deficient strain. *J. Biol. Chem.* 276, 7762–7768
- Fox TM, Guerinot ML** (1998): Molecular biology of cation transport in plants. *Annu Rev Plant Physiol Plant Mol Biol* 49: 669–96
- Frausto da Silva JJR, Williams RJP** (2001): *The Biological Chemistry of the Elements*, second edition. Clarendon Press, Oxford
- Frazer DM, Vulpe CD, McKie AT, Wilkins SJ, Trinder D, Cleghorn GJ, Anderson GJ** (2001): Cloning an gastrointestinal expression of rat hephaestin: relationship to other iron transport proteins. *Am J Physiol* 281: G931-G939
- Freeman JL, Persans MW, Nieman K, Albrecht C, Peer W, Pickering IJ, Salt DE** (2004): Increased glutathione biosynthesis plays a role in nickel tolerance in thlaspi nickel hyperaccumulators. *Plant Cell* 16(8): 2176-91
- Freeman JL, Salt DE** (2007): The metal tolerance profile of *Thlaspi goesingense* is mimicked in *Arabidopsis thaliana* heterologously expressing serine acetyl-transferase. *BMC Plant Biol* 7:63
- Gad N** (2006): Increasing the efficiency of nitrogen fertilization through cobalt application to pea plant. *Research J Agr Biol Sc* 2(6): 433-442
- Gaither LA, Eide DJ** (2001): Eukaryotic zinc transporters and their regulation. *Biometals* 14: 251-270
- Ganz T** (2003): Heparin, a key regulator of iron metabolism and mediator of anemia of inflammation. *Blood* 102 (3): 783-788.
- Gerendás J, Zhu Z, Sattelmacher B** (1998): Influence of N and Ni supply on nitrogen metabolism and urease activity in rice (*Oryza sativa* L.). *J Exp Bot* 49(326):1545-1554

- Gerendás J, Polacco JC, Freyermuth SK, Sattelmacher B** (1999): Significance of nickel for plant growth and metabolism. *J Plant Nutr Soil Sci* 162: 241-256
- Gietz D, St Jean A, Woods RA, Schiestl RH** (1992): Improved method for high efficiency transformation of intact yeast cells. *Nucleic Acids Res.* 20, 1425
- Gonçalves AS, Muzeau F, Blaybel R, Hetet G, Driss F, Delaby C, Canonne-Hergaux F, Beaumont C** (2006): Wild-type and mutant ferroportins do not form oligomers in transfected cells. *Biochem J* 396(2):265-75
- Govoni G, Gros P** (1998): Macrophage NRAMP1 and its role in resistance to microbial infections. *Inflamm Res* 47(7): 277-84
- Green LS, Rogers EE** (2004): FRD3 controls iron localization in Arabidopsis. *Plant Physiol.* 136(1):2523-31.
- Grotz N, Fox T, Connolly E, Park W, Guerinot ML, Eide D** (1998): Identification of a family of zinc transporter genes from *Arabidopsis thaliana* that respond to zinc deficiency. *Proc Natl Acad Sci* 93: 7220–7224
- Guerinot ML and Yi Y** (1994): Iron: nutritious, noxious, and not readily available. *Plant Physiol* 104, 815–820
- Guerinot ML** (1994): Microbial iron transport. *Annu Rev Microbiol* 48: 743-72
- Guerinot ML** (2000): The ZIP family of metal transporters. *Biochim Biophys Acta* 1465: 4956-4960
- Gunshin H, Mackenzie B, Berger UV, Gunshin Y, Romero MF, Boron WF, Nussberger S, Gollan JL, Hediger MA** (1997): Cloning and characterization of a mammalian proton-coupled metal ion-transporter. *Nature* 388: 482-488
- Hajdukiewicz P, Svab Z, Maliga P** (1994): The small, versatile pPZP family of *Agrobacterium* binary vectors for plant transformation. *Plant Mol. Biol.* 25, 989–994
- Hall JL** (2002): Cellular mechanisms for heavy metal detoxification and tolerance. *J Exp Bot* 53: 1-11
- Hall JL, Williams LE** (2003): Transition metal transporters in plants. *J Exp Bot* 54: 2601-2613
- Halliwell B, Gutteridge JMC** (1986): Iron and free radical reactions: two aspects of antioxidant protection. *Trends Biochem Sci* 11: 372-375
- Halliwell B, Gutteridge JMC** (1990): Role of free radicals and catalytic metal ions in human disease - an overview. *Methods Enzymol* 186:1-85
- Hallsworth EG, Wilson SB, Adams WA** (1965): Effect of cobalt on the non-nodulated legume. *Nature* 205: 307-8
- Hartley J, Cairney JWG, Meharg AA** (1997): Do ectomycorrhizal fungi exhibit adaptive tolerance to potentially toxic metals in the environment? *Plant Soil* 189(2): 303-319
- Hellens RP, Edwards EA, Leyland NR, Bean S, Mullineaux PM** (2000): pGreen: a versatile and flexible binary Ti vector for *Agrobacterium*-mediated plant transformation. *Plant Mol. Biol.* 42, 819–832
- Hellmann NE, Gitlin JD** (2002): Ceruloplasmin metabolism and function. *Annu Rev Nutr* 22: 439-458
- Henriques R, Jásik J, Klein M, Martinoia E, Feller U, Schell J, Pais MS, Koncz C** (2002): Knock-out of *Arabidopsis* metal transporter gene IRT1 results in iron deficiency accompanied by cell differentiation defects. *Plant Mol Biol* 50: 587–597

- Hewitt EJ, Bond G** (1966): The Cobalt Requirement of Non-legume Root Nodule Plants. *J Exp Bot* 17(3): 480-491
- Hirayama T, Kieber JJ, Hirayama N, Kogan M, Guzman P, Nourizadeh S, Alonso JM, Dailey WP, Dancis A, Ecker JR** (1999): Responsive-to-antagonist 1, a Menkes/Wilson disease related copper transporter is required for ethylene signalling in *Arabidopsis*. *Cell* 97, 383-393
- Horton P, Park KJ, Obayashi T, Nakai K** (2006): Protein Subcellular Localization Prediction with WoLF PSORT, Proceedings of the 4th Annual Asia Pacific Bioinformatics Conference APBC06, Taipei, Taiwan: 39-48
- Huang X, Frenkel K, Klein C, Costa M** (1993): Nickel induces increased oxidants in intact cultured mammalian cells as detected by dichlorofluorescein fluorescence. *Toxic Appl Pharmacol* 120, 29-36
- Hussain D, Haydon MJ, Wang Y, Wong E, Sherson SM, Young J, Camakaris J, Harper JF, Cobbett CS** (2004): P-type ATPase heavy metal transporters with roles in essential zinc homeostasis in *Arabidopsis*. *Plant Cell* 16: 1327-1339
- Jakoby M, Wang HY, Reidt W, Weisshaar B, Bauer P** (2004): FRU (BHLH029) is required for induction of iron mobilization genes in *Arabidopsis thaliana*. *FEBS Lett* 577: 528-34
- Kaiser BN, Moreau S, Castelli J, Thomson R, Lambert A, Bogliolo S, Puppo A, Day DA** (2003): The soybean NRAMP homologue, GmDMT1, is a symbiotic divalent metal transporter capable of ferrous iron transport. *Plant J* 35: 295-304
- Kamizono A, Nishizawa M, Teranishi Y, Murata K, Kimura A** (1989): Identification of a gene conferring resistance to zinc and cadmium ions in the yeast *Saccharomyces cerevisiae*. *Mol. Gen. Genet.* 219, 161-167
- Kawabata H, Fleming RE, Gui D, Moon SY, Saitoh T, O'Kelly J, Umehara Y, Wano Y, Said JW, Koeffler HP** (2005): Expression of hepcidin is down-regulated in TfR2 mutant mice manifesting a phenotype of hereditary hemochromatosis. *Blood* 105 (1): 376-381
- Kim D, Gustin JL, Lahner B, Persans MW, Baek D, Yun DJ, Salt DE** (2004): The plant CDF family member TgMTP1 from the Ni/Zn hyperaccumulator *Thlaspi goesingense* acts to enhance efflux of Zn at the plasma membrane when expressed in *Saccharomyces cerevisiae*. *Plant J* 39: 237-251
- Kim S, Takahashi M, Higuchi K, Tsunoda K, Nakanishi H, Yoshimura E, Mori S, Nishizawa NK** (2005): Increased nicotianamine biosynthesis confers enhanced tolerance of high levels of metals, in particular nickel, to plants. *Plant Cell Physiol.* 46, 1809-1818
- Kim SA, Punshon T, Lanzirotti A, Li L, Alonso JM, Ecker JR, Kaplan J, Guerinot ML** (2006): Localization of Iron in *Arabidopsis* Seed Requires the Vacuolar Membrane Transporter VIT1. *Science* 314(5803):1295-8
- Kim S, Guerinot ML** (2007): Mining iron: Iron uptake and transport in plants. *FEBS Letters* 581 (12): 2273-2280
- Kobae Y, Uemura T, Sato MH, Ohnishi M, Mimura T, Nakagawa T, Maeshima M** (2004): Zinc transporter of *Arabidopsis thaliana* AtMTP1 is localized to vacuolar membranes and implicated in zinc homeostasis. *Plant Cell Physiol* 45:1749-1758
- Koo AJ, Ohlrogge JB** (2002): The predicted candidates of *Arabidopsis* plastid inner envelope membrane proteins and their expression profiles. *Plant Physiol* 130: 823-36
- Korshunova YO, Eide D, Clark WG, Guerinot ML, Pakrasi HB** (1999): The IRT1 protein from *Arabidopsis thaliana* is a metal transporter with a broad substrate range. *Plant Mol Biol* 40: 37-44

- Krämer U** (2005): MTP1 mops up excess zinc in Arabidopsis cells. *Trends Plant Sci* 10: 313–315
- Krämer U, Talke IN, Hanikenne M** (2007): Transition metal transport. *FEBS Lett* 581(12): 2263-72
- Kukier U, Chaney RL** (2001): Amelioration of nickel phytotoxicity in muck and mineral soils. *J. Environ. Qual.* 30, 1949–1960
- Lanquar V, Lelievre F, Bolte S, Hames C, Alcon C, Neumann D, Vansuyt G, Curie C, Schroder A, Krämer U** (2005): Mobilization of vacuolar iron by AtNramp3 and AtNramp4 is essential for seed germination on low iron. *EMBO J* 24: 4041-4051
- Li CZ, Wang D, Wang GX** (2005): The protective effects of cobalt on potato seedling leaves during osmotic stress. *Bot Bull Acad Sin* 46: 119-125
- Li L, Kaplan J** (1998): Defects in the yeast high affinity iron transport system result in increased metal sensitivity because of the increased expression of transporters with a broad transition metal specificity. *J Biol Chem* 273(35): 22181-7
- Li L, Chen OS, McVey Ward D, Kaplan J** (2001): CCC1 is a transporter that mediates vacuolar iron storage in yeast. *J Biol Chem* 276:29515–19
- Li L, He Z, Pandey GK, Tsuchiya T, Luan S** (2002): Functional cloning and characterization of a plant efflux carrier for multidrug and heavy metal detoxification. *J Biol Chem* 277: 5360-5368
- Li YM, Chaney RL, Brewer E, Roseberg RJ, Angle JS, Baker AJM, Reeves RD, Nelkin J** (2003): Development of a technology for commercial phytoextraction of nickel: Economic and technical considerations. *Plant Soil* 249:107-115
- Lin H, Kumánovics A, Nelson J, McVey Ward D, Kaplan J** (2008): A single amino acid change in the yeast vacuolar metal transporters ZRC1 and COT1 alters their substrate specificity. *JBC Papers in Press*. Manuscript M804377200
- Ling HQ, Bauer P, Berezky Z, Keller B, Ganai M** (2002): The tomato *fer* gene encoding a bHLH protein controls iron-uptake responses in roots. *Proc Natl Acad Sci* 99(21): 13938-43
- Liu LH, Ludwig U, Frommer WB, von Wirén N** (2003): AtDUR3 encodes a new type of high-affinity urea/H<sup>+</sup> symporter in Arabidopsis. *Plant Cell* 15, 790–800
- Magalhaes JV, Liu J, Guimaraes CT, Lana UGP, Alves VMC, Wang YH, Schaffert RE, Hoekenga OA, Pineros MA, Shaff JE, Klein PE, Carneiro NP, Coelho CM, Trick HN, Kochian LV** (2007): A gene in the multidrug and toxic compound extrusion (MATE) family confers aluminum tolerance in sorghum. *Nature Genetics* 39: 1156-1161
- Marschner H** (1995): Function of mineral nutrients: micronutrients. In *Mineral Nutrition of Higher Plants*, 2<sup>nd</sup> Edition, Academic Press
- Mäser P, Thomine S, Schroeder JI** (2001): Phylogenetic relationships within cation transporter families of Arabidopsis. *Plant Physiol* 126: 1646-1667
- McBride MB** (1994): *Environmental chemistry of soils*. NY Oxford University Press
- Mena NP, Esparza A, Tapia V, Valdes P, Nunez MT** (2008): Heparin inhibits apical iron uptake in intestinal cells. *Am J Physiol Gastrointest Liver Physiol* 294 (1): G192-128
- McKie AT, Barlow DJ** (2004): The SLC40 basolateral iron transporter family (IREG1/ferroportin/MTP1). *Pflugers Arch – Eur J Physiol* 447:801-806

- McKie AT, Barrow D, Latunde-Daha GO, Rolfs A, Sager G, Mudaly E, Mudaly M, Richardson C, Barlow D, Bomford A, Peters TJ, Raja KB, Shirali S, Hediger MA, Farzaneh F, Simpson RJ** (2001): An iron-regulated ferric reductase associated with the absorption of dietary iron. *Science* 291: 1755-1759
- McKie AT, Marciani P, Rolfs A, Brennan K, Wehr K, Barrow D, Miret S, Bomford A, Peters TJ, Farzaneh F, Hediger MA, Hentze MW, Simpson RJ** (2000): A novel duodenal iron-regulated transporter, IREG1, implicated in the basolateral transfer of iron to the circulation. *Mol Cell* 5: 299-309
- Mills RF, Krijger GC, Baccarini PJ, Hall JL, Williams LE** (2003): Functional expression of AtHMA4, a P1B-type ATPase in the Zn/Co/Cd/Pb subclass. *Plant J* 35: 164-175
- Mills RF, Francini A, Ferreira da Rocha PS, Baccarini PJ, Aylett M, Krijger GC, Williams LE** (2005): The plant P1B-type ATPase AtHMA4 transports Zn and Cd and plays a role in detoxification of transition metals supplied at elevated levels. *FEBS Lett* 579(3): 783-91
- Moog PR, Brüggemann W** (1994): Iron reductase systems on the plant plasma membrane-A review. *Plant Soil* 165, 241-260
- Moreau S, Thomson RM, Kaiser BN, Trevaskis B, Guerinot ML, Udvardi MK, Puppo A, Day DA** (2002): *GmZIP1* encodes a symbiosis-specific zinc transporter in soybean. *J Biol Chem* 277: 4738-4746
- Mukherjee I, Campbell NH, Ash JS, Connolly EL** (2006): Expression profiling of the Arabidopsis ferric chelate reductase (*FRO*) gene family reveals differential regulation by iron and copper. *Planta* 223(6): 1178-90
- Nemeth E, Valore EV, Territo M, Schiller G, Lichtenstein A, Ganz T** (2003): Hepcidin, a putative mediator of anemia of inflammation, is a type II acute-phase protein. *Blood* 101: 2461-2463
- Nemeth E, Tuttle MS, Powelson J, Vaughn MB, Donovan A, Ward DM, Ganz T, Kaplan J** (2004): Hepcidin regulates cellular iron efflux by binding to ferroportin and inducing its internalization. *Science* 306: 2090-2093
- Nemeth E, Roetto A, Garozzo G, Ganz T, Camaschella C** (2005): Hepcidin is decreased in TFR2 hemochromatosis. *Blood* 105 (4): 1803-1806
- Nicolas G, Bennoun M, Devaux I, Beaumont C, Grandchamp B, Kahn A, Vaulont S** (2001): Lack of hepcidin gene expression and severe tissue iron overload in upstream stimulatory factor 2 (USF2) knockout mice. *Proc Natl Acad Sci* 98: 8780-8785
- Nicolas G, Viatte L, Bennoun M, Beaumont C, Kahn A, Vaulont S** (2002): Hepcidin, a new iron regulatory peptide. *Blood Cells Mol Dis.* 29 (3): 327-335.
- Nicolas G, Andrews NC, Kahn A, Vaulont S** (2003): Hepcidin, a candidate modifier of the hemochromatosis phenotype in mice. *Blood* 103 (7): 2841-2843
- Noctor G, Strohm M, Jouanin L, Kunert KJ, Foyer CH, Rennenberg H** (1996): Synthesis of Glutathione in Leaves of Transgenic Poplar Overexpressing [gamma]-Glutamylcysteine Synthetase. *Plant Physiol* 112: 1071-1078
- Noctor G, Foyer CH** (1998): Ascorbate and Glutathione: Keeping Active Oxygen Under Control. *Annu Rev Plant Physiol Plant Mol Biol* 49: 249-279
- Olsen RA, Clark RB, Bennett JH** (1981): The enhancement of soil fertility by plant roots. *Am Scientist* 69: 378-384
- Ouariti O, Boussama N, Zarrouk M, Cherif A, Ghorbal MH** (1997): Cadmium- and copper-induced changes in tomato membrane lipids. *Phytochemistry* 45(7): 1343-50

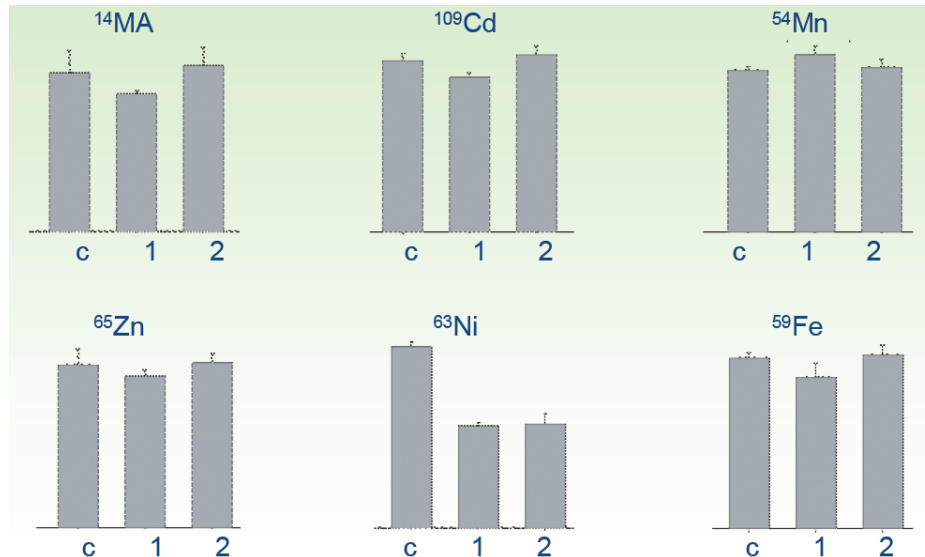
- Pence NS, Larsen PB, Ebbs SD, Letham DLD, Lasat MM, Garvin DF, Eide D, Kochian LV** (2000): The molecular physiology of heavy metal transport in the Zn/Cd hyperaccumulator *Thlaspi caerulescens*. *Proc Natl Acad Sci* 97: 4956-4960
- Persans MW, Nieman K, Salt DE** (2001): Functional activity and role of cation-efflux family members in Ni hyperaccumulation in *Thlaspi goesingense*. *Proc Natl Acad Sci* 98: 9995-10000
- Peuke AD, Rennenberg H** (2005): Phytoremediation. *EMBO Rep* 6(6):497-501
- Pianelli K, Mari S, Marques L, Lebrun M, Czernic P** (2005): Nicotianamine over-accumulation confers resistance to nickel in *Arabidopsis thaliana*. *Transgenic Res.* 14, 739–748
- Pigeon C, Ilyin G, Courselaud B, Leroyer P, Turlin B, Brissot P, Loreal O** (2001): A new mouse liver-specific gene, encoding a protein homologous to human antimicrobial peptide hepcidin, is overexpressed during iron overload. *J Biol Chem* 276: 7811-7819
- Pignatti E, Mascheroni L, Sabelli M, Barelli S, Biffo S, Pietrangelo A** (2006): Ferroportin is a monomer in vivo in mice. *Blood Cells Mol Dis* 36: 26-32
- Pittman JK** (2005): Managing the manganese: molecular mechanisms of manganese transport and homeostasis. *New Phytol* 167(3):733-42
- Reisenauer HM** (1960): Cobalt in nitrogen fixation by a legume. *Nature* 186: 375-6
- Rentsch D, Laloi M, Rouhara I, Schmelzer E, Delrot S, Frommer WB** (1995): NTR1 encodes a high affinity oligopeptide transporter in *Arabidopsis*. *FEBS Lett.* 370, 264–268
- Roberts SK, Herderson RW, Young GP** (1993): Modulation of uptake of heme by rat small intestinal mucosa in iron-deficiency. *Am J Physiol* 265: G712-G718
- Robinson NJ, Proctor CM, Connolly EL, Guerinot ML** (1999): A ferric-chelate reductase for iron uptake from soils. *Nature* 397: 694–697.
- Rogers EE, Eide DJ, Guerinot ML** (2000): Altered selectivity in an *Arabidopsis* metal transporter. *PNAS* 97: 12356-60
- Rogers EE, Guerinot ML** (2002): FRD3, a member of the multidrug and toxin efflux family, controls iron deficiency responses in *Arabidopsis*. *Plant Cell* 14: 1787-1799
- Römheld V** (1987): Different strategies for iron acquisition in higher plants. *Physiol Plant* 70: 231–234
- Sambrook J, Russell DW** (2001): *Molecular Cloning: A Laboratory Manual*, 3rd Ed., Cold Spring Harbor Laboratory Press, Cold Spring Harbor, NY
- Sancenon V, Puig S, Mira H, Thiele DJ, Penarrubia L** (2003): Identification of a copper transporter family in *Arabidopsis thaliana*. *Plant Mol Biol* 51: 577-587
- Schaaf G, Ludewig U, Erenoglu BE, Mori S, Kitahara T, von Wirén N** (2004): ZmYS1 functions as a proton-coupled symporter for phytosiderophore- and nicotianamine-chelated metals. *J Biol Chem* 279(10): 9091-6
- Schaaf G, Schikora A, Haberle J, Vert G, Ludewig U, Briat JF, Curie C, von Wirén N** (2005): A putative function for the *Arabidopsis* Fe-phytosiderophore transporter homolog AtYSL2 in Fe and Zn homeostasis. *Plant Cell Physiol* 46:762-774
- Schimanski LM, Drakesmith H, Talbott C, Horne K, James JR, Davis SJ, Sweetland E, Bastin J, Cowley D, Townsend AR** (2008): Ferroportin: lack of evidence for multimers. *Blood Cells Mol Dis* 40(3):360-9

- Schützendübel A, Polle A** (2002): Plant responses to abiotic stresses: heavy metal-induced oxidative stress and protection by mycorrhization. *J Exp Bot* 53(372): 1351-65
- Schwarz G, Mendel RR** (2006): Molybdenum cofactor biosynthesis and molybdenum enzymes. *Ann Rev Plant Biol* 57: 623-647
- Seigneurin-Berny D, Gravot A, Auroy P, Mazard C, Kraut A, Finazzi G, Grunwald D, Rappaport F, Vavasseur A, Joyard J** (2005): HMA1, a new Cu-ATPase of the chloroplast envelope, is essential for growth under adverse light conditions. *J Biol Chem* 281: 2882-2892
- Sharma RK, Agrawal M** (2005): Biological effects of heavy metals: an overview. *Environ Biol* 26(2 Suppl):301-13
- Shigaki T, Pittmann JK, Hirschi KD** (2003): Manganese specificity determinants in the Arabidopsis metal/H<sup>+</sup> antiporter CAX2. *J Biol Chem* 278(8): 6610-7
- Shikanai T, Müller-Moulé P, Munekage Y, Niyogi KK, Pilon M** (2003): PAA1, a P-type ATPase of Arabidopsis functions in copper transport in chloroplasts. *Plant Cell* 15, 1333-1346
- Sirko A, Brodzik R** (2000): Plant ureases: roles and regulation. *Acta Biochim Pol* 47(4): 1189-95
- Solioz M, Odermatt A** (1995): Copper and silver transport by CopB-ATPase in membrane vesicles of *Enterococcus hirae*. *J Biol Chem* 270(16): 9217-21
- Stadler JA, Schweyen RJ** (2002): The yeast iron regulon is induced upon cobalt stress and crucial for cobalt tolerance. *J. Biol. Chem.* 277, 39649–39654
- Stearman R., Yuan DS, Yamaguchi-Iwai Y, Klausner RD, Dancis A** (1996): A permease-oxidase complex involved in high-affinity iron uptake in yeast. *Science* 271, 1552–1557
- Stohs SJ, Bagchi D** (1995): Oxidative mechanisms in the toxicity of metal ions. *Free Radical Biol & Med* 18(2): 321-336
- Takagi S, Nomoto K, Takemoto S** (1984): Physiological aspect of mugineic acid, a possible phytosiderophore of graminaceous plants. *J Plant Nutr* 7: 469–477
- Takano J, Miwa K, Yuan LX, von Wirén N, Fujiwara T** (2005): Endocytosis and degradation of BOR1, a boron transporter of *Arabidopsis thaliana*, regulated by boron availability. *Proc. Natl. Acad. Sci. U. S. A.* 102, 12276–12281
- Talke IN, Hanikenne M, Krämer U** (2006): Zinc-dependent global transcriptional control, transcriptional deregulation, and higher gene copy number for genes in metal homeostasis of the hyperaccumulator *Arabidopsis halleri*. *Plant Physiol* 142(1):148-67
- Thomine S, Wang R, Ward JM, Crawford NM, Schroeder JI** (2000): Cadmium and iron transport by members of a plant metal transporter family in Arabidopsis with homology to *Nramp* genes. *Proc Natl Acad Sci* 97: 4991-4996
- Thomine S, Lelievre F, Debarbieux E, Schroeder JI, Barbier-Brygoo H** (2003): AtNramp3, a multispecific vacuolar metal transporter involved in plant responses to iron deficiency. *Plant J* 34: 685-695
- Vacchina V, Mari S, Czernic P, Marquès L, Pianelli K, Schaumlöffel D, Lebrun M, Lobiński R** (2003): Speciation of nickel in a hyperaccumulating plant by high-performance liquid chromatography-inductively coupled plasma mass spectrometry and electrospray MS/MS assisted by cloning using yeast complementation. *Anal. Chem.* 75, 2740-2745

- van der Zaal BJ, Neuteboom LW, Pinas JE, Chardonens AN, Schat H, Verkleij JA, Hooykaas PJ** (1999): Overexpression of a novel Arabidopsis gene related to putative zinc-transporter genes from animals can lead to enhanced zinc resistance and accumulation. *Plant Physiol* 119: 1047-1055
- Varotto C, Maiwald D, Pesaresi P, Jahns P, Francesco S, Leister D** (2002): The metal ion transporter IRT1 is necessary for iron homeostasis and efficient photosynthesis in *Arabidopsis thaliana*. *Plant J* 31: 589-599
- Verret F, Gravot A, Auroy P, Leonhardt N, David P, Nussaume L, Vavasseur A, Richaud P** (2004): Overexpression of AtHMA4 enhances root-to-shoot translocation of zinc and cadmium and plant metal tolerance. *FEBS Lett* 576:306-312
- Vert G, Briat JF, Curie C** (2001): Arabidopsis IRT2 gene encodes a root-periphery iron transporter. *Plant J* 26(2): 181-9
- Vert G, Grotz N, Dedaldechamp F, Gaymard F, Guerinot ML, Briat JF, Curie C** (2002): IRT1, an Arabidopsis transporter essential for iron uptake from the soil and plant growth. *Plant Cell* 14: 1223-1233
- Von Wirén N, Mori S, Marschner H, Römheld V** (1994): Iron Inefficiency in Maize Mutant *ys1* (*Zea mays L.* cv Yellow-Stripe) Is Caused by a Defect in Uptake of Iron Phytosiderophores. *Plant Physiol.* 106, 71-77
- Von Wirén N, Marschner H, Römheld V** (1996): Roots of iron-efficient maize also absorb phytosiderophore-chelated zinc. *Plant Physiol* 111(4): 1119-1125
- Vulpe CD, Kuo YM, Murphy TL, Cowley L, Askwith C, Libina N, Gitschier J, Anderson GJ** (1999): Hephaestin, a ceruloplasmin homologue implicated in intestinal iron transport, is defective in the sla mouse. *Nat Genet* 21: 195-199
- Welch RM, Norvell WA, Schaefer SC, Shaff JE, Kochian LV** (1993): Induction of iron (III) and copper (II) reduction in pea (*Pisum sativum L.*) roots by Fe and Cu status: does the root-cell plasmalemma Fe(III)-chelate reductase perform a general role in regulating cation uptake? *Planta* 190: 555-561
- Walsh CT, Orme-Johnson WH** (1987): Nickel enzymes. *Biochemistry* 26(16): 4901-6
- Wang HY, Klatte M, Jakoby M, Bäumlein H, Weisshaar B, Bauer P** (2007): Iron deficiency-mediated stress regulation of four subgroup Ib *BHLH* genes in *Arabidopsis thaliana*. *Planta* 226(4): 897-908
- Waters BM, Lucena C, Romera FJ, Jester GG, Wynn AN, Rojas CL, Alcántara E, Pérez-Vicente R** (2007): Ethylene involvement in the regulation of the H(+)-ATPase CSHA1 gene and of the new isolated ferric reductase CsFRO1 and iron transporter CsIRT1 genes in cucumber plants. *Plant Physiol Biochem* 45(5): 293-301
- Wiberg E** (1985): *Lehrbuch der Anorganischen Chemie*. Walter de Gruyter, Berlin, New York
- Williams LE, Pittman JK, Hall JL** (2000): Emerging mechanisms for heavy metal transport in plants. *Biochim Biophys Acta* 1465(1-2): 104-26
- Williams LE, Mills RF** (2005): P(1B)-ATPases - an ancient family of transition metal pumps with diverse functions in plants. *Trends Plant Sci* 10: 491-502
- Wintz H, Fox T, Wu YY, Feng V, Chen W, Chang HS, Zhu T, Vulpe C** (2003): Expression profiles of *Arabidopsis thaliana* in mineral deficiencies reveal novel transporters involved in metal homeostasis. *J Biol Chem* 278: 47644-47653

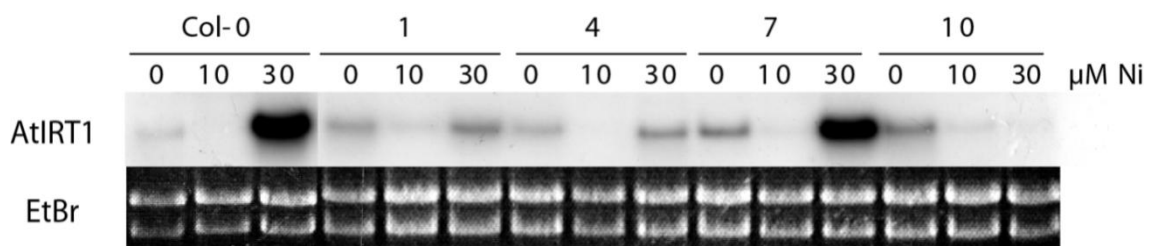
- Witte CP, Tiller SA, Taylor MA, Davies HV** (2002a): Addition of nickel to Murashige and Skoog medium in plant tissue culture activates urease and may reduce metabolic stress. *Plant Cell Tissue and Organ Culture* 68, 103–104
- Witte CP, Tiller SA, Taylor MA, Davies HV** (2002b): Leaf urea metabolism in potato. Urease activity profile and patterns of recovery and distribution of  $^{15}\text{N}$  after foliar urea application in wild-type and urease-antisense transgenics. *Plant Phys* 128, 1129–1136
- Witte CP, Tiller SA, Isidore E, Davies HV and Taylor MA** (2005): Analysis of two alleles of the urease gene from potato: polymorphisms, expression, and extensive alternative splicing of the corresponding mRNA. *J Exp Bot* 56(409): 91–99
- Woeste KE, Kieber JJ** (2000): A strong loss-of-function mutation in RAN1 results in constitutive activation of the ethylene response pathway as well as a rosette-lethal phenotype. *Plant Cell* 12, 443–455
- Wu H, Li L, Du J, Yuan Y, Cheng X, Ling HQ** (2005): Molecular and biochemical characterization of the Fe(III) chelate reductase gene family in *Arabidopsis thaliana*. *Plant Cell Physiol* 46(9): 1505–14
- Yang F, Liu XB, Quinones M, Melby PC, Ghio A, Haile DJ** (2002): Regulation of reticuloendothelial iron transporter MTP1 (Slc11a3) by inflammation. *J Biol Chem* 277: 39786–39791
- Yi Y, Guerinot ML** (1996): Genetic evidence that induction of root Fe(III) chelate reductase activity is necessary for iron uptake under iron deficiency. *Plant J* 10: 835–844
- Yuan Y, Wu H, Wang N, Li J, Zhao W, Du J, Wang D, Ling HQ** (2008): FIT interacts with AtbHLH38 and AtbHLH39 in regulating iron uptake gene expression for iron homeostasis in *Arabidopsis*. *Cell Research* 18: 385–397
- Zhao H, Eide D** (1996a): The yeast ZRT1 gene encodes the zinc transporter protein of a high-affinity uptake system induced by zinc limitation. *Proc Natl Acad Sci* 93: 2454–2458
- Zhao H, Eide D** (1996b): The ZRT2 gene encodes the low affinity zinc transporter in *Saccharomyces cerevisiae*. *J Biol Chem* 271: 23203–23210

## 7 Appendix



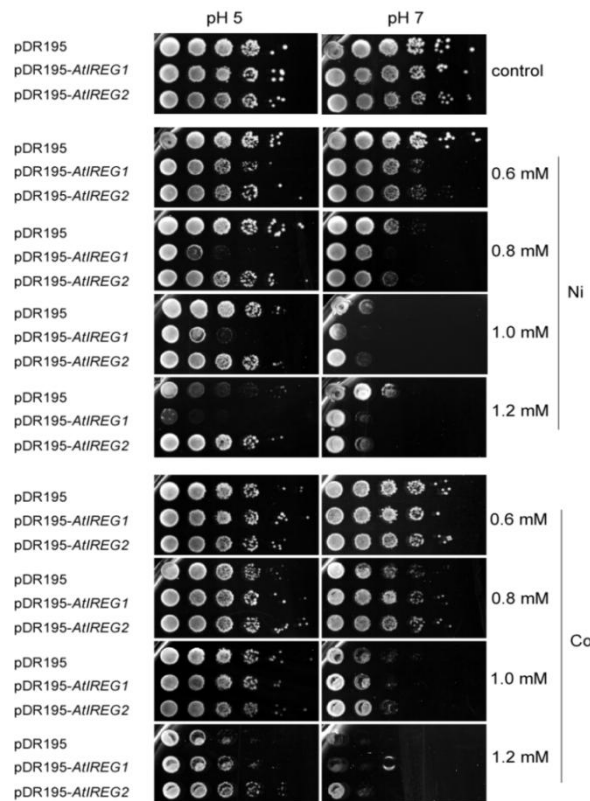
### Appendix 1: Metal content of *AtIREG*-expressing yeast mutants.

Yeast wildtype (BY4741) cells were transformed with the empty vector pDR195 (c) or with pDR195-*AtIREG1* (1) or pDR195-*AtIREG2* (2). Yeast was grown in selective media for 5 d. Cells were plated on medium supplemented with radiolabeled metals ( $^{14}\text{Methylammonium}$  (MA),  $^{109}\text{Cd}$ ,  $^{54}\text{Mn}$ ,  $^{65}\text{Zn}$ ,  $^{63}\text{Ni}$  or  $^{59}\text{Fe}$ ). Cells were washed, and radioactivity was detected by scintillation counting.



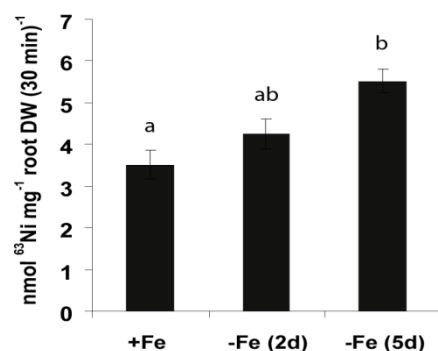
### Appendix 2: Expression of *AtIRT1* in *AtIREG2* overexpressing Arabidopsis lines.

RNA gel blot analysis was performed to determine *AtIRT1* expression in roots from hydroponically grown plants that were precultured for 5 weeks in presence of 50  $\mu\text{M}$  Fe(III)-EDTA and then cultured for 3 d with 0, 10 or 30  $\mu\text{M}$  Ni supply. Total RNA from roots was used for hybridization to the complete ORF of *AtIRT1*. EtBr-stained gel is shown as loading control.



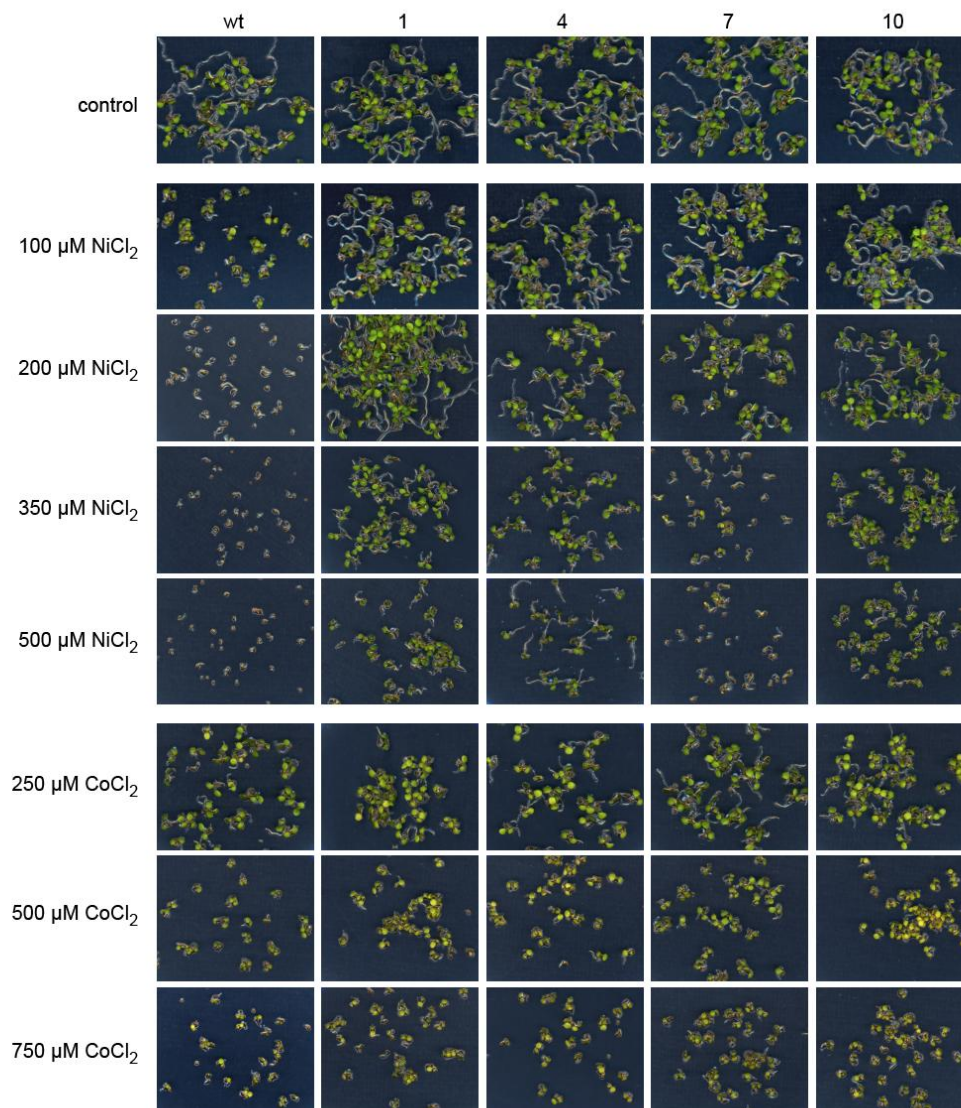
### Appendix 3: Growth of *AtIREG1* or *AtIREG2* expressing yeast on nickel and cobalt.

Yeast wildtype (BY4741) cells were transformed with the empty vector pDR195 or with pDR195-*AtIREG1* or pDR195-*AtIREG2*. Single colonies were cultured in selective media for 48 h and adjusted to an optical density of 1.0 before spotting 5-fold dilutions on uracil-free YNB medium or medium supplemented with NiCl<sub>2</sub> or CoSO<sub>4</sub>. The pH was adjusted to pH 5 or 7 by 50 mM MES/TRIS.



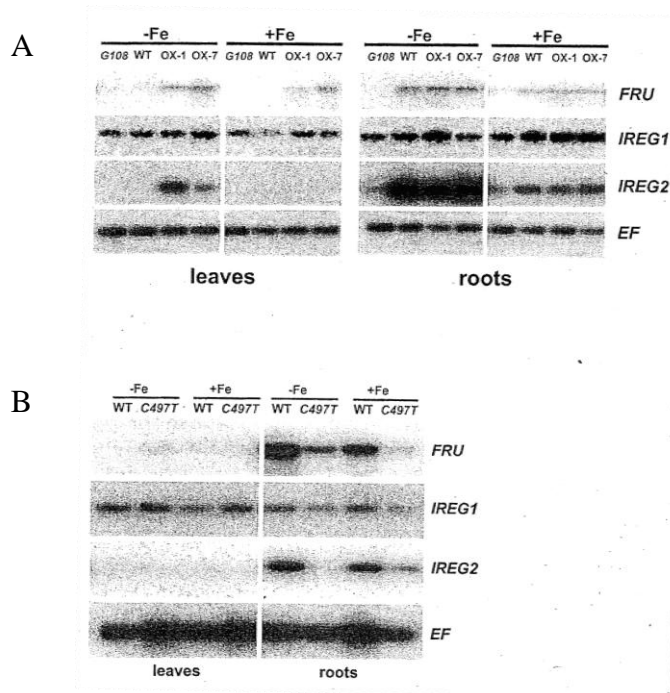
### Appendix 4: Enhanced nickel accumulation in iron-deficient plants.

Wildtype *Arabidopsis* plants were precultured for 16 days and then transferred to Fe-sufficient (+ Fe) or Fe-deficient (- Fe) medium containing 25 μM <sup>63</sup>Ni-labeled NiCl<sub>2</sub>. Plants were harvested after 11 days and wet digested for <sup>63</sup>Ni analysis by liquid scintillation counting.



**Appendix 5: Growth phenotype of 35S:AtIREG2 plants under nickel and cobalt stress.**

Wildtype and 35S:AtIREG2 seeds (lines 1, 4, 7, 10) were germinated for 9 days on agar supplemented with 100-500  $\mu\text{M}$  Ni or 250-750  $\mu\text{M}$  Co.



#### Appendix6: Analysis of *AtIREG1* and *AtIREG2* regulation by *FRU* (=former name of *FIT*)

**A:** Analysis of *AtIREG1* and *AtIREG2* expression in pCaMV35S-*FRU* lines. Reverse transcription-PCR expression analysis of *FRU*, *AtIREG1* and *AtIREG2* in leaves (left) and roots (right) of a *FRU* T-DNA insertion line (G108), two *FRU*-overexpression lines (OX-1 and OX-7) and wildtype (WT). -Fe, 0  $\mu$ M Fe / 50  $\mu$ M Ferrozine; +Fe, 50  $\mu$ M FeEDTA. *EF* (*EF1 B- $\alpha$* ) gene expression served as a control.

**B:** Analysis of *AtIREG1* and *AtIREG2* expression in *fru* mutant plants. Reverse transcription-PCR expression analysis of *FRU* (*FIT*), *AtIREG1* and *AtIREG2* in leaves (left) and roots (right) of a *FRU* EMS-induced loss-of-function mutant line (C497T) and wildtype (WT). -Fe, 0  $\mu$ M Fe / 50  $\mu$ M Ferrozine; +Fe, 50  $\mu$ M FeEDTA. *EF* (*EF1 B- $\alpha$* ) gene expression served as a control.

Figure kindly provided by Petra Bauer, Saarland University.

## 8 Acknowledgements

First of all, special thanks go to Prof. Dr. Nico von Wirén for giving me the opportunity to do my PhD thesis at his institute. Nico, I thank you for your understanding in hard times, for your readiness to discuss and for always being helpful and patient. Special thanks also for giving me the freedom to develop myself into the direction I wanted, and thus to find the right way for my future. Many thanks also for the fast correction of my thesis and the helpful comments.

I also thank Prof. Dr. Weber for accepting to evaluate my thesis and Prof. Dr. Hanke for taking part in the final examination.

Special thanks to Mrs. Schölhammer for helping me in so many ways, especially when I started my work at the institute, but also during all the time there. Sincere thanks also go to Mrs. Berghammer for her continuous help, her friendly ways and finally for helping me with the submission of my thesis.

I also thank Mrs. Ruckwied for always managing to measure my samples in time, for helpful discussions and for many nice conversations. Thanks to Hans Bucher for his help and Hinrich, Charlotte and Mrs. Dachtler for their tireless effort in all kinds of things.

Of course very special thanks go to the „S1-group“. Due to the good atmosphere and the friendly and helpful people I immediately felt welcome when I arrived, and always enjoyed the work at the institute. Thank you all for the “balancing” to my work: the barbecues, the “friday-night-colloquium”, the “Cannstatter Wasen” and all other good times we had, especially during the first two years of my PhD position. I also thank you for the good cooperation and the assistance in work. In this regard, my special thanks go to Anderson Rotter Meda, who introduced me to plant work (which was completely new to me) and who shared all his methodological and professional knowledge with me. I also thank Anderson, as well as Gabriel Schaaf and Annegret Honsbein, also for the work they did on the IREGs. This pre-work made the start very easy for me and I could directly “kick off”.

Special thanks also to the people of my office, you were the cause that I always looked forward to working. Thanks to Brigitte (who enriched our office life a lot, but unfortunately left too early), Uta Lintner, Lilia Carvalhais (greetings to Berlin) and especially to Claudia Weishaar, Bernhard Bauer and Enrico Scheuermann for all the serious, strange, cheerful, loud and funny discussions. Thanks to Claudi for joining me in the dancing course (I never would have dared to go alone!).

Very special thanks also go to Susanne Reiner, who was always helpful, no matter if the problems regarded work or private life. I wish you all the best, Susanne!

Thanks to all the S1-group: Anne Bohner for a lot of help and discussions, our “Brazilian gang” Ricardo, Joni and Anderson, Caro, Olga, Dmitriy, Rongli and all the others. Thanks also to the people that left during the time I was at the institute: Lixing Yuan and Soichi Kojima for a lot of technical advice, Ruth for her help and very interesting talks, Anne Rubel, Dominique (thanks for the great time in the Normandy), Sara, Sabine, Desiree and Bülent. Thanks also go to the three students (Miriam, Anne and Andi) I supervised for a whole semester each and who were very engaged in work and integrated very well to our group.

I also thank Prof. Römheld for his helpful comments and discussions, and Prof. Müller and his group, especially Angelika Kania who answered a lot of my questions. And of course very special thanks go to Silke Will (and her two little sunshines), for her mental support and for her friendship.

Finally, deep thanks go to my family and to Sven Nold for their support and their love.

Last but not least I want to thank Dr. Wilhelm Herzog and Dr. Martina Würfel from The Binding Site GmbH, for their support in finishing this thesis and preparing for the final defence.

## 9 Curriculum vitae

### Silvia Kirchner

Lindenstraße 23  
68723 Schwetzingen

Date of birth: 05/29/1975 in Neu-Ulm

Nationality: German

E-mail: silvia.kirchner@gmx.net

### Education

---

- 2004 - 2008 PhD position at the University of Hohenheim, Institute of Plant Nutrition. Title of the PhD thesis: “The AtIREGs – Characterization of a new family of metal transporters in *Arabidopsis thaliana*”, supervised by Prof. Dr. Nicolaus von Wirén
- 2004 Diploma thesis at the University of Ulm, Institute of Molecular Biology. Title of the diploma thesis: “Untersuchung der funktionellen Domänen der tRNase Z Enzyme aus *Saccharomyces cerevisiae* und *Arabidopsis thaliana*”, supervised by PD Dr. Anita Marchfelder
- 1999 - 2004 Studies in biology at the University of Ulm, Germany
- 1997 – 1999 High school degree (fachgebundene Hochschulreife) at the technical high school (technische Oberschule) in Ulm
- 1993 – 1996 Apprenticeship as pharmaceutical technical assistant

### Publications

---

**Späth B\*, Kirchner S\*, Vogel A, Schubert S, Meinschmidt P, Aymanns S, Nezzar J, Marchfelder A** (2005): Analysis of the functional modules of the rRNA 3' endonuclease (tRNaseZ). *J Biol Chem* 280(42): 35440-7. \*both authors contributed equally to this work

**Schaaf G, Honsbein A, Meda AR, Kirchner S, Wipf D, von Wirén N** (2006): *AtIREG2* encodes a tonoplast transport protein involved in iron-dependent nickel detoxification in *Arabidopsis thaliana* roots. *J Biol Chem* 281(35): 25532-40

### **Congresses, Advanced Training and Teaching Experience**

---

Poster presentation at the “XIII International Symposium on Iron Nutrition and Interactions in Plants” (13th ISINIP, 2007) in Montpellier, France

Poster presentation at the “XIV International Workshop on Plant Membrane Biology” (2007), Valencia, Spain

Poster presentation at the conference „Plant Nutrition meets Plant Breeding“ (2006) in Hohenheim, Germany; award for outstanding poster (2<sup>nd</sup> prize)

Supervision of the part “xylem exudate analysis of maize plants” of a practical course in plant nutrition (2005 – 2008)

Organization and supervision of a practical course in agricultural biotechnology (Großpraktikum Agrarbiotechnologie, 2005 – 2008)

Participation in the training course „Sicherheit im Laborbetrieb“ (safety in laboratory administration) for project leaders

### **Languages and Computer Science**

---

Languages                      German (mother tongue), English (fluent), French (basic knowledge)

Computer science            MS Office (Word, Excel, PowerPoint), Internet, DNASTar programs (EditSeq, Amplify, SeqMan, MapDraw, MegAlign), Adobe programs (Photoshop, Illustrator, Acrobat), statistical data analysing tools (SigmaStat), basic knowledge in programming

Silvia Kirchner